Waves and Oscillations in Model Neuronal Networks

by

Rodica Curtu

B.S. in Mathematics and Computer Science,
Transilvania University of Braşov, Romania, 1995

M.A. in Mathematics, University of Pittsburgh, 1999

Submitted to the Graduate Faculty of

Arts and Sciences in partial fulfillment

of the requirements for the degree of

Doctor of Philosophy

University of Pittsburgh

2003

UNIVERSITY OF PITTSBURGH

FACULTY OF ARTS AND SCIENCES

This dissertation was presented

by

Rodica Curtu

It was defended on

June 6, 2003

and approved by

Prof. Carson C. Chow, Mathematics

Prof. Jonathan Rubin, Mathematics

Prof. Daniel J. Simons, Neurobiology

Prof. William C. Troy, Mathematics

Committee Chairperson: Prof. G. Bard Ermentrout, Mathematics

WAVES AND OSCILLATIONS IN MODEL NEURONAL NETWORKS

Rodica Curtu, Ph.D.

University of Pittsburgh, 2003

In this thesis methods from nonlinear dynamical systems, pattern formation and bifurcation theory, combined with numerical simulations, are applied to three models in neuroscience.

In Chapter 1 we analyze the Wilson-Cowan equations for a single self-excited population of cells with absolute refractory period. We construct the normal form for a Hopf bifurcation, and prove that by increasing the refractory period the network switches from a steady state to an oscillatory behavior. Numerical simulations indicate that for large values of refractoriness the oscillation converges to a relaxation-like pattern, the period of which we estimate.

Chapter 2 brings new results for the rate model introduced by Hansel and Sompolinsky who study feature selectivity in local cortical circuits. We study their model with a more general, nonlinear sigmoid gain function, and prove that the system can exhibit different kind of patterns such as stationary states, traveling waves and standing waves.

Standing waves can be obtained only if the threshold is sufficiently high and only for intermediate values of the strength of adaptation. A large adaptation strength destabilizes the pattern. Therefore the localized activity starts to propagate along the network, resulting in a traveling wave.

We construct the normal form for Hopf and Takens-Bogdanov with $O(2)$-symmetry bifurcations and study the interactions between spatial and spatio-temporal patterns in the neural network. Numerical simulations are provided.

Chapter 3 addresses several questions with regard to the traveling wave propagation in a leaky-integrate-and-fire model for a network with purely excitatory (exponentially decaying) synaptic

coupling. We analyze the case when the neurons fire multiple spikes and derive a formula for the voltage.

We compute in a certain parameter space, the curves that delineate the region where single-spike traveling wave solutions exist, and show that there is a region of parameter space where neurons can propagate a two-spike traveling wave.

To my husband Iulian, for his love and understanding

Acknowledgments

I would like to thank the members of my committee, Prof. Carson Chow, Prof. Jon Rubin, Prof. Simons and Prof. Troy for their guidance throughout the writing of this thesis. I would also like to acknowledge Prof. Bryce McLeod for his advice and insightful comments.

I am especially grateful to my thesis advisor, Prof. Bard Ermentrout, for a wonderful interaction, scientific and otherwise. I thank him for his constant support during my graduate studies, and for giving me independence in pursuing research. You have shown me how effectively mathematics can be used as a tool for investigating other fields.

Thanks go to my colleagues and friends. To Pranay Goel for interesting and endless discussions, not always scientific, and to Dr. Remus Oşan for a good collaboration. To Stephanie Hoogendoorn and Jon Drover for a stimulating work environment.

Last but not least, I am deeply grateful to my family for believing in me and for their help and patience during my doctoral studies.

Table of Contents

List of Figures

Introduction

In this thesis methods from nonlinear dynamical systems, pattern formation and bifurcation theory are applied to three models in neuroscience.

Despite the fact that models for the behavior of individual neurons are relatively well developed, the question of how the brain, as a whole, processes and encodes the information received from external stimuli remains open. The huge amount of data collected from experiments needs to be interpreted, and as a first step computational models are used. Nevertheless most of the computational models are themselves complicated because of the large number of variables and parameters they include, thus the necessity of construction of much simpler models becomes apparent. These models try to capture the main characteristics of the phenomenon under scrutiny, and discard the rest of the unknowns. They have the advantage that they can be analyzed with tools such as dynamical systems and bifurcation theory in a framework proven already useful in other quantitative fields. As a consequence, the theoretical approach allows for a better understanding of the phenomenon, and may suggest new hypotheses to be tested in later experimental studies.

A dynamical system is a mathematical model of a deterministic process. Since real processes depend on different parameters, a small change in one parameter value implies a change in the system's behavior and this change can be negligible or, in contrast, substantial. Bifurcation theory helps at this point, allowing one to predict the critical regime of the parameters, that is, to find those parameters associated with dramatic changes in the system. There are two main types of bifurcations that we use in this thesis: the Hopf bifurcation and the Takens-Bogdanov bifurcation with $O(2)$-symmetry. The Hopf bifurcation is a very useful tool to prove the existence of oscillations in a system. When certain conditions are satisfied a constant state becomes unstable and it is replaced by small amplitude oscillations with finite frequency. The Takens-Bogdanov bifurcation provides us with an additional insight on how the system's behavior changes from stationary to

oscillatory (not necessary of small amplitude) solutions, and proves that bistable regimes exist. The $O(2)$-symmetry means that the system we analyze does not change with respect to rotations and reflection. In addition to the above mentioned methods, in Chapter 2 we apply results from the general theory of pattern formation.

Many experimental studies report spatial and spatio-temporal patterns in the brain. As an example, patients under drug induced hallucinations describe a series of simple geometric patterns such as spirals, tunnels, cones or grating honeycombs [77]. Based on experiments with LSD when even blind subjects report visual hallucinations, the hypothesis that this phenomenon is independent of external stimuli, and the patterns are generated in the visual cortex, was formulated. Motivated by this question, neural models [37, 39, 12] were constructed and analyzed with the goal of reproducing the patterns, and making predictions about the structure and organization of the visual cortex. On the other hand, patterns in the form of sustained oscillations [1, 22, 24, 31, 42, 49, 93, 101], or propagating waves [17, 18, 43, 52, 66, 67, 76, 98, 105], are frequently reported in experimental studies.

In this thesis we discuss two types of models that are commonly used in computational and mathematical neuroscience. They are rate models and the leaky-integrate-and-fire (LIF) spiking model. Both rate models and spiking models present advantages and disadvantages, depending on the context in which they are used.

A rate model accounts for a population activity and works with variables that correspond to an averaged firing rate measured usually through local field potential recordings. Essentially, rate models rely on the hypothesis that a large number of neurons are involved in different functions of the brain, such as sensory information processing, and so an approach at the level of averaged activity is better suited than one at the single cell level.

Obviously, rate models do not include individual spikes and as a result, the temporal details of neuronal activity cannot be considered. The advantage of the spiking models such as the LIF is that, in contrast, they do include the temporal details.

Thesis description

The thesis is structured in three chapters. We analyze two different rate models in Chapters 1 and 2, and study traveling wave propagation in the LIF spiking model in Chapter 3.

Chapter 1 is dedicated to the analysis of the Wilson-Cowan model [104] in its original form that includes an absolute refractory period. This model was introduced in 1972, and since then was used in a simplified form (by assuming that the refractory period is zero or very small) in many theoretical and computational studies.

The neurons in the population are assumed to be in close spatial proximity with random, but dense enough interconnections, so that any two neurons within the population are connected through a direct or indirect path. Therefore spatial interactions may be neglected and only the temporal dynamics of the network are considered. Usually two population of neurons, one excitatory and one inhibitory, are included. The rate variable in the Wilson-Cowan model represents the proportion of neurons in the population which become active per unit of time. Therefore the relevant aspect of a single cell activity is considered to be the spike frequency rather than the single spike.

We investigate the consequences of keeping the original form of the Wilson-Cowan equations for a single self-excited population of cells with absolute refractory period. We prove that by increasing the refractory period, the network switches from a randomly firing activity, that mathematically corresponds to a steady state (or fixed point) to a synchronized activity translated into an oscillatory behavior. Moreover the period of the oscillation scales linearly with the absolute refractory period for large values of the latter.

The work presented in this chapter resulted in a paper [25].

Chapter 2 brings new results for the rate model introduced by Hansel and Sompolinsky [58] who study feature selectivity in local cortical circuits. Since the spatial connectivity plays an important role in this case, it was included in the equations.

There is still a debate [7] about the role of the local cortical interactions in shaping the response properties of cortical neurons to sensory stimuli. One hypothesis is that the receptive field properties of simple cells in primary visual cortex are a reflection of the feedforward afferents from the lateral geniculate nucleus (LGN). In contrast, the other hypothesis is that recurrent cortical circuitry plays an important role in shaping the orientation tuning in cortex.

The Hansel-Sompolinsky model belongs to the group of models [7, 8, 59, 91] constructed to test if the second hypothesis holds. Their analysis shows that a stationary profile, called a tuning curve, can be obtained. Thus in their model, the local cortical connections are indeed capable of

playing a central role in generating the sharp selectivity of cortical neurons to the orientation of visual stimuli.

Hansel and Sompolinsky added an adaptation current to the rate model and proved that in this case, for sufficiently strong (or slow) adaptation, the stationary profile (steady state) tends to destabilize, and intrinsic moving profiles (traveling waves) occur. They also assumed that the stable state of the network is such that all the neurons are far from their saturation level. As a consequence they used a semilinear gain function.

We considered the Hansel-Sompolinsky model with a more general, nonlinear sigmoid gain function, and proved that the system can exhibit different kind of patterns than those previously reported. These are standing waves and are characterized by an oscillatory behavior in time at a fixed position in space, and an oscillatory behavior in space for any given moment of time.

The standing wave pattern can be obtained only if the threshold is sufficiently high and only for intermediate values of the strength of adaptation. When the adaptation strength increases the pattern is destabilized, and the localized activity starts to travel along the network, resulting in a traveling wave pattern.

The interactions between stationary and spatio-temporal patterns in the neural network are analyzed by considering a Takens-Bogdanov bifurcation with $O(2)$-symmetry.

Our theoretical approach is completely different from that followed in [58]. The tools we used to prove the existence and stability of the patterns come from those of pattern formation and bifurcation theory.

Chapter 3 addresses several questions with regard to the traveling wave propagation in a leaky-integrate-and-fire model for a network with purely excitatory synaptic coupling.

Previous theoretical studies [10, 33, 45, 44] developed methods for studying the existence of traveling waves of activity in networks of LIF cells, sometimes incorporating additional features such as synaptic delays. This work was motivated by experiments in which a wave of activity that propagates across the network was observed in slices of cortical tissue subjected to a local shock stimulus, and with all inhibition blocked [17, 18, 43, 66, 98]. However, these theoretical studies, with few exceptions, required *each neuron to fire exactly once* during wave propagation.

We considered the LIF model with exponential coupling and analyzed the case when the neurons were allowed to fire multiple spikes. We proved two equivalent formulas for general traveling wave

solutions and used them to prove that in a certain parameter space, there are curves that delineate the region on which single-spike traveling wave solutions exist.

We have also proved that in another region of parameter space, neurons can propagate a two-spike traveling wave. It remains open to determine where such solutions actually exist, by rigorously specifying the set of parameter values for which neurons stop spiking after exactly two spikes.

The general traveling wave formula provides a relationship that can, in theory, be used in an iterative way to solve for as many spike-times as desired in a traveling wave with any countable number of spikes, for fixed parameter values and a fixed wave speed. The iterative scheme is provided.

This work was part of a group research effort, and a more complete analysis including a dispersion relationship for periodic solutions, the effect of absolute refractory period, the connection between infinitely-countable multiple-spike waves and period wave, and numerical simulations are presented in [78].

Chapter 1

Oscillations in a refractory neural network

1.1 Introduction

Wilson and Cowan [104] introduced a class of neural network equations modeling the excitatory and inhibitory interactions between two populations of cells. Each population obeys a functional-differential equation of the form

$$\tau \frac{du(t)}{dt} = -u(t) + (1 - \int_{t-R}^{t} u(s)\ ds) f(I(t))$$

where τ is the time constant, $I(t)$ represents inputs to the population, f is the firing rate curve, and R is the absolute refractory period of the neurons. The function $u(t)$ is the fraction of the population of neurons which is firing. It can also be regarded as the actual firing rate of the population. The refractory term premultiplying the firing rate was approximated (by assuming that R is small) as

$$1 - \int_{t-R}^{t} u(s)\ ds \approx 1 - Ru(t).$$

All subsequent analyses of these equations either make this assumption or set $R = 0$.

Assumptions and derivation of equations for Wilson-Cowan model. The model assumes two population of neurons, one excitatory and one inhibitory, and it is described by two variables, $E(t)$ and $I(t)$, the proportion of excitatory, respectively inhibitory, cells firing per unit time at t. The resting state $E(t) = I(t) = 0$ is taken to be a state of low-level background activity.

By assumption, the value of E and I at time $t + \tau$ is equal to the proportion of cells which are sensitive (not refractory), and which receive at least threshold excitation at time t. If the probability that a cell is sensitive is independent of the probability that it is currently excited above its threshold, then the expression for E and I is obtained as a product between 'sensitivity' and 'excitation'.

If the absolute refractory period is of R msec, then $\int_{t-R}^{t} E(s)\,ds$ represents the proportion of excitatory cells which are refractory, and so $\left[1 - \int_{t-R}^{t} E(s)\,ds\right]$ gives the proportion of excitatory cells which are sensitive. A similar expression is obtained for inhibitory cells, i.e. $\left[1 - \int_{t-R}^{t} I(s)\,ds\right]$.

The 'excitation factor' is given by a response function $S_e(x)$, respectively $S_i(x)$, that describes the expected proportion of cells in a subpopulation which would respond to a given level of excitation if none of them were initially in absolute refractory period [104]. Therefore, $E(t + \tau) = \left[1 - \int_{t-R}^{t} E(s)\,ds\right] S_e(x)$ and $I(t + \tau) = \left[1 - \int_{t-R}^{t} I(s)\,ds\right] S_i(y)$.

The form of the response functions S_e and S_i results from the following assumptions: (1) the total number of afferents reaching a neuron is sufficiently large, (2) there is a distribution of individual neural thresholds within subpopulation characterized by the distribution function $D(\theta)$ which is unimodal (that is, it has only one maximum), and (3) on the average, all cells are subjected to the same excitation $x(t)$. Therefore the response function, defined as $S(x) = \int_0^{x(t)} D(\theta)\,d\theta$, takes a sigmoid form and can be described by $S(x) = \frac{1}{1 + e^{-a(x-\theta)}}$. A similar result is obtained in the hypotheses that all cells within a subpopulation have the same threshold θ and there is a (unimodal) distribution $C(w)$ of the number of afferent synapses per cell, and $x(t)$ is the average excitation per synapse. In this case $S(x) = \int_{\theta/x(t)}^{\infty} C(w)\,dw$ and still takes a sigmoid form.

An additional assumption is that individual cells sum their inputs and the effect of stimulation decays with a time course $\alpha(t)$, so the average level of excitation generated in an excitatory cell (similar for inhibitory cell) is describes by the integral term $\int_{-\infty}^{t} \alpha(t-s)[c_1 E(s) - c_2 I(s) + P(s)]\,ds$ where c_1, c_2 (positive constants) represent the average number of excitatory and inhibitory synapses per cell, and $P(t)$ is the external input to the subpopulation. Then we obtain

$$E(t + \tau) = \left[1 - \int_{t-R}^{t} E(s)\,ds\right] \cdot S_e\left(\int_{-\infty}^{t} \alpha(t-s)[c_1 E(s) - c_2 I(s) + P(s)]\,ds\right),$$

$$I(t + \tau) = \left[1 - \int_{t-R}^{t} I(s)\,ds\right] \cdot S_i\left(\int_{-\infty}^{t} \alpha(t-s)[c_3 E(s) - c_4 I(s) + Q(s)]\,ds\right).$$

If $\alpha(t)$ is close to 1 for $0 \leq t \leq R$ and drops rapidly to 0 for $t > R$, then the term $\int_{-\infty}^{t} \alpha(t-s)E(s)\,ds$ can be replaced by $k\overline{E}(t)$ where k is a constant and $\overline{E}$ is an average value of E over time. In addition $E(t + \tau)$ is written as $E(t + \tau) \approx \overline{E}(t) + \tau\frac{d\overline{E}}{dt}$.

Therefore, the resulting Wilson-Cowan equations are

$$\tau\frac{d\overline{E}}{dt} = -\overline{E}(t) + \left[1 - \int_{t-R}^{t} \overline{E}(s)\,ds\right] \cdot S_e\left(kc_1\overline{E} - kc_2\overline{I} + kP(t)\right),$$

$$\tau'\frac{d\overline{I}}{dt} = -\overline{I}(t) + \left[1 - \int_{t-R}^{t} \overline{I}(s)\,ds\right] \cdot S_i\left(k'c_3\overline{E} - k'c_4\overline{I} + k'Q(t)\right).$$

Wilson-Cowan model for a self-excited population of neurons with absolute refractory period. There have been numerous analyses of neural networks with delays. Castelfranco and Stech [16] prove the existence of oscillatory solutions to a two-dimensional model due to Plant which has delayed negative feedback. Similar results are described by Campbell et.al in a model for pupillary control [14]. Marcus and Westervelt [74] linearize a Hopfield symmetrically coupled network and show that the fixed points are asymptotically stable. Ye et.al [106] improve on this result by rigorously showing global stability of fixed points for the Hopfield network with delay.

In this chapter we will explore the consequences of keeping the original form of the Wilson-Cowan equations. In particular, we will look at a self-excited population of cells.

We consider the functional-differential equation

$$\tau\frac{du}{dt} = -u + \left(1 - \frac{1}{R}\int_{t-R}^{t} u(s)\,ds\right) f(u)$$

where f is a smooth monotonically increasing function ($f' > 0$) which takes values between 0 and 1. We have normalized the integral term in order to study the temporal effects of altering this absolute refractory period.

By rescaling the time $t \mapsto t/R$ and letting $r = R/\tau$ denote the ratio of the absolute refractory period to the time constant of the network, the equation becomes

$$\frac{du}{dt} = r\left[-u + \left(1 - \int_{t-1}^{t} u(s)\,ds\right) f(u)\right]. \tag{1.1}$$

Remark 1.1. We can alternatively rescale time as $t \mapsto t/\tau$. Then instead of equation (1.1) we obtain $\frac{du}{dt} = -u + \left(1 - \frac{1}{r}\int_{t-r}^{t} u(s)\,ds\right) f(u)$. In this rescaling, it is clear that this is a "delayed negative-feedback" system and that in the limit as $r \to 0$ we obtain the original Wilson-Cowan equations $\frac{du}{dt} = -u + (1-u)f(u)$. Because the calculations are simpler, we will use the first rescaling,
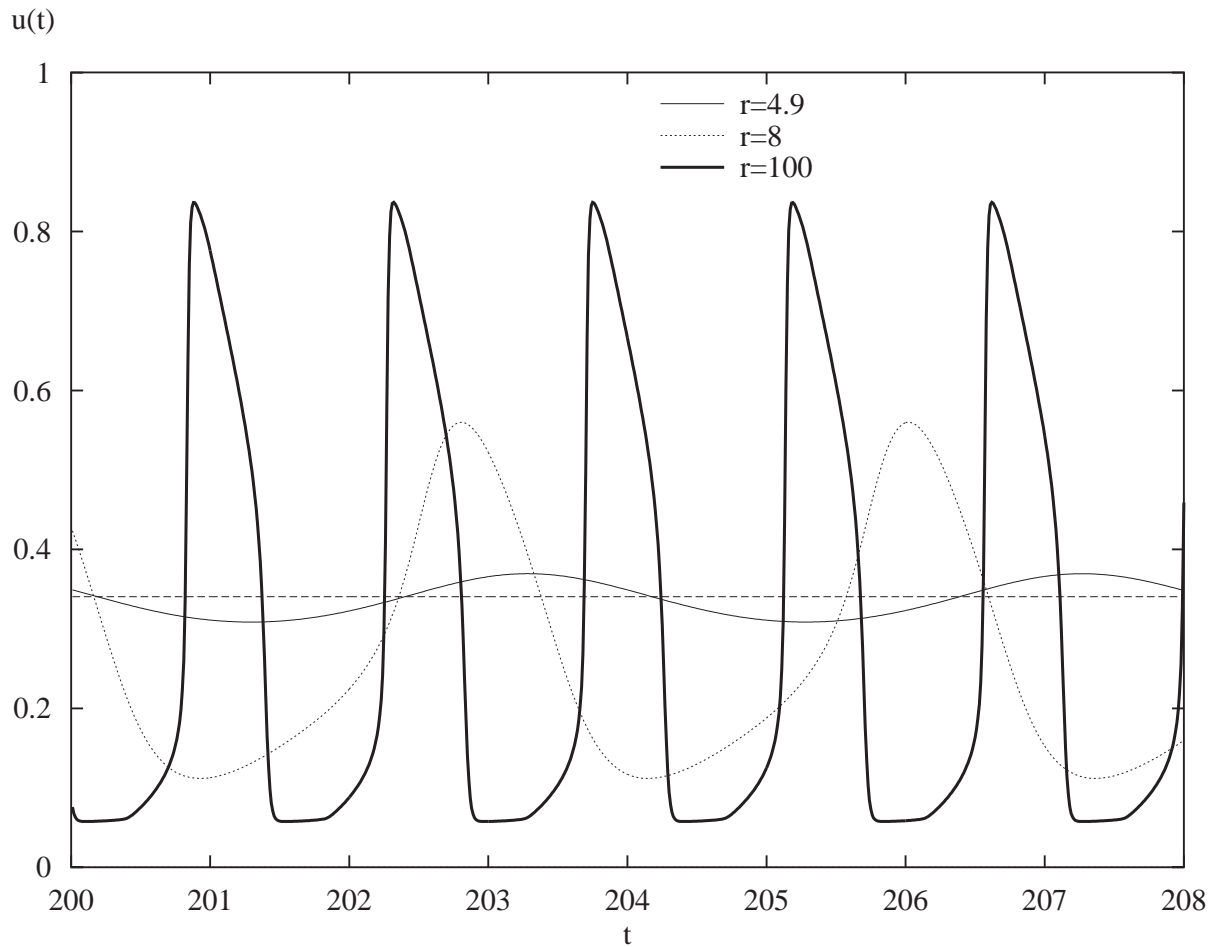
Figure 1.1. The behavior of (1.1) for different values of the parameter $r = R/\tau$ with $f(u) = 1/(1 + \exp(-8(u - .333)))$. The period of the smallest oscillation is 4 and that of the largest is 1.43.

(1.1) in the remainder of the chapter.

Remark 1.2. Figure 1.1 shows a simulation of (1.1) for a variety of values of the parameter r. The horizontal line corresponds to a fixed point. For the choice of parameters in the figure, solutions converge to the fixed point for $r < 4.7$ and for $r > 4.8$ all solutions numerically converge to a periodic orbit. Thus, it appears that as the refractoriness r increases, the constant solution loses stability through a Hopf bifurcation. For all larger values of r, solutions converge to a family of periodic orbits whose amplitude increases. Our goal in the subsequent sections is to show that this is in fact the correct picture. Section 1.2.1 is devoted to the analysis of fixed points and their stability. In Section 1.2.2 , we find the normal form for the Hopf bifurcation and show that the bifurcation is supercritical. We then look at the limit as r gets large. We show that the resulting equation behaves like a relaxation oscillator and compute the period for this system. We close with some simulations of waves and related phenomena in a locally connected network.

1.2 Oscillations in the refractory neural network obtained through a Hopf bifurcation

1.2.1 Fixed points and stability

The fixed points for (1.1) are $u = \bar{u}$ for all t and $\bar{u}$ satisfies

$$-\bar{u} + (1 - \bar{u})f(\bar{u}) = 0 \tag{1.2}$$

It is easy to check that because $0 < f < 1$ there is no equilibrium point in $(-\infty, 0] \cup [\frac{1}{2}, \infty)$, but there is at least one in $(0, \frac{1}{2})$, say $\bar{u}$.

For such an equilibrium we can rewrite equation (1.1), by defining $u := \bar{u} + y$ and using the Taylor expansion for the function f about $\bar{u}$, as

$$\frac{dy}{dt} = r\left[-y + y(1 - \bar{u})f'(\bar{u}) - f(\bar{u})\int_{t-1}^{t} y(s)\, ds\right] + r\left[-y f'(\bar{u})\int_{t-1}^{t} y(s)\, ds + y^2(1 - \bar{u})\frac{f''(\bar{u})}{2}\right]$$
$$+ r\left[-y^2\frac{f''(\bar{u})}{2}\int_{t-1}^{t} y(s)\, ds + y^3(1 - \bar{u})\frac{f'''(\bar{u})}{6}\right] + \mathcal{O}(y^4). \tag{1.3}$$

Remark 1.3. We define the coefficients $A = 1 - (1 - \bar{u}) f'(\bar{u}) < 1$ and $b = f(\bar{u}) \in (0, 1)$. Then as a first step in our analysis we consider only the linearized part of the equation (1.3), i.e.

$$\frac{dy}{dt} = r \left(-A y - b \int_{t-1}^{t} y(s) \, ds \right).$$

The stability of this equation is determined by studying the roots of the characteristic equation obtained by substituting $y(t) = \exp \lambda t$ into the linearized equation. This results in

$$\lambda + A r + b r \frac{1 - e^{-\lambda}}{\lambda} = 0. \tag{1.4}$$

A very similar equation to this is studied in Diekmann et. al, Chapter XI.4.3. We summarize the main points as they apply to the present equations. First, $\lambda = 0$ if and only if $A + b = 0$ and furthermore as long as $b \neq 0$, $\lambda = 0$ is a simple root. All roots with positive real part are bounded by the following inequality:

$$|\lambda| < r(|A| + |b|).$$

Thus, the only way that roots can enter the right-half plane is to go through the imaginary axis. Clearly if $b = 0$ and $A > 0$, then all roots have negative real parts. Furthermore, as we just noted, roots can cross 0 only if $A + b = 0$. Thus, we are interested in when there are roots of the form $\lambda = i\omega$. Substituting this into (1.4) we see that

$$Ar = -\frac{\omega \sin \omega}{1 - \cos \omega}, \tag{1.5}$$

$$br = \frac{\omega^2}{1 - \cos \omega}. \tag{1.6}$$

Since there are singularities at $\omega = 2k\pi$, these equations define a series of parametric curves defined in the regions $\omega \in (2k\pi, 2(k + 1)\pi)$ for k an integer. The first two of these curves are plotted in Figure 1.2. Crossing these curves results in new complex eigenvalues with positive real parts. To study stability as a function of the parameter r, we note that (Ar, br) defines a line through the origin with slope b/A as r varies in the the (Ar, br) plane shown in the figure. If this line crosses the lower emphasized curve then stability is lost through a pair of complex eigenvalues as the parameter
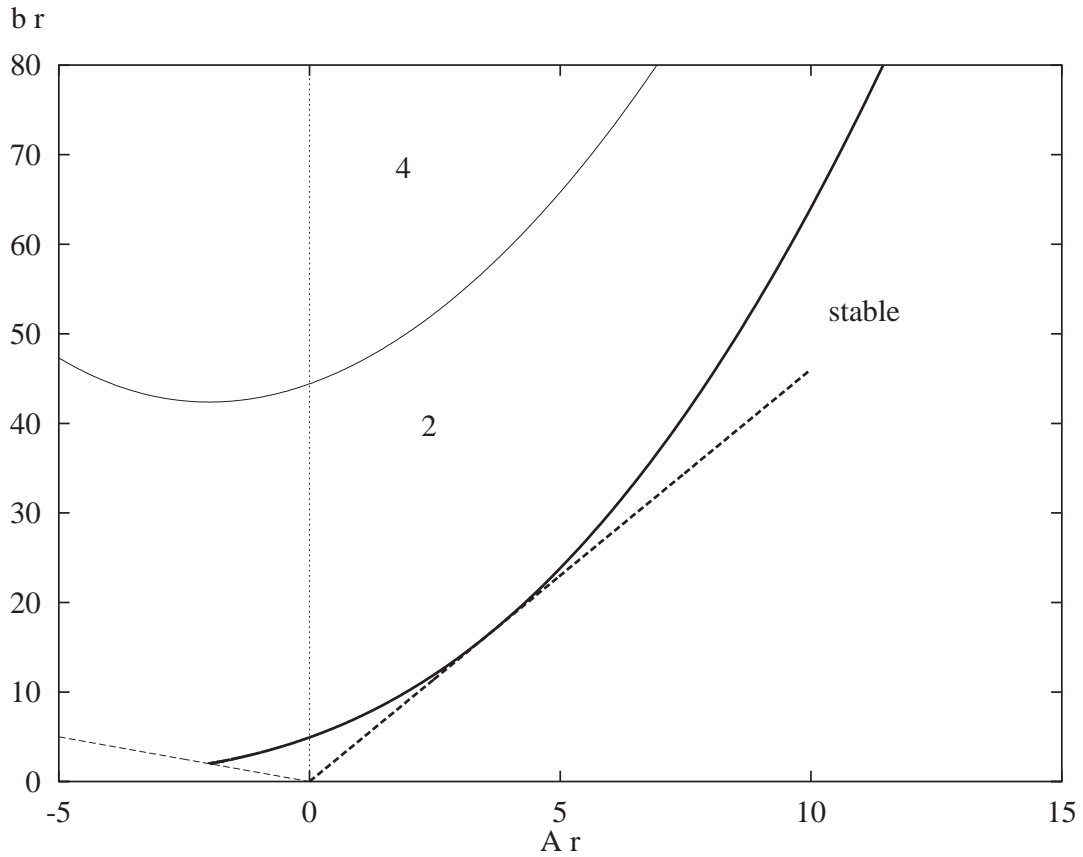
Figure 1.2. Stability diagram for (1.4) as a function of $A\,r$ and $b\,r$. Straight lines depicts the curve $b = -A$ and $b = A/M$ where M is defined in the text. The remaining curves depict lines along which there are purely imaginary roots. Numbers denote the number of eigenvalues with positive real parts.

r increases. Taking the ratio of the two above equations, we see that there will be such a root if and only if

$$\frac{A}{b} = -\frac{\sin\omega}{\omega}. \tag{1.7}$$

The minimum of this function is -1 and the maximum is $M = -\sin(\xi)/\xi$ where ξ is the smallest root of $\tan(x) = x$ greater than π. Thus, the slope of the line b/A must lie between $1/M \approx 4.60334$ and -1. These two lines are illustrated in Figure 1.2. If b/A lies between -1 and $4.6033\ldots$, then starting at small values of r as r increases, it pierces the lower stability curve and a pair of complex conjugate eigenvalues cross the imaginary axis resulting in a loss of stability. Clearly, if b/A is within these bounds, then we can solve (1.7) for a value of ω between 0 and 2π. Then we can use (1.6) to find $\tilde{r}_0 = \frac{1}{b}\frac{\omega^2}{1-\cos\omega}$ the critical value of r (which is always positive). If b/A is positive and less than $1/M$ then no increases in r can ever lead to a loss of stability. If the slope b/A is negative and shallower than -1, then for all positive values of r there is a real positive root to (1.4). To see this, note that we can rewrite (1.4) as

$$br\frac{1-e^{-\lambda}}{\lambda} = -(\lambda + Ar).$$

The left-hand side is monotonically decreasing, positive, and starts at br at $\lambda = 0$. Suppose that $-Ar > br$. Then $-(\lambda + Ar)$ is larger than br at $\lambda = 0$ and crosses the x-axis when $\lambda = -Ar > 0$. Thus, there is an intersection of the two for a positive value of λ between 0 and $-Ar$.

We summarize these calculations in the following theorem.

Theorem 1.1. *Suppose $\bar{u}$ is a fixed point of equation (1.1). Let $A = 1 - (1 - \bar{u}) f'(\bar{u})$ and $b = f(\bar{u})$.*

(i) Suppose that $-b < A < bM$ where $M = -\sin(\xi)/\xi \approx 1/4.60334 = 0.2172336$ with ξ the smallest root greater than π to $\tan(x) = x$. Then for r small enough, the fixed point is stable. As r increases, stability is lost when r crosses $\tilde{r}_0$ where

$$\tilde{r}_0 = \frac{1}{b}\frac{\omega_0^2}{1 - \cos\omega_0}$$

and ω_0 is the unique root to

$$\frac{A}{b} = -\frac{\sin\omega}{\omega}$$

between 0 and 2π.

    (ii) If $A > Mb$ *then the fixed point is stable for all values of* r.

    (iii) If $A < -b$ *then the fixed point is unstable for all positive* r.

1.2.2   Normal form

The numerical simulations in Figure 1.1 indicate that there exist oscillatory solutions for large enough r. Because of the above stability analysis we suspect the presence of an Andronov-Hopf bifurcation point for certain values of the parameter r. The next reasonable step would be the construction of the corresponding normal form and this is exactly what we do in this section.

Remark 1.4. The Hopf bifurcation theorem has been rigorously proven for (1.1) and related equations in Diekmann, et.al.[30]. Indeed, the authors compute the normal form for a related equation in Chapter XI4.3. Faria and Magalhães [41] describe a method to compute normal forms using the adjoint for equations of the form

$$\frac{dz}{dt} = L(p)z_t + F(z_t, p)$$

where p represents parameters. Our approach is similar to theirs. With minor modifications, we could apply the formula in Theorem 3.9 Diekmann, et.al.[30] (page 298), but for completeness, we derive the coefficients for the normal form here.

Let us consider equation (1.3) and define the linear operators

$$Ly := \frac{dy}{dt} + A\,\tilde{r}_0\,y + b\,\tilde{r}_0 \int_{t-1}^{t} y(s)\,ds\,, \quad \Lambda y := -A\,y - b\int_{t-1}^{t} y(s)\,ds$$

as well as the quadratic and cubic forms

$$B(y_1, y_2) := \tilde{r}_0 \left[\frac{(1-\bar{u})f''(\bar{u})}{2}\, y_1\, y_2 - \frac{f'(\bar{u})}{2}\, y_1 \int_{t-1}^{t} y_2(s)\,ds - \frac{f'(\bar{u})}{2}\, y_2 \int_{t-1}^{t} y_1(s)\,ds \right]$$

$$C(y_1, y_2, y_3) := \tilde{r}_0 \left[\frac{(1-\bar{u})f'''(\bar{u})}{6}\, y_1\, y_2\, y_3 - \frac{f''(\bar{u})}{6}\, y_1\, y_2 \int_{t-1}^{t} y_3(s)\,ds - \frac{f''(\bar{u})}{6}\, y_2\, y_3 \int_{t-1}^{t} y_1(s)\,ds \right.$$
$$\left. - \frac{f''(\bar{u})}{6}\, y_3\, y_1 \int_{t-1}^{t} y_2(s)\,ds \right].$$

Taking a small perturbation of the parameter $(r = \tilde{r}_0 + \alpha)$, the equation (1.3) can be rewritten as

$$Ly = \alpha \Lambda y + B(y, y) + C(y, y, y) + \alpha B(y, y) + \mathcal{O}(y^4). \qquad (1.8)$$

Since we are interested in finding small oscillatory solutions we can consider the following asymptotic expansion for (small) y and α

$$\alpha = \epsilon\,\alpha_1 + \epsilon^2\alpha_2 + \epsilon^3\alpha_3 + \cdots, \quad y(t) = \epsilon\,u_0(t) + \epsilon^2 u_1(t) + \epsilon^3 u_2(t) + \cdots, \quad \epsilon \to 0,$$

and obtain, instead of (1.8), $\epsilon\,Lu_0 + \epsilon^2 Lu_1 + \epsilon^3 Lu_2 + \mathcal{O}(\epsilon^4) = [\epsilon\,\alpha_1 + \epsilon^2\alpha_2 + \epsilon^3\alpha_3 + \cdots] \cdot [\epsilon\,\Lambda u_0 + \epsilon^2\Lambda u_1 + \epsilon^3\Lambda u_2 + \cdots] + [1 + \epsilon\,\alpha_1 + \cdots] \cdot B(\epsilon\,u_0 + \epsilon^2 u_1 + \epsilon^3 u_2 + \cdots, \epsilon\,u_0 + \epsilon^2 u_1 + \epsilon^3 u_2 + \cdots) + C(\epsilon\,u_0 + \epsilon^2 u_1 + \epsilon^3 u_2 + \cdots, \epsilon\,u_0 + \epsilon^2 u_1 + \epsilon^3 u_2 + \cdots, \epsilon\,u_0 + \epsilon^2 u_1 + \epsilon^3 u_2 + \cdots) + \mathcal{O}(\epsilon^4)$, i.e.

$$\epsilon\,Lu_0 + \epsilon^2 Lu_1 + \epsilon^3 Lu_2 + \mathcal{O}(\epsilon^4) = \epsilon^2\left[\alpha_1\,\Lambda u_0 + B(u_0, u_0)\right]$$

$$+ \epsilon^3\left[\alpha_1\,\Lambda u_1 + \alpha_2\,\Lambda u_0 + 2B(u_0, u_1) + C(u_0, u_0, u_0) + \alpha_1\,B(u_0, u_0)\right] + \mathcal{O}(\epsilon^4). \qquad (1.9)$$

Based on the fact that the equation $Ly = 0$ has two independent solutions $(e^{\pm i\omega_0 t})$ on the center manifold and by the asymptotic expansion $Lu_0 = \epsilon\left[\alpha_1\,\Lambda u_0 + B(u_0, u_0) - Lu_1\right] + \cdots$ we can choose

$$u_0(t) = z(t)e^{i\omega_0 t} + \bar{z}(t)e^{-i\omega_0 t}$$

with z depending on ϵ (e.g. $z = z(\epsilon^2 t)$). The expansion with respect to ϵ gives $z = z(0) + \epsilon^2 t z'(0) + \mathcal{O}(\epsilon^4)$ as ϵ tends to 0. We then use z and the properties of the defined operators in (1.9) to obtain

$$0 = \epsilon\left[\alpha_1\,z(0)\,\Lambda(e^{i\omega_0 t}) + \alpha_1\,\bar{z}(0)\,\Lambda(e^{-i\omega_0 t}) + 2z(0)\bar{z}(0)\,B(e^{i\omega_0 t}, e^{-i\omega_0 t}) + z(0)^2 B(e^{i\omega_0 t}, e^{i\omega_0 t})\right.$$

$$+ \bar{z}(0)^2 B(e^{-i\omega_0 t}, e^{-i\omega_0 t}) - Lu_1\left.\right] + \epsilon^2\left[-Lu_2 - z'(0)\,L(te^{i\omega_0 t}) - \bar{z}'(0)\,L(te^{-i\omega_0 t}) + \alpha_1\,\Lambda u_1\right.$$

$$+ \alpha_2\,z(0)\,\Lambda(e^{i\omega_0 t}) + \alpha_2\,\bar{z}(0)\,\Lambda(e^{-i\omega_0 t}) + 2B(u_0, u_1) + \alpha_1\,B(u_0, u_0) + C(u_0, u_0, u_0)\left.\right] + \mathcal{O}(\epsilon^3).$$

$$(1.10)$$

Therefore the coefficient of ϵ in the above expansion implies $Lu_1 = g$, with the given function g,

$$g(t) = \alpha_1 \, z(0) \, \Lambda(e^{i\omega_0 t}) + \alpha_1 \, \bar{z}(0) \, \Lambda(e^{-i\omega_0 t})$$
$$+ 2z(0)\bar{z}(0) \, B(e^{i\omega_0 t}, e^{-i\omega_0 t}) + z(0)^2 B(e^{i\omega_0 t}, e^{i\omega_0 t}) + \bar{z}(0)^2 B(e^{-i\omega_0 t}, e^{-i\omega_0 t}) \,.$$

Remark 1.5. In order to ensure the existence of a solution for the equation $Lu_1 = g$ we need the inhomogeneous term $g(t)$ to be orthogonal to the solutions of the adjoint homogeneous equation. The adjoint operator of L (see Appendix A.0.1) is $L^* y := -\frac{dy}{dt} + A\,\tilde{r}_0\, y + b\,\tilde{r}_0 \int_t^{t+1} y(s)\, ds$, and on the two-dimensional center manifold $e^{i\omega_0 t}$ and $e^{-i\omega_0 t}$ are independent solutions for L^*. The inner product is the usual $< \phi, \psi >= \int_0^{\frac{2\pi}{\omega_0}} \phi(t)\bar{\psi}(t)\, dt$, so we need $\int_0^{\frac{2\pi}{\omega_0}} g(t) e^{\pm i\omega_0 t}\, dt = 0$. The definition of the operators L, Λ, B, C implies immediately that $L(e^{\lambda t}) = \tilde{L}(\lambda)\, e^{\lambda t}$, $\Lambda(e^{\lambda t}) = \tilde{\Lambda}(\lambda)\, e^{\lambda t}$, $B(e^{\lambda_1 t}, e^{\lambda_2 t}) = \tilde{B}(\lambda_1, \lambda_2)\, e^{(\lambda_1 + \lambda_2)t}$, $C(e^{\lambda_1 t}, e^{\lambda_2 t}, e^{\lambda_3 t}) = \tilde{C}(\lambda_1, \lambda_2, \lambda_3)\, e^{(\lambda_1 + \lambda_2 + \lambda_3)t}$ with $\tilde{L}, \tilde{\Lambda}, \tilde{B}$ and $\tilde{C}$ given in Appendix A.0.2. Therefore g can be expressed as a linear combination of powers of $e^{i\omega_0 t}$ and $e^{-i\omega_0 t}$.

The orthogonality condition becomes $[\alpha_1\, \bar{z}(0)\, \frac{2\pi}{\omega_0}\, \tilde{\Lambda}(-i\omega_0) = 0, \ \alpha_1\, z(0)\, \frac{2\pi}{\omega_0}\, \tilde{\Lambda}(i\omega_0) = 0]$. Obviously in this case α_1 is zero, and the equation $Lu_1 = g$ becomes

$$Lu_1 = z(0)^2\, \tilde{B}(i\omega_0, i\omega_0)\, e^{2i\omega_0 t} + \bar{z}(0)^2\, \tilde{B}(-i\omega_0, -i\omega_0)\, e^{-2i\omega_0 t} + 2z(0)\bar{z}(0)\, \tilde{B}(i\omega_0, -i\omega_0)\,. \quad (1.11)$$

We choose $u_1 = a_1 z^2 e^{2i\omega_0 t} + 2a_2 z\bar{z} + a_3\bar{z}^2 e^{-2i\omega_0 t}$ which implies $u_1 = a_1 z^2(0)e^{2i\omega_0 t} + 2a_2 z(0)\bar{z}(0) + a_3\bar{z}^2(0)e^{-2i\omega_0 t} + \mathcal{O}(\epsilon^2 t)$, as $\epsilon \to 0$, substitute into L, and compare with (1.11). We get the coefficients a_1, a_2, a_3, with $a_2 \in \mathbf{R}$ and $\bar{a}_1 = a_3$,

$$a_1 = \frac{\tilde{B}(i\omega_0, i\omega_0)}{\tilde{L}(2i\omega_0)}, \quad a_2 = \frac{\tilde{B}(i\omega_0, -i\omega_0)}{\tilde{L}(0)}, \quad a_3 = \frac{\tilde{B}(-i\omega_0, -i\omega_0)}{\tilde{L}(-2i\omega_0)}\,.$$

So far we have calculated u_0, u_1, α_1. We can now conclude that in equation (1.10), u_2 should satisfy

$$Lu_2 = -\, z'(0)\, L(te^{i\omega_0 t}) - \bar{z}'(0)\, L(te^{-i\omega_0 t}) + \alpha_2\, z(0)\, \tilde{\Lambda}(i\omega_0)e^{i\omega_0 t} + \alpha_2\, \bar{z}(0)\tilde{\Lambda}(-i\omega_0)e^{-i\omega_0 t}$$
$$+ 2a_1\, z^3(0)\, B(e^{i\omega_0 t}, e^{2i\omega_0 t}) + 4a_2\, z^2(0)\bar{z}(0)\, B(e^{i\omega_0 t}, 1) + 2a_3\, \bar{z}^3(0)\, B(e^{-i\omega_0 t}, e^{-2i\omega_0 t})$$
$$+ 4a_2\, z(0)\bar{z}^2(0)\, B(e^{-i\omega_0 t}, 1) + 2a_1\, z^2(0)\bar{z}(0)\, B(e^{-i\omega_0 t}, e^{2i\omega_0 t}) + 2a_3\, z(0)\bar{z}^2(0)\, B(e^{i\omega_0 t}, e^{-2i\omega_0 t})$$
$$+ z^3(0)\, C(e^{i\omega_0 t}, e^{i\omega_0 t}, e^{i\omega_0 t}) + 3z^2(0)\bar{z}(0)\, C(e^{i\omega_0 t}, e^{i\omega_0 t}, e^{-i\omega_0 t}) + \bar{z}^3(0)\, C(e^{-i\omega_0 t}, e^{-i\omega_0 t}, e^{-i\omega_0 t})$$
$$+ 3z(0)\bar{z}^2(0)\, C(e^{i\omega_0 t}, e^{-i\omega_0 t}, e^{-i\omega_0 t})$$

16

Similar to u_1, for solutions, we need the right hand side to be orthogonal to $e^{\pm i\omega_0 t}$, i.e.

$$z'(0) \int_0^{\frac{2\pi}{\omega_0}} e^{-i\omega_0 t} L(te^{i\omega_0 t})\, dt + \bar{z}'(0) \int_0^{\frac{2\pi}{\omega_0}} e^{-i\omega_0 t} L(te^{-i\omega_0 t})\, dt = \alpha_2\, z(0)\, \tilde{\Lambda}(i\omega_0) \frac{2\pi}{\omega_0}$$

$$+2a_1\, z^2(0)\bar{z}(0)\, \tilde{B}(-i\omega_0, 2i\omega_0) \frac{2\pi}{\omega_0} + 4a_2\, z^2(0)\bar{z}(0)\, \tilde{B}(i\omega_0, 0) \frac{2\pi}{\omega_0} + 3z^2(0)\bar{z}(0)\, \tilde{C}(i\omega_0, i\omega_0, -i\omega_0) \frac{2\pi}{\omega_0} \ .$$

This immediately implies

$$z'(0) = \frac{i\,\omega_0\,\alpha_2}{\tilde{r}_0 \left[2 + A\,\tilde{r}_0 + i(\omega_0 - \frac{A\tilde{r}_0 + b\tilde{r}_0}{\omega_0})\right]}\, z(0)$$

$$+ \frac{4a_2\, \tilde{B}(i\omega_0, 0) + 2a_1\, \tilde{B}(-i\omega_0, 2i\omega_0) + 3\tilde{C}(i\omega_0, i\omega_0, -i\omega_0)}{2 + A\,\tilde{r}_0 + i(\omega_0 - \frac{A\tilde{r}_0 + b\tilde{r}_0}{\omega_0})}\, z^2(0)\bar{z}(0) \quad (1.12)$$

where

$$\tilde{B}(i\omega_0, 0) = \left[\tilde{r}_0 \frac{1 - \bar{u}}{2}\, f''(\bar{u}) + \frac{A}{2b}\, f'(\bar{u})\, \tilde{r}_0 - \frac{1}{2} f'(\bar{u})\, \tilde{r}_0\right] + i\, \frac{\omega_0}{2b}\, f'(\bar{u}),$$

$$\tilde{B}(-i\omega_0, 2i\omega_0) = \left[\tilde{r}_0 \frac{1 - \bar{u}}{2}\, f''(\bar{u}) + \left(\frac{A\,\tilde{r}_0}{b} - \frac{A\,\omega_0^2}{2b^2}\right) f'(\bar{u})\right] + i\, \frac{\tilde{r}_0\,\omega_0}{4b^2}\left[A^2 - \frac{\omega_0^2}{\tilde{r}_0^2}\right] f'(\bar{u}),$$

$$\tilde{C}(i\omega_0, i\omega_0, -i\omega_0) = \left[\tilde{r}_0 \frac{1 - \bar{u}}{6}\, f'''(\bar{u}) + \frac{A}{2b}\, f''(\bar{u})\, \tilde{r}_0\right] + i\, \frac{\omega_0}{6b}\, f''(\bar{u}).$$

We have just proven the following theorem.

Theorem 1.2. *Suppose that $\bar{u}$ is an equilibrium point of the equation (1.1) and that A, b satisfy $-b < A < Mb$ where M is as in Theorem 1.1. Take $\tilde{r}_0$ and ω_0 as in Theorem 1.1 and denote by δ the coefficient of $z^2(0)\bar{z}(0)$ in (1.12).*

Then the normal form on the center manifold at $r = \tilde{r}_0$ is given by (1.12). If $Re(\delta) < 0$ $(Re(\delta) > 0)$ then at $r = \tilde{r}_0$ the system passes through a supercritical (subcritical) Andronov-Hopf bifurcation which proves the existence of a small amplitude periodic stable (unstable) solution in the vicinity of the steady state near the bifurcation point.

Proof: The nondegeneracy condition requires the real part of the coefficient of $z(0)$ to be nonzero. The real part of the coefficient is

$$\frac{\omega_0^2 - (A + b)r_0}{r_0[(2 + Ar_0)^2 + (\omega_0 - (A + b)r_0/\omega_0)^2]} \ .$$

Using the substitution of $r_0 = \omega_0^2/[b(1 - \cos\omega_0)]$ into the numerator and the fact that $A/b = -\sin(\omega_0)/\omega_0$ we find that the numerator is $\frac{\omega_0^2}{1 - \cos\omega_0}\left(\frac{\sin\omega_0}{\omega_0} - \cos\omega_0\right)$. The first term cannot vanish

17

since $\omega_0 \in (0, 2\pi)$. Thus, the coefficient will be zero if and only if $\frac{\sin \omega_0}{\omega_0} = \cos \omega_0$. Recall that the extrema of $\sin(\omega)/\omega = -A/b$ can occur only when $\sin(\omega)/\omega = \cos \omega$ so that the numerator will vanish only along the lines $A = -b$ and $A = Mb$. Since $-b < A < bM$ this is impossible.

1.2.3 Example

Let us consider the function

$$f(x) = \frac{1}{1 + e^{-a(x+\theta)}} \quad \text{with} \quad a = 8, \quad \theta = -0.333$$

that has only one equilibrium point $\bar{u}$. We compute A, b and the values for the first three derivatives, i.e. $\bar{u} = 0.335909$, $A = -0.328002$, $b = 0.505818$, $f'(\bar{u}) = 1.99973$, $f''(\bar{u}) = -0.186145$, $f'''(\bar{u}) = -63.9653$, and solve for ω and r; we find here a unique solution $\omega_0 = 1.541455$, $\tilde{r}_0 = 4.839469881$.

By immediate calculation we have $\sin(\omega_0)/\omega_0 - \cos \omega_0 = 0.619121$, so the linear coefficient in the normal form is positive and the rest state loses stability when the value of r increases through $r = \tilde{r}_0$. At $r = \tilde{r}_0$ a stable periodic orbit is born. In this example the quantities which appear in the formula for the coefficient of $z^2 \bar{z}$ in the normal form are

$$2 + A\tilde{r}_0 + i(\omega_0 - \frac{\tilde{r}_0(A+b)}{\omega_0}) = 0.4126442001 + 0.9831933729\, i\,,$$

$$\tilde{B}(i\omega_0, 0) = -8.275709357 + 3.047038468\, i\,, \quad \tilde{B}(-i\omega_0, 2i\omega_0) = -3.52893752 + 0.0893831027\, i\,,$$

$$\tilde{C}(i\omega_0, i\omega_0, -i\omega_0) = -33.97038306 - 0.0945445928\, i\,,$$

$$a_1 = 4.172849433 + 0.097025506\, i\,, \quad a_2 = -7.640204473\,, \quad \delta = -36.6125 - 138.977\, i\,,$$

therefore since $Re(\delta) < 0$, this is a supercritical Andronov-Hopf bifurcation.

We note that Figure 1.1 shows the numerical solutions for a variety of values of r. In particular, the fixed point is the only attractor for $r = 4.7$ but clearly, when $r = 4.9$ there is a stable periodic solution. The period computed analytically is $2\pi/\omega_0 = 4.08$ which agrees well with the numerically found period of 4.00. Thus, the numerical solutions and the Hopf calculations are consistent.

1.3   Relaxation oscillator approximation

We now consider equation (1.1) for large values of the parameter r. By introducing $\epsilon = \frac{1}{r}$ and the function $z(t)$

$$z(t) := \int_{t-1}^{t} u(s)\, ds$$

equation (1.1) is equivalent to the two-dimensional delay-differential equation

$$\begin{cases} \epsilon \frac{du}{dt} &= -u + (1-z)\, f(u) \\[2mm] \frac{dz}{dt} &= u(t) - u(t-1) \end{cases} \qquad (1.13)$$

We recall that (1.1) is obtained by rescaling time t with respect to the parameter R in the original equation, so t represents a *slow time*. We analyze the solution by treating ϵ as a small positive parameter. We will first point out how to construct a singular periodic orbit for this system and then we will estimate the period T for the relaxation oscillator.

Remark 1.6. Mallet-Paret and Nussbaum [73] have extensively and rigorously analyzed an equation similar to (1.13), $\epsilon \frac{dx(t)}{dt} = -x(t) + f(x(t-1))$ where f is an odd negative feedback function (that is, $xf(x) \leq 0$). In particular, they consider a step function for f. Hale and Huang [57] have studied the vector analogue, $\epsilon \frac{dx(t)}{dt} = -Ax(t) + Af(\lambda, x(t-1))$ where A is an invertible matrix and f is smoothly dependent on x and the free parameter λ. They assume that the map $x \longrightarrow f(\lambda, x)$ undergoes a period-doubling bifurcation at $\lambda = 0$ and then prove that the delay-differential equation undergoes a similar bifurcation. More recent work by Hale and Huang [56] shows a similar behavior as well as a Hopf bifurcation. As far as we know, however, the rigorous analysis of equation (1.13) has not been done and remains an open problem.

By setting $\epsilon = 0$ in (1.13), we obtain the equations corresponding to the slow flow

$$\begin{cases} 0 = -u + (1-z)\, f(u)\,, \\[2mm] \frac{dz}{dt} = u(t) - u(t-1) \end{cases} \qquad (1.14)$$

For the fast flow we consider the original integro-differential equation. In this case the function z is $z(t) = \frac{1}{r} \int_{t-r}^{t} u(s)\, ds$ and it satisfies $dz/dt = (u(t) - u(t-r))/r$. When r tends to infinity (ϵ

tends to zero), the system becomes

$$\begin{cases} \frac{du}{dt} = -u + (1-z)\,f(u)\,, \\ \\ \frac{dz}{dt} = 0 \end{cases}$$

Thus, the two-dimensional system is decomposed in two one-dimensional equations, the solutions of which we now characterize.

Consider the graph for $0 = -u + (1-z)\,f(u)$ with $f(x) = \frac{1}{1+e^{-a\,(x+\theta)}}$, $a = 8$, $\theta = -0.333$. The sign of $(-u + (1-z)\,f(u))$ is negative above the graph and positive below it. Consider the points A, B, C, D on the graph with corresponding coordinates $A(u_1, z_{\min})$, $B(u_{\max}, z_{\min})$, $C(u_2, z_{\max})$, $D(u_{\min}, z_{\max})$ (see Figure 1.3).

We begin with the system at the point A at $t = 0$, where z cannot decreases anymore so a jump up takes place to the BC branch ($z = $ constant and u suddenly increases by the fast system). On this branch the system's law of motion is (1.14). Here $dz/dt > 0$ so z increases until the point reaches C. We remark that in order to have $dz/dt > 0$ on BC branch we need $u(t) > u(t-1)$ all the time. This is obviously true at B since $u_B = u(t = 0+) = u_{\max} > u(t = -1)$. In order to have $u_C = u(t = T_d) > u(t = T_d - 1)$ we need $u(t = T_d - 1)$ to be on the DA branch. This implies that T_d, the time the system stays on the upper branch BC, must be less than 1.

At the point C since z cannot increases anymore there is a jump down to the branch DA ($z = $ constant and u decreases by the fast system). On the branch DA, z decreases from $z_{\max}$ to $z_{\min}$. In order to have $dz/dt < 0$ we need $u(t) < u(t-1)$, in particular $u_D = u(t = T_d+) = u_{\min} < u(t = T_d - 1)$ and $u_A = u(t = T) < u(t = T - 1)$, which means that it is necessary that $u(T-1)$ be on the BC branch, i.e. $T-1$ is positive and less than T_d.

Following these considerations we see that in order to construct a singular periodic solution it has to be true that

$$0 < T - 1 < T_d < 1 < T \qquad (\Rightarrow T < 2)$$

where T is the period of oscillation. We estimate T and T_d considering u constant, $u = u_H$, on the
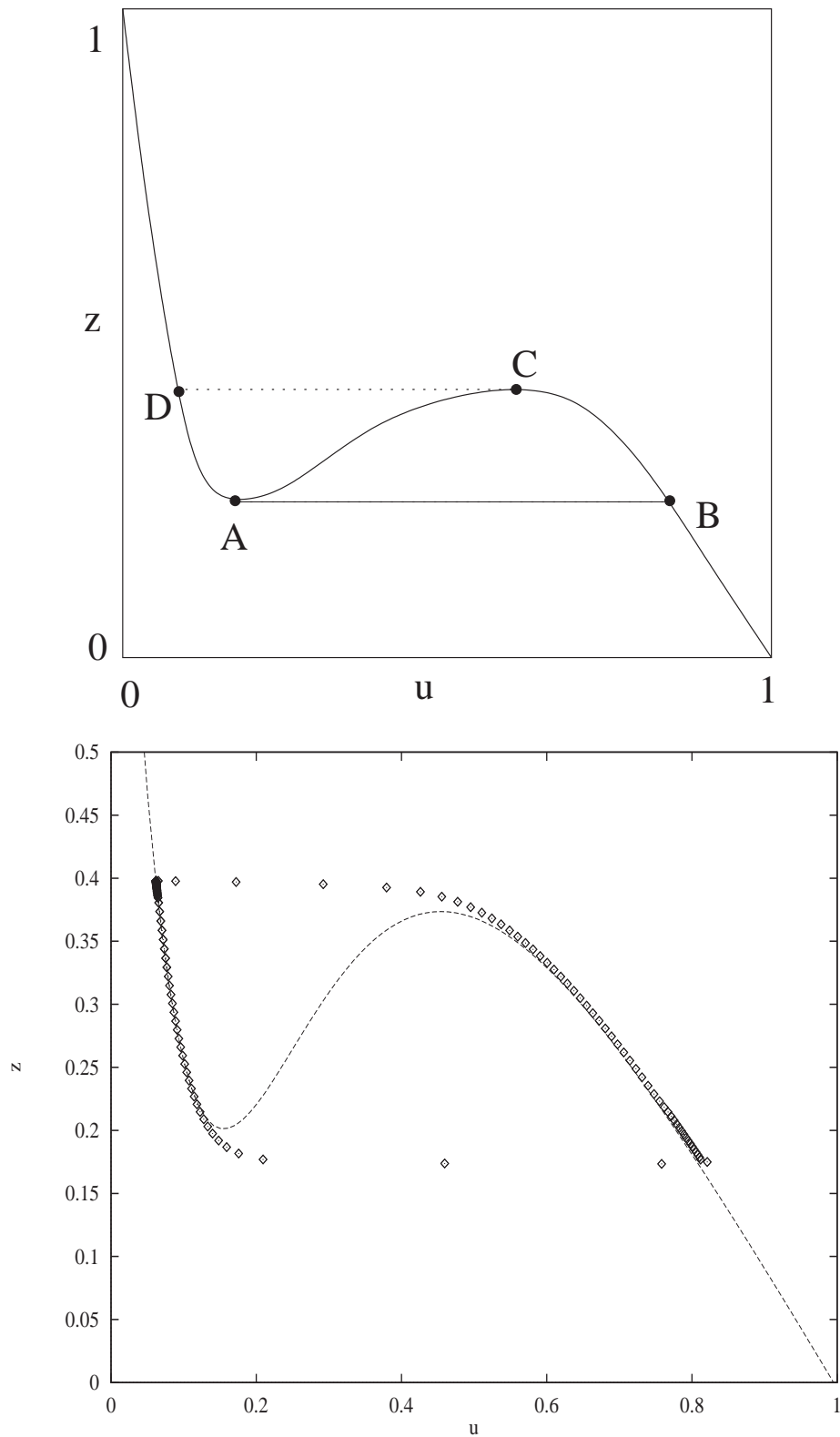
Figure 1.3. Plot of $0 = -u + (1 - z)f(u)$ with points relevant to the relaxation oscillation labeled. Below is a numerically computed solution with $r = 300$ illustrating the relaxation character of the oscillation.

21

branch BC, and $u = u_L$ on the branch DA. At $t = 0, z = z_{\min}, u = u_H$ and

$$dz/dt = u(t) - u(t-1) = \begin{cases} 0 & , t \in [0, T_d + 1 - T] \\ u_H - u_L & , t \in [T_d + 1 - T, T_d] \\ 0 & , t \in [T_d, 1] \\ u_L - u_H & , t \in [1, T] \end{cases}$$

equivalently with

$$z(t) = \begin{cases} z_{\min} & , t \in [0, T_d + 1 - T] \\ (u_H - u_L) t + C_1 & , t \in [T_d + 1 - T, T_d] \\ C_2 & , t \in [T_d, 1] \\ (u_L - u_H) t & , t \in [1, T] \end{cases}$$

with $z(T) = z_{\min}$ and $z(T_d) = z_{\max}$. Using this and the identity $z(t = 0) = z_{\min} = \int_{-1}^{0} u(s)\, ds$ we obtain an approximating formula for T and T_d

$$T \approx 1 + \frac{z_{\max} - z_{\min}}{u_H - u_L} \qquad \text{and} \qquad T_d \approx \frac{z_{\max} - u_L}{u_H - u_L}.$$

Remark 1.7. For our example, $u_{\min} = 0.065$, $u_1 = 0.15957447$, $u_{\max} = 0.777$, $u_2 = 0.45106383$, $z_{\min} = 0.20141882$, $z_{\max} = 0.37353106$. Choosing $u_H = u_{\max}$ and $u_L = u_{\min}$ we obtain $T = 1.2417$ and $T_d = 0.4333$. The period for the oscillation shown in Figure 1.3 is 1.35. Given that u is not really constant on the branches, this is a pretty good estimate of the period. We can improve this approximation with just a minor change in the choice of u_L and u_H. Above, we chose $u_{\max}$ and $u_{\min}$; a better approximation is to choose the mean value

$$u_L = \frac{u_{\min} + u_1}{2}, \quad u_H = \frac{u_2 + u_{\max}}{2}.$$

For our example, this implies $u_L = 0.1122872$, $u_H = 0.6140319$ and $T = 1.3430$, $T_d = 0.5206$. This is a considerably better approximation of the period without any extra work.

22

1.4 Conclusions

We have analyzed the original Wilson-Cowan model for an excitatory population of neurons with an absolute refractory period. It is not surprising that there exist oscillations as the system is essentially a delayed negative feedback model. Curiously, however, as the effective delay increases, the oscillation converges to a relaxation-like pattern and the frequency goes to a nice limit. In terms of the original time, the actual oscillation period scales linearly with R the absolute refractory period.

We have looked only at oscillatory solutions of the scalar problem. An interesting subject for future research is to investigate what happens when two populations are coupled and answer the question if the resulting oscillations synchronize, or not.

Based on the fact that if we let a be larger in the definition of the function f, the system is not oscillatory but rather excitable, another interesting question is the existence of a traveling wave when such (1.1) units are coupled locally on a line. An analytical approach is possible by letting $a \to \infty$ so that f can be approximated by a step function.

Chapter 2

Pattern formation in a network of excitatory and inhibitory cells with adaptation

2.1 Introduction

We analyze in this chapter a rate model that describe the activity of two populations of neurons coupled together, one excitatory and one inhibitory, in the presence of adaptation. Our goal is to investigate what types of patterns can be obtained in the system as a consequence of changing the strength of synaptic coupling and/or the strength of the adaptation variable.

The model was introduced by Hansel and Sompolinsky [58] when studying feature selectivity in local cortical circuits. In that context the network of neurons was assumed to code for a sensory or movement scalar feature x (for example the angle a bar is rotated in the subject receptor field, so that x can be taken in the interval $[-\frac{\pi}{2}, \frac{\pi}{2}]$). The local cortical network consists of ensembles of neurons that respond (are tuned) to a particular feature of an external stimulus, and so are called 'feature columns', and that are interconnected by recurrent synaptic connections. In other words, each neuron in the network is selective, firing maximally when a feature ('preferred feature' of the neuron) with a particular value is present. The synaptic interactions between a presynaptic neuron y from the β-population and a postsynaptic neuron x from the α-population are denoted by a function $J^{\alpha\beta}(x-y) = j_0^{\alpha\beta} + j_2^{\alpha\beta}\cos(2(x-y))$ where α and β indices stand for E (excitatory) and/or I (inhibitory) population of neurons, depending on the context. We take $j_0^{\alpha E} \geq j_2^{\alpha E} \geq 0$ for input coming from the excitatory population, and $j_0^{\alpha E} \leq j_2^{\alpha E} \leq 0$ for input coming from the inhibitory population.

Hansel and Sompolinsky collapsed both excitatory and inhibitory populations into a single equivalent population. In this case the synaptic connectivity function J is defined as $J(x-y) = j_0 + j_2\cos(2(x-y))$ with no restrictions on the sign of coefficients, and the rate model has a single rate variable $m(x,t)$ that represents the activity of the population of neurons in the column x at

time t. Moreover the population is assumed to display adaptation. The resulting model [58] is

$$
\begin{aligned}
\tau_0 \frac{\partial m}{\partial t}(x,t) &= -m(x,t) + F\left(\frac{1}{\pi}\int_{-\frac{\pi}{2}}^{\frac{\pi}{2}} J(x-y)\, m(y,t)\, dy + I^0(x-x_0) - I_a(x,t) - T\right) \\
\tau_a \frac{\partial I_a}{\partial t}(x,t) &= -I_a(x,t) + J_a\, m(x,t)\,.
\end{aligned}
\tag{2.1}
$$

I^0 stands for the synaptic currents from the external neurons, T is the neuronal threshold, I_a is the adaptation current, $\tau_a > \tau_0$ is its time constant, and J_a measures the strength of adaptation.

An additional assumption for (2.1) is that the stable state of the network is such that all the neurons are far from their saturation level, allowing the gain function F to be in a semilinear form $F(I) = I$ for $I > 0$, and zero otherwise.

The model we analyze in this chapter is based on the above Hansel and Sompolinsky model, but includes a more general nonlinear sigma-shaped gain function F. It can be also used in a more general context of synaptically coupled populations of excitatory and inhibitory neurons with adaptation.

2.1.1 Biological model description

The problem we are interested in, concerns the possible patterns that can be obtained in a neuronal network consisting of both excitatory and inhibitory cells, and in the presence of adaptation.

The network model consists of two homogeneous populations of neurons, one excitatory (E), displaying adaptation, and the other one inhibitory (I), without adaptation. This is a reasonable assumption, for example, for *cortical neurons*, since experimental studies report that in cortex most of the inhibitory neurons do not display spike adaptation ([22], [23], [52]).

The spatial connectivity is assumed to be all-to-all from E to E, E to I, and I to E cells, and in all cases the strength of interactions decreases with the distance between neurons according to a Gaussian distribution with zero mean, say J_{EE}, J_{IE} and J_{EI} respectively. No I to I interactions are included. In addition, the network is considered one-dimensional in space.

We assume in the following a *linear adaptation*, and describe the neuronal activity by a rate

model. That is we have

$$\tau_E \frac{du_E}{dt} = -u_E + F_E(J_{EE} * u_E - J_{EI} * u_I - gA),$$

$$\tau_I \frac{du_I}{dt} = -u_I + F_I(J_{IE} * u_E),$$

$$\tau_A \frac{dA}{dt} = -A + u_E, \tag{2.2}$$

where τ_E, τ_I, τ_A are the time constants for the excitatory and inhibitory neurons, and for adaptation respectively; A is the variable that defines the adaptation; g is the strength of adaptation; F_E and F_I are the firing-rate functions; and $J_{ij} * u_j$, with $i, j \in \{E, I\}$, is the convolution $J_{ij} * u_j(x, t) = \int_{-\infty}^{\infty} J_{ij}(x - y) u_j(y, t) \, dy$.

One simplification is to assume that the inhibition is much faster than the excitation, and that the firing rate for inhibitory population is linear. That allows us to replace the equation for I cells by its steady state, i.e. to take $u_I \approx F_I(J_{IE} * u_E) = J_{IE} * u_E$.

Then, since a convolution of two Gaussians with zero mean is still a Gaussian with zero mean, we have $(J_{EE} * u_E - J_{EI} * u_I)(x, t) = (J_{EE} - J_{EI} * J_{IE}) * u_E(x, t) = J * u_E(x, t)$, where $J(x)$ is a difference of two Gaussians.

Therefore the system (2.2) can be reduced to a rate model for only one variable u in which we include the neuronal activity for both excitatory and inhibitory populations, and with the synaptic coupling defined by a function J as in Figure 2.1a (the "Mexican hat"). This means that we assume to have a network characterized by local excitation and long range (lateral) inhibition.

2.1.2 Mathematical model

Under the assumptions considered in the previous section, the mathematical model equivalent to (2.2) is

$$\frac{\partial u}{\partial t} = -u(x, t) + F(\alpha \, J * u \, (x, t) - g \, v(x, t)),$$

$$\tau \frac{\partial v}{\partial t} = -v(x, t) + u(x, t) \tag{2.3}$$

with $x \in \mathbb{R}$ the one-dimensional spatial coordinate, and α, g and τ positive parameters.

The variables u and v represent the neuronal activity and adaptation respectively, τ and g

correspond to the time constant and the strength of adaptation, and α is a parameter that controls the strength of the synaptic coupling J.

Synaptic coupling J is a continuous and even function, $J(-x) = J(x)$, $\forall x \in \mathbb{R}$, and absolutely integrable on the interval $[-l, l]$ where $l \in \mathbb{R}_+ \cup \{\infty\}$. If $l = \infty$ we ask that $\lim_{x \to -\infty} J(x) = \lim_{x \to \infty} J(x) = 0$. Otherwise, J is assumed to be periodic of period $2l$. Then the operator $J * u$ is defined as

$$J * u\,(x, t) = \int_{-l}^{l} J(x - y)\, u(y, t)\, dy\,. \tag{2.4}$$

There is an operator associated to J, which is defined on the frequency space, and that is

$$\hat{J}(k) = \int_{-l}^{l} J(x)\, e^{ikx}\, dx\,. \tag{2.5}$$

Remark 2.1.   If we consider an infinite neural network, we take $l = \infty$ and the function J is typically as in Figure 2.1a. For example, we can define J as

$$J(x) = \frac{1}{\sqrt{\pi}} \left[A\sqrt{a}\, e^{-ax^2} - B\sqrt{b}\, e^{-bx^2} \right]\,, \quad x \in \mathbb{R} \tag{2.6}$$

where $A \geq B > 0$, $a > b > 0$. Then $\hat{J}(k) = A\, e^{-k^2/4a} - B\, e^{-k^2/4b}$, $k \in \mathbb{R}$ and $\hat{J}$ has the graph as in Figure 2.1b. Nevertheless, in numerical simulations we cannot consider an infinite domain. Therefore we have to restrict ourselves to a finite domain $[-l, l]$ with $l \in \mathbb{R}_+$ and work with periodic boundary conditions. In order to maintain the assumptions of local excitation and long range inhibition, J is typically as in Figure 2.2a. For example, we can take J as

$$J(x) = \frac{1}{2l} \left[a + b \cos\left(\frac{\pi x}{l}\right) + c \cos\left(\frac{2\pi x}{l}\right) \right]\,, \quad x \in \mathbb{R} \tag{2.7}$$

where a, b, c are real parameters. Therefore $\hat{J}$ (see Figure 2.2b) is

$$\hat{J}(0) = a\,, \;\; \hat{J}(\pm \pi/l) = b/2\,, \;\; \hat{J}(\pm 2\pi/l) = c/2\,, \;\; \hat{J}(\pm j\pi/l) = 0 \;\; (j \in \mathbb{N} \setminus \{0, 1, 2\})\,,$$

$$\hat{J}(k) = \frac{\sin(lk)\left[(a - b + c)(lk/\pi)^4 + (-5a + 4b - c)(lk/\pi)^2 + 4a \right]}{lk\left[(lk/\pi)^2 - 1 \right]\left[(lk/\pi)^2 - 4 \right]}\,, \;\; k \notin \pm\frac{\pi}{l}\mathbb{N}\,.$$
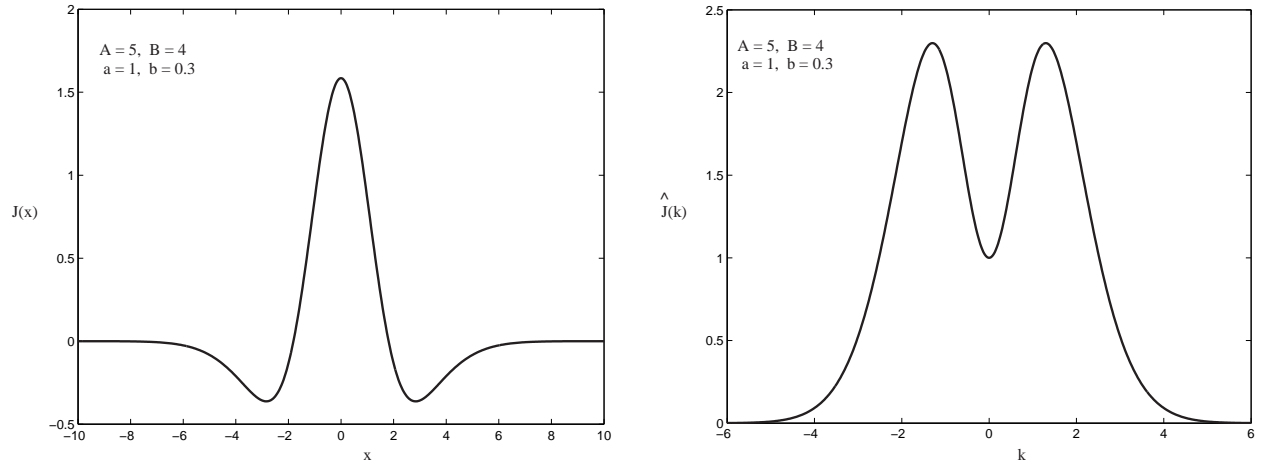
Figure 2.1. (a) The coupling $J(x) = \frac{1}{\sqrt{\pi}} \left[A\sqrt{a}\, e^{-ax^2} - B\sqrt{b}\, e^{-bx^2} \right]$ for $A = 5$, $B = 4$, $a = 1$, $b = 0.3$; (b) The function $\hat{J}$.
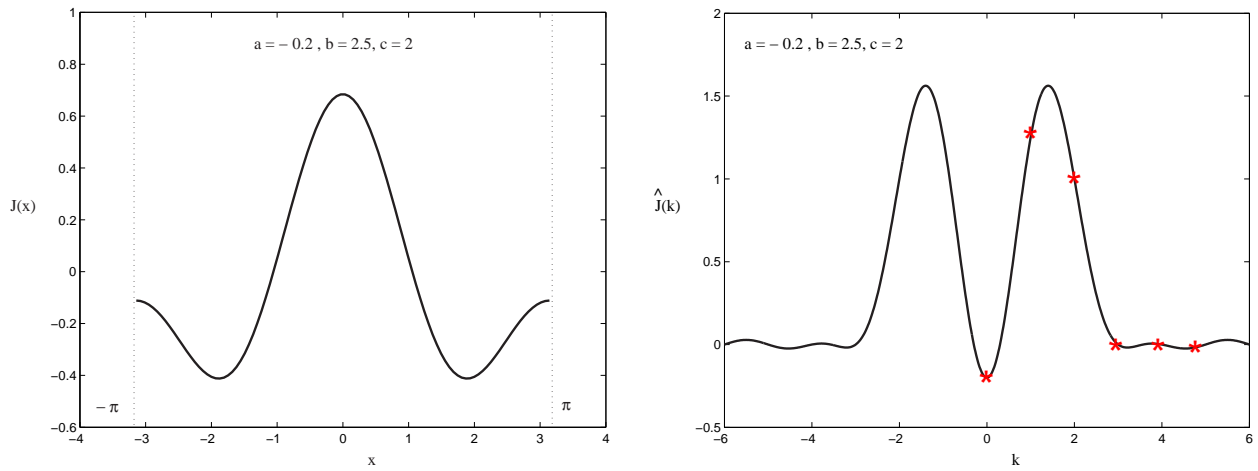
Figure 2.2. (a) The periodic coupling $J(x) = \frac{1}{2l} \left[a + b\cos(\frac{\pi x}{l}) + c\cos(\frac{2\pi x}{l}) \right]$ for $l = \pi$ and $a = -0.2$, $b = 2.5$, $c = 2$; (b) The function $\hat{J}$.
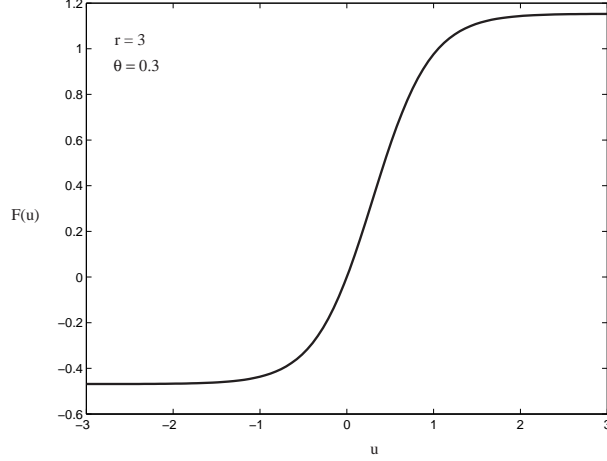
Figure 2.3. The firing rate (2.8) for $r = 3$ and $\theta = 0.3$.

Firing rate F in (2.3) is a sigmoid function (Figure 2.3) assumed to satisfy

$$F(0) = 0, \ F'(0) = 1.$$

The first condition translates the steady state to the origin $\bar{u} = 0$, $\bar{v} = 0$. The second condition brings additional simplifications to our calculations. A typical expression for F is then $F(u) = K\left[\frac{1}{1+e^{-r(u-\theta)}} - \frac{1}{1+e^{r\theta}}\right]$, with r and θ positive parameters, and $K = (1 + e^{r\theta})^2\, e^{-r\theta}/r$, i.e.

$$F(u) = \frac{1 + e^{r\theta}}{r} \cdot \frac{1 - e^{-ru}}{1 + e^{-r(u-\theta)}} . \tag{2.8}$$

Remark 2.2. The condition $F'(0) = 1$ is not essential. As long as $F'(0)$ is nonzero and positive, the results proved in the following sections remain valid. To see this, let us assume that $F'(0) \neq 1$. Then, by the change of variables $u_{\text{new}} = u/F'(0)$, $v_{\text{new}} = v/F'(0)$, the change of parameters $\alpha_{\text{new}} = F'(0)\,\alpha$, $g_{\text{new}} = F'(0)\,g$, and the change of function $F_{\text{new}} = F/F'(0)$ we obtain a system topologically equivalent to (2.3) where F_{new} satisfies the constraints $F_{\text{new}}(0) = 0$ and $F'_{\text{new}}(0) = 1$.

2.1.3 Linear stability analysis and pattern initiation mechanism

Previous studies on reaction diffusion pattern generation mechanisms (see [77] for a review) and neural models of pattern generation (such as a mechanism for stripe formation in the visual cortex

[96], a model for the brain mechanism underlying visual hallucination patterns [37], [39], or a neural activity model for shell patterns [38]) indicate that in one-dimensional structures the linear theory turns out to be a good predictor of the ultimate steady state of the full nonlinear system. There is very good agreement between the theoretical solutions obtained from the linearized problem, and the numerical simulations of the original nonlinear system with initial conditions taken to be small random perturbations about the steady state.

Nevertheless, in order to find the solution of the linearized problem that corresponds to the stable spatial or spatio-temporal pattern that appears when the zero steady state loses stability, nonlinear terms of the original system must be taken into account, and a singular perturbation analysis around a bifurcation point must be pursued.

In the following we investigate the possible spatial and spatio-temporal patterns that can occur in the neuronal system with adaptation (2.3), as a dependence on the parameters α, g and τ.

Based on the hypotheses $F(0) = 0$, $F'(0) = 1$, the expansion of (2.3) in linear and higher order terms becomes

$$\frac{\partial u}{\partial t} = -u + (\alpha J * u - gv) + \frac{F''(0)}{2}(\alpha J * u - gv)^2 + \frac{F'''(0)}{6}(\alpha J * u - gv)^3 + \dots,$$
$$\frac{\partial v}{\partial t} = (-v + u)/\tau, \tag{2.9}$$

and then the linear operator is

$$L_0 U = \frac{\partial}{\partial t} U - \begin{pmatrix} -1 + \alpha J * (\cdot) & -g \\ 1/\tau & -1/\tau \end{pmatrix} U \tag{2.10}$$

where $U = (u, v)^T$. We are looking for solutions of $L_0 U = \mathbf{0}$ that are bounded and have the form $\xi(t) e^{ikx}$ with $k \in \mathbb{R}$.

Let us assume first that $l = \infty$. Then, according to (2.4) and (2.5), the equation (2.10) can be written as $\left[\frac{d\xi}{dt} - \hat{L}(k)\xi(t)\right] e^{ikx} = \mathbf{0}$ where

$$\hat{L}(k) = \begin{pmatrix} -1 + \alpha\hat{J}(k) & -g \\ 1/\tau & -1/\tau \end{pmatrix}. \tag{2.11}$$

30

Since we work on an infinite domain ($l = \infty$) and J is symmetric, this statement is true for all values of $k \in \mathbb{R}$. Moreover, we have $\hat{J}(-k) = \hat{J}(k)$.

The equation to be solved now is the ODE $\frac{d\xi}{dt} = \hat{L}(k)\xi$ which has two independent solutions $\xi_{1k} e^{\lambda_{1k}t}$, $\xi_{2k} e^{\lambda_{2k}t}$ where $\xi_{1,2\,k}$ are two-dimensional complex vectors. Therefore the eigenfunctions of L_0 have the form $\xi_{1,2\,k} e^{\lambda_{1,2\,k}t \pm ikx}$ and $\overline{\xi}_{1,2\,k} e^{\overline{\lambda}_{1,2\,k}t \mp ikx}$, where $\lambda_{1,2\,k}$ are the eigenvalues defined by $\lambda_{1,2\,k} = \frac{1}{2}\left[Tr(\hat{L}(k)) \pm \sqrt{Tr(\hat{L}(k))^2 - 4\,det(\hat{L}(k))} \right]$.

If $det(\hat{L}(k)) > 0$ and $Tr(\hat{L}(k)) < 0$ for all k, i.e. $\alpha\,\hat{J}(k) < g + 1$ and $\alpha\,\hat{J}(k) < 1/\tau + 1$, then all eigenfunctions of L_0 correspond to the stable manifold , and they decay exponentially in time to zero. The trivial solution is asymptotically stable.

Remark 2.3. The eigenvalues k represent a measure of the wave-like pattern that can occur in the system. That is why k are called *wavenumbers*, or *modes* of the system, and $2\pi/k$ are called *wavelengths*.

We consider k_0 to be *the most unstable mode*, defined as

$$\hat{J}(k_0) = \max_{k \geq 0}\hat{J}(k) = \max_{k \geq 0}\left(\int_{-\infty}^{\infty} J(x)\, e^{ikx}\, dx \right) \tag{2.12}$$

and assume that

$$k_0 \neq 0 \quad \text{and} \quad \hat{J}(k_0) > 0\,, \tag{2.13}$$

$$\hat{J}(k_0) \neq \hat{J}(k)\,, \forall k \neq \pm k_0\,. \tag{2.14}$$

This is true for functions J as in Figure 2.1.

There are only two ways the trivial solution can lose its stability: either when the determinant, or the trace becomes zero. We notice that (2.12), with additional conditions (2.13), (2.14), implies that $Tr(\hat{L}(k)) < Tr(\hat{L}(k_0))$ and $det(\hat{L}(k)) > det(\hat{L}(k_0))$ for $k \neq \pm k_0$. Therefore k_0 is the first eigenvalue where the system may lose its stability, that is k_0 is the most unstable mode of the system (2.3). For all $k \neq \pm k_0$ the eigenfunctions belong to the stable manifold. On the other hand, the eigenfunctions with $\pm k_0$ wavenumber may form a basis for the center manifold that becomes our point of interest.

The wavenumber k_0 determines then the mechanism that generates the emerged pattern. There are basically two possible cases. At $\alpha\,\hat{J}(k_0) = g + 1$, $g < 1/\tau$ the determinant becomes zero and a

spatial pattern (steady state SS) bifurcates. At $\alpha \hat{J}(k_0) = 1 + 1/\tau$, $g > 1/\tau$ the trace becomes zero and a spatio-temporal pattern (traveling wave TW /standing wave SW) bifurcates.

Let us assume now that l is finite There is a considerable difference when working with finite domains as the interval $[-l, l]$ and periodic boundary conditions. The difference comes from the fact that in this case there is only a discrete set of possible wavenumbers. The wavenumbers k must satisfy the condition $k \in \left(\pm \frac{\pi}{l}\mathbb{N}\right)$ in order for the integral $\int_{-l}^{l} J(x-y)\, e^{ik(x-y)}\, dy$ to be independent of x and so equal to $\hat{J}(k) = \int_{-l}^{l} J(y)\, e^{iky}\, dy$.

This allows us to use the matrix $\hat{L}(k)$ from (2.11) and construct the eigenvalues and eigenfunctions of the linear operator as in the case of infinite domain. Moreover, the discussion from the previous paragraph remains valid here with the observation that in the case of l finite we consider *only* those values of k belonging to the set $\left(\pm \frac{\pi}{l}\mathbb{N}\right)$.

The most unstable mode k_0 is then defined as

$$\hat{J}(k_0) = \hat{J}\left(\frac{\pi n_0}{l}\right) = \max_{k \in \frac{\pi \mathbb{N}}{l}} \left(\int_{-l}^{l} J(x)\, e^{ikx}\, dx\right) \tag{2.15}$$

and we assume again that $k_0 \neq 0$ and $\hat{J}(k_0) > 0$, $\hat{J}(k_0) \neq \hat{J}(k)$, $\forall k = \pm \pi n/l$, $n \in \mathbb{N}$ such that $n \neq n_0$. This is true for functions J as in Figure 2.2.

Remark 2.4. In the next sections we analyze the case of spatial and spatio-temporal patterns that occur in the system when at the most unstable mode $k_0 \neq 0$ either the trace $Tr(\hat{L}(k_0))$ becomes zero, or *both* the trace $Tr(\hat{L}(k_0))$ and the determinant $det(\hat{L}(k_0))$ become zero.

2.2 Spatio-temporal patterns obtained by a loss of stability at a pure imaginary pair of eigenvalues

In the case of $Tr(\hat{L}(k_0)) = 0$ and $det(\hat{L}(k_0)) > 0$, at the most unstable mode k_0 defined by (2.12), or (2.15), with conditions (2.13), (2.14), the eigenvalues of the associated ODE $\frac{d\xi}{dt} = \hat{L}(k_0)\xi$ are complex with zero real part. This happens when the parameters of the system (2.3) satisfy

$$g > 1/\tau \quad \text{and} \quad \alpha^* = \frac{1 + 1/\tau}{\hat{J}(k_0)}. \tag{2.16}$$

Remark 2.5. In the following we fix the values of τ and g as above, and take α as the bifurcation parameter. The bifurcation value around which we will consider the singular perturbation analysis is α^*. Therefore on the entire Section 2.2, the operator L_0 defined by (2.10), and the matrix $\hat{L}(k)$ defined by (2.11) for all k where it makes sense, will be evaluated at $\alpha = \alpha^*$.

The matrix $\hat{L}(k_0)$ has pure imaginary eigenvalues $\pm i\omega_0$ with corresponding eigenvectors Φ_0 and $\overline{\Phi}_0$ such that

$$\omega_0 = \frac{1}{\tau}\sqrt{g\tau - 1}\,, \tag{2.17}$$

$$\hat{L}(k_0)\Phi_0 = i\omega_0\Phi_0 \quad \text{with} \quad \Phi_0 = \left(\phi\,,\ \frac{\phi}{1 + i\sqrt{g\tau - 1}}\right)^T. \tag{2.18}$$

Based on the general theory [37], in the case of a pair of pure imaginary eigenvalues that arises at the most unstable mode k_0, the solution U of the nonlinear system (2.3) can be approximated by

$$U(x,t) \approx 2\mathrm{Re}\left[z(t)\,\Phi_0\,e^{i(\omega_0 t + k_0 x)} + w(t)\,\Phi_0\,e^{i(\omega_0 t - k_0 x)}\right], \tag{2.19}$$

where z, w are time-dependent functions that satisfy the ODE system

$$\begin{cases} z' = z(a + bz\overline{z} + cw\overline{w})\,, \\ w' = w(a + bw\overline{w} + cz\overline{z})\,, \end{cases} \tag{2.20}$$

called *the normal form for the Turing-Hopf bifurcation* in the time-and-space-variable case, with $a = a_1 + ia_2$, $b = b_1 + ib_2$, $c = c_1 + ic_2$ complex coefficients.

The importance of the normal form becomes apparent when we write it in polar coordinates. It provide us with essential information about the existence and stability of the (new) bifurcating solutions. We notice that actually only the sign and values of the real part a_1, b_1, c_1 of the coefficients a, b and c play a role in the matter.

In that sense let us define $z(t) = re^{i\theta_1}$ and $w(t) = Re^{i\theta_2}$. Then (2.20) is equivalent to the system $r' = r[a_1 + b_1 r^2 + c_1 R^2]$, $R' = R[a_1 + b_1 R^2 + c_1 r^2]$, $\theta_1' = a_2 + b_2 r^2 + c_2 R^2$, $\theta_2' = a_2 + b_2 R^2 + c_2 r^2$, and the normal form is basically reduced to

$$r' = r\left[a_1 + b_1 r^2 + c_1 R^2\right], \quad R' = R\left[a_1 + b_1 R^2 + c_1 r^2\right]. \tag{2.21}$$

33

There are two distinct qualitative pictures of small amplitude bifurcating patterns in a system with normal form (2.20), and so (2.21), as long as $-a_1/b_1 < 0$ and $-a_1/(b_1 + c_1) < 0$ (Ermentrout B. [37]).

One corresponds to the solution $\tilde{r} = 0, \tilde{R} = \sqrt{-a_1/b_1}$ of (2.21) (or $\tilde{R} = 0, \tilde{r} = \sqrt{-a_1/b_1}$), and it represents a traveling periodic wave train with velocity $c = \pm\omega_0/k_0$ (''traveling wave''). This can be understood easily by using the formula (2.19): up to a translation in time, an approximation of the solution $U(x,t)$ is then $2\sqrt{-a_1/b_1}\mathrm{Re}\left[\Phi_0\, e^{i(\omega_0 t \pm k_0 x)}\right] = 2\sqrt{-a_1/b_1}\mathrm{Re}\left[\Phi_0\, e^{\mp i k_0(ct-x)}\right]$. Therefore the pattern will change with time and position in space, according to the traveling wave coordinate $\xi = ct - x$ (see for an example Figure 2.6).

The other case corresponds to the solution $\tilde{r} = \tilde{R} = \sqrt{-a_1/(b_1 + c_1)}$, and it represents a standing oscillation, periodic in space with spatial frequency k_0, and periodic in time with temporal frequency ω_0 (''standing wave''). The approximating solution of $U(x,t)$ (up to a translation in time) is now $4\sqrt{-a_1/(b_1 + c_1)}\mathrm{Re}\left[\Phi_0\, e^{i\omega_0 t}\right]\cos(k_0 x)$, and the pattern consists of oscillations with respect to the position x in space, for any fixed time t, respectively in oscillations with respect to time at any fixed position x (see for an example Figure 2.5).

They cannot be simultaneously stable, therefore physically only one of these patterns is selected ([37], [35], [39]). The traveling wave solution TW has the corresponding eigenvalues $\lambda_1 = -2a_1$, $\lambda_2 = -\frac{a_1(c_1-b_1)}{b_1}$ with eigenvectors $(1,0)^T$, $(0,1)^T$. Therefore *the traveling wave exists and it is stable* if and only if $a_1 > 0$, $b_1 < 0$ and $c_1 - b_1 < 0$. The standing wave solution SW has the corresponding eigenvalues $\lambda_1 = -2a_1$, $\lambda_2 = -\frac{2a_1(b_1-c_1)}{b_1+c_1}$ with eigenvectors $(1,1)^T$ and $(1,-1)^T$. Therefore *the standing wave exists and it is stable* if and only if $a_1 > 0$, $b_1 + c_1 < 0$ and $c_1 - b_1 > 0$.

Since the goal of our study is to investigate the existence of stable TW and/or SW patterns in the neural network (2.3), we have to construct the normal form for the Hopf bifurcation case. More precisely, according to the general theory summarized above, we have to determine the coefficients a, b and c in (2.20), and then, their real part.

2.2.1 Hopf bifurcation and pattern formation

The construction of the normal form uses a singular perturbation approach with a proper scaling of the variables, parameters, and time with respect to ϵ, the small pertubation quantity. The Fredholm alternative method is then used to identify solutions for the functional equations

obtained from the ϵ-power series expansion.

In the case of a pair of pure imaginary eigenvalues, a good scaling for the bifurcation parameter α and the solution U we are seeking, is

$$\alpha - \alpha^* = \epsilon^2\, \gamma\,,\ \gamma \in \mathbb{R}\,,$$

$$U(x,t) = \epsilon\, U_0(x,t) + \epsilon^2\, U_1(x,t) + \epsilon^3\, U_2(x,t) + \cdots = \epsilon \begin{pmatrix} u_0 \\ v_0 \end{pmatrix} + \epsilon^2 \begin{pmatrix} u_1 \\ v_1 \end{pmatrix} + \epsilon^3 \begin{pmatrix} u_2 \\ v_2 \end{pmatrix} + \cdots\,.$$

$$(2.22)$$

The system (2.9) can be written in the equivalent form

$$L_0 U = (\alpha - \alpha^*)\,(J * u\,,\ 0)^T + B(U,U) + C(U,U,U) + \ldots \tag{2.23}$$

with $B(U,U) = \left(\frac{F''(0)}{2}(\alpha\, J * u - gv)^2\,,\ 0 \right)^T$ and $C(U,U,U) = \left(\frac{F'''(0)}{6}(\alpha\, J * u - gv)^3\,,\ 0 \right)^T$.

With the notation $\boldsymbol{E} = (1,0)^T$, (2.22) and (2.23) imply

$$\epsilon L_0 U_0 + \epsilon^2 L_0 U_1 + \epsilon^3 L_0 U_2 + \mathcal{O}(\epsilon^4) = \epsilon^2 \boldsymbol{E}\, \frac{F''(0)}{2}[\alpha^* J * u_0 - gv_0]^2 + \epsilon^3 \boldsymbol{E}\left[\gamma\,(J * u_0) \right.$$

$$\left. + F''(0)[\alpha^* J * u_0 - gv_0][\alpha^* J * u_1 - gv_1] + \frac{F'''(0)}{6}[\alpha^* J * u_0 - gv_0]^3 \right] + \mathcal{O}(\epsilon^4)\,. \tag{2.24}$$

Remark 2.6. The calculation of the normal form is cumbersome. For this reason we prefer to present in this section only the main steps and results, and to leave the details of proofs for Appendices B.0.1 and B.0.2.

The first equation to be solved is $L_0 U_0 = \boldsymbol{0}$. The nullspace of L_0 corresponding to the center manifold is four-dimensional and it has the basis $\left\{\ \Phi_0\, e^{i(\omega_0 t \pm k_0 x)}, \overline{\Phi}_0\, e^{-i(\omega_0 t \pm k_0 x)}\right\}$, therefore U_0 can be written as

$$U_0 = z\,\Phi_0\, e^{i(\omega_0 t + k_0 x)} + w\,\Phi_0\, e^{i(\omega_0 t - k_0 x)} + \overline{z}\,\overline{\Phi}_0\, e^{-i(\omega_0 t + k_0 x)} + \overline{w}\,\overline{\Phi}_0\, e^{-i(\omega_0 t - k_0 x)}\,.$$

Since in (2.24), $L_0 U_0 = \mathcal{O}(\epsilon)$, we have z and w as ϵ-dependent. By considering $z = z(\epsilon^2 t)$ and $w = w(\epsilon^2 t)$ and expanding them as $z = z(0) + z'(0)\epsilon^2 t + \mathcal{O}(\epsilon^4)$ and $w = w(0) + w'(0)\epsilon^2 t + \mathcal{O}(\epsilon^4)$ as

$\epsilon \to 0$, we then obtain

$$U_0 = \left[z(0)\, \Phi_0\, e^{i(\omega_0 t + k_0 x)} + w(0)\, \Phi_0\, e^{i(\omega_0 t - k_0 x)} + \overline{z}(0)\, \overline{\Phi}_0\, e^{-i(\omega_0 t + k_0 x)} + \overline{w}(0)\, \overline{\Phi}_0\, e^{-i(\omega_0 t - k_0 x)} \right] + \mathcal{O}(\epsilon^2)\,.$$

The equation that defines U_1 is

$$L_0 U_1 = \left\{ \left[A^2 z(0)^2\, e^{2i(\omega_0 t + k_0 x)} + A^2 w(0)^2\, e^{2i(\omega_0 t - k_0 x)} + 2A^2 z(0) w(0)\, e^{2i\,\omega_0 t} + cc \right] \right.$$
$$\left. + 2A\,\overline{A}\left[z(0)\overline{z}(0) + w(0)\overline{w}(0) + z(0)\overline{w}(0)\, e^{2ik_0 x} + \overline{z}(0)w(0)\, e^{-2ik_0 x} \right] \right\} \frac{F''(0)}{2} E\,,$$

where cc denotes the complex conjugation of the previous expression, and

$$A = \Phi_0^T \cdot (1 + 1/\tau\,,\ -g) = \phi\,(1 + i\omega_0)\,. \tag{2.25}$$

Therefore U_1 can be constructed as

$$U_1 = \left(\xi_1\, z^2\, e^{2i(\omega_0 t + k_0 x)} + \xi_2\, w^2\, e^{2i(\omega_0 t - k_0 x)} + \xi_3\, z\, w\, e^{2i\omega_0 t} + \xi_4\, z\, \overline{w}\, e^{2ik_0 x} + cc \right) + \xi_5\, z\, \overline{z} + \xi_6\, w\, \overline{w}$$

with ξ_i, $i = 1,\dots,6$, vectors in $\mathbb{C}^2$ that depend on g, τ, $\hat{J}(k_0)$, $\hat{J}(0)$, $\hat{J}(2k_0)$, and $F''(0)$. With the use of formula (B.15), we then obtain the equation for U_2

$$L_0 U_2 = Q_{(1)} E - \left(z'(0)\, \Phi_0\, e^{i(\omega_0 t + k_0 x)} + w'(0)\, \Phi_0\, e^{i(\omega_0 t - k_0 x)} + cc \right)\,,$$

that provides the explicit normal form for the Hopf bifurcation

$$\begin{cases} z'(0) = z(0)\left(\tilde{a} + b\, z(0)\overline{z}(0) + c\, w(0)\overline{w}(0) \right)\,, \\[2mm] w'(0) = w(0)\left(\tilde{a} + b\, w(0)\overline{w}(0) + c\, z(0)\overline{z}(0) \right)\,, \end{cases} \tag{2.26}$$

where the time variable is $\epsilon^2 t$, and $\tilde{a} = a/\epsilon^2$, with a, b, c of order 1 (see Appendix B.0.1). We proved then the following result.

Proposition 2.2.1. *If $g > 1/\tau$, in the neighborhood of the bifurcation value $\alpha^* = \frac{1 + 1/\tau}{\hat{J}(k_0)}$, the system (2.3) has the normal form (2.20) with $a_1 = Re(a) = \frac{1}{2}\left[\alpha\, \hat{J}(k_0) - (1 + \frac{1}{\tau}) \right]$, and $b_1 = Re(b)$,*

$c_1 = Re(c)$ *satisfying the equations*

$$b_1 = \frac{\tau + 1}{4\tau}|A|^2 \left[F'''(0) + F''(0)^2 \cdot \left(-3 + \frac{2}{g + 1 - \frac{(1+1/\tau)\hat{J}(0)}{\hat{J}(k_0)}} + \frac{M_B}{N_B} \right) \right], \qquad (2.27)$$

$$c_1 + b_1 = \frac{\tau + 1}{4\tau}|A|^2 \cdot \left[3\left[F'''(0) - 3F''(0)^2 \right] \right.$$

$$\left. + F''(0)^2 \cdot \left(\frac{2}{g + 1 - \frac{(1+1/\tau)\hat{J}(2k_0)}{\hat{J}(k_0)}} + \frac{4}{g + 1 - \frac{(1+1/\tau)\hat{J}(0)}{\hat{J}(k_0)}} + 2\frac{M_C}{N_C} + \frac{M_B}{N_B} \right) \right], \qquad (2.28)$$

$$c_1 - b_1 = \frac{\tau + 1}{4\tau}|A|^2 \cdot \left[\left[F'''(0) - 3F''(0)^2 \right] + F''(0)^2 \cdot \left(\frac{2}{g + 1 - \frac{(1+1/\tau)\hat{J}(2k_0)}{\hat{J}(k_0)}} + 2\frac{M_C}{N_C} - \frac{M_B}{N_B} \right) \right].$$

$$(2.29)$$

Here we have $M_B = M\left(\frac{\hat{J}(2k_0)}{\hat{J}(k_0)} \right)$, $M_C = M\left(\frac{\hat{J}(0)}{\hat{J}(k_0)} \right)$, $N_B = N\left(\frac{\hat{J}(2k_0)}{\hat{J}(k_0)} \right)$, $N_C = N\left(\frac{\hat{J}(0)}{\hat{J}(k_0)} \right)$, *where* M *and* N *are functions defined as*

$$M(X) = (4g\tau - 3)[2g\tau - (\tau + 1)(\tau + 2)]X + 4(g\tau - 1)(\tau + 1)^2 + (3g\tau - 4 - \tau)^2 + g\tau(g\tau + \tau - 2),$$

and

$$N(X) = (4g\tau - 3)(\tau + 1)^2 X^2 + 2\tau(\tau + 1)(3 - g - 4g\tau)X + [4(g\tau - 1)(\tau + 1)^2 + (3g\tau - 4 - \tau)^2].$$

Proof: The normal form (2.20) is obtained directly from (2.26) as a result of the scaling $\epsilon z(0) \leftrightarrow z$, $\epsilon w(0) \leftrightarrow w$, and $\epsilon^2 t \leftrightarrow t$.

2.2.2 Traveling wave and standing wave patterns in the neural system

Based on the formulas (2.27), (2.28), (2.29) from Proposition 2.2.1 we obtain the first important result regarding the type of patterns that can be selected by the neural system (2.3).

Theorem 2.1. *Let us assume that the most unstable mode k_0 of the system (2.3) satisfies the conditions (2.13), (2.14), and at k_0 a pair of pure imaginary eigenvalues appears.*

If the firing rate function F is such that $F(0) = 0$, $F'(0) > 0$, $F''(0) = 0$, and $F'''(0) < 0$, then the system (2.3) has a traveling wave (TW) and a standing wave (SW) solution for $\alpha > \alpha^*$, α close to α^*. The SW solution is unstable. The TW solution is stable.

Proof: First we notice that there exist sigmoid functions F that satisfy the theorem hypotheses.

For example, if $\theta = 0$, we have from (2.8), $F(u) = \frac{2}{r} \tanh\left(\frac{ru}{2}\right)$ and so $F(0) = 0$, $F'(0) = 1$, $F''(0) = 0$, $F'''(0) = -\frac{r^2}{2} < 0$.

In this case $b_1 = \frac{\tau+1}{4\tau}|A|^2 F'''(0) < 0$, $c_1 = 2b_1$, and therefore $c_1 + b_1 < 0$ and $c_1 - b_1 < 0$. Both standing and traveling waves bifurcate from the trivial solution at $\alpha = \alpha^*$, but only the TW is stable.

Remark 2.7. The condition $F''(0) = 0$ on the firing rate function is quite restrictive. We are interested to see what happens in the general case of $F''(0) \neq 0$ (then the firing rate function F as in (2.8) has the second and third derivatives $F''(0) = r \frac{1-e^{-r\theta}}{1+e^{-r\theta}}$, $F'''(0) = \frac{r^2\left(e^{-2r\theta} - 4e^{-r\theta} + 1\right)}{(1+e^{-r\theta})^2}$). In that sense, the coefficients of the normal form (2.20) computed in the previous section provide us with some useful information. They have indeed a complicated expression that does not allow us to give a general, theoretical prediction. Nevertheless we can use the equations (2.27), (2.28), (2.29) in Matlab, for example, to search for possible parameter values of g, τ, r, θ, plus coupling J, such that the stable pattern *selected* in the bifurcation at α^* is SW. The importance of the construction of the normal form (2.20) becomes clear, since this allows us to show that *both* traveling wave *and* standing wave patterns can be found in the neural system (2.3).

Proposition 2.2.2. *Let us assume that the hypotheses in Proposition 2.2.1 are true.*

i) If $b_1 < 0$ and $c_1 - b_1 < 0$, then for $\alpha > \alpha^*$, sufficiently close to α^*, the system (2.3) has a traveling wave solution TW that is stable. The velocity of the TW is approximately $\left(\pm\frac{\sqrt{g\tau-1}}{\tau k_0}\right)$, and the solution can be approximated by

$$U(x,t) \approx \sqrt{\frac{2\hat{J}(k_0)(\alpha - \alpha^*)}{(-b_1)}} \, Re\left[\Phi_0 e^{i(\omega_0 t \pm k_0 x)}\right]$$

with Φ_0 and ω_0 defined by (2.17) and (2.18).

ii) If $c_1 + b_1 < 0$ and $c_1 - b_1 > 0$, then for $\alpha > \alpha^*$, sufficiently close to α^*, the system (2.3) has a standing wave solution SW that is stable. The solution can be approximated by

$$U(x,t) \approx 2\cos(k_0 x)\sqrt{\frac{2\hat{J}(k_0)(\alpha - \alpha^*)}{(-b_1 - c_1)}} \, Re\left[\Phi_0 e^{i\omega_0 t}\right].$$

Proof: The solution U can be approximated by its projection onto the eigenvectors space, i.e. $U \approx 2\epsilon \, Re\left[z(0) \Phi_0 e^{i(\omega_0 t + k_0 x)} + w(0) \Phi_0 e^{i(\omega_0 t - k_0 x)}\right]$, where as we mentioned above $\epsilon z(0) \leftrightarrow z$ and

$\epsilon w(0) \leftrightarrow w$. Therefore (2.19) results immediately.

When the TW exists, $z = \tilde{r}e^{i\theta_1} = 0$ and $w = \tilde{R}e^{i\theta_2}$, $\tilde{R} = \sqrt{-a_1/b_1}$ and $\theta_2(t) = -t(\alpha - \alpha^*)\frac{\hat{J}(k_0)}{2}[\frac{1}{\sqrt{g\tau-1}} + \frac{b_2}{b_1}]$. Since we have $\omega_0 t + \theta_2(t) \approx \omega_0 t$ at $\alpha \to \alpha^*$, we obtain the conclusion (i).

In a similar manner one can show that when SW exists, we use in (2.19) $z = w = \tilde{r}e^{i\theta_1} = \tilde{R}e^{i\theta_2}$ with $\tilde{r} = \tilde{R} = \sqrt{-a_1/(b_1 + c_1)}$ and $\theta_1(t) = \theta_2(t) = -t(\alpha - \alpha^*)\frac{\hat{J}(k_0)}{2}[\frac{1}{\sqrt{g\tau-1}} + \frac{b_2+c_2}{b_1+c_1}]$. The conclusion (ii) follows immediately.

Example. If we consider an infinite domain ($l = \infty$), the synaptic coupling J is defined by (2.6) with a graph as in Figure 2.1. For example for $A = 5$, $B = 4$, $a = 1$, $b = 0.3$ we have $k_0 = 1.2967$, $\hat{J}(0) = 1$, $\hat{J}(k_0) = 2.2988$, $\hat{J}(2k_0) = 0.9158$, and at $\tau = 4$ we obtain $\alpha^* = 0.5438$. We choose the function F as in (2.8) with $r = 3$ and $\theta = 0.3$. The theory predicts that there exist values of g such that the stable pattern in the neural network (2.3) that occurs through the Hopf bifurcation is the TW, and there exist values of g such that the SW pattern is stable. For example, at $g = 0.34$, both TW and SW bifurcate, but only SW is stable ($b_1 = -0.0651$, $c_1 + b_1 = -0.0955$, $c_1 - b_1 = 0.0347$). On the other hand at $g = 0.35$, both TW and SW bifurcate, but only TW is stable ($b_1 = -0.1283$, $c_1 + b_1 = -0.2873$, $c_1 - b_1 = -0.0306$).

2.2.3 Numerical results

A good agreement is obtained between the theoretical prediction (based on the normal form construction), and the numerical simulation of the full nonlinear system (2.3).

For numerical simulations we need to consider a finite domain together with periodic boundary conditions. The synaptic coupling J is defined by (2.7) with a graph as in Figure 2.2, and there is only a discrete set of wavenumbers. We choose the gain function F as in (2.8) with $r = 3$ and $\theta = 0.3$, or $\theta = 0$, and $l = \pi$ and $a = -0.2$, $b = 2.5$, $c = 2$ in J. Then $k_0 = 1$, $\hat{J}(0) = -0.2$, $\hat{J}(k_0) = 1.25$, $\hat{J}(2k_0) = 1$, and at $\tau = 4$ we obtain $\alpha^* = 1$. The simulations for the system (2.3) were run in Xppaut [32], [36] on a network of 100 neurons, with the method of integration Runge-Kutta RK4 and step size $dt = 0.25$.

At $\theta = 0.3$, the theory predicts that, for example, at $g = 0.45$, both TW and SW bifurcate, but only SW is stable ($b_1 = -3.4412$, $c_1 + b_1 = -5.1928$, $c_1 - b_1 = 1.6895$). At $g = 0.7$, both TW and SW bifurcate, but only TW is stable ($b_1 = -3.1939$, $c_1 + b_1 = -7.7540$, $c_1 - b_1 = -1.3661$).

At $\theta = 0$, for any $g > 1/\tau = 0.25$, we can obtain both SW and TW solutions, but the stable pattern is always TW.

These results are confirmed by the numerical simulations of the full model (2.3).

Remark 2.8. In the figures below we represent the space x on the horizontal axis, the time t on the vertical axis, and the value of the variable $u(x,t)$ by the level of color. The upper left corner corresponds to the minum value of x that increases to the right. The value of time increases in the up-to-down direction. In general, the time is represented after $t = 3000$ transients. We choose two different sets of initial conditions to illustrate the possible behaviors in the system (2.3).

Let us consider first the case $\theta = 0.3$.

For different values of the parameter g, e.g. $g = 0.45$ and $g = 0.7$, before the bifurcation point, at $\alpha = 0.99$, by choosing random initial conditions around the origin, the solution decays in time to zero. After the bifurcation point, at $\alpha = 1.01$, both traveling and standing waves patterns can be obtained, depending on the choice of the initial conditions. In order to test what pattern is stable, we have also run the simulations of the system (2.3) in the presence of white noise add to the first equation and scaled by a factor of 0.001 (Figure 2.4(b)-Figure 2.7(b))

As a consequence we notice that at $g = 0.45$, the stable pattern is SW (Figure 2.4, Figure 2.5), and at $g = 0.7$ the stable pattern is TW (Figure 2.6, Figure 2.7). This means that for both sets of initial conditions that in the absence of noise might produce different patterns, we obtain *the same pattern in the presence of noise*, that is SW at $g = 0.45$, respectively TW at $g = 0.7$.

At $\theta = 0$ the stable pattern obtained as a result af added noise is always TW. We present the numerical results in Figure 2.8 and Figure 2.9 for $g = 0.45$, respectively 2.10 and Figure 2.11 for $g = 0.7$.
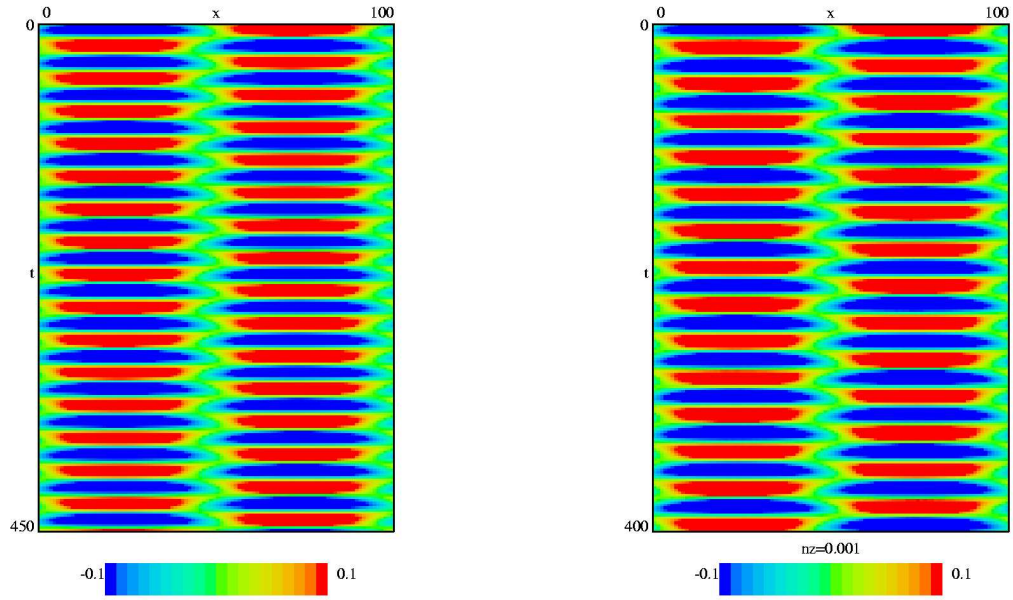
Figure 2.4. (a) SW is the pattern obtained at $g = 0.45$, $\theta = 0.3$, and set 1 of initial conditions; (b) in the presence of noise SW is preserved.
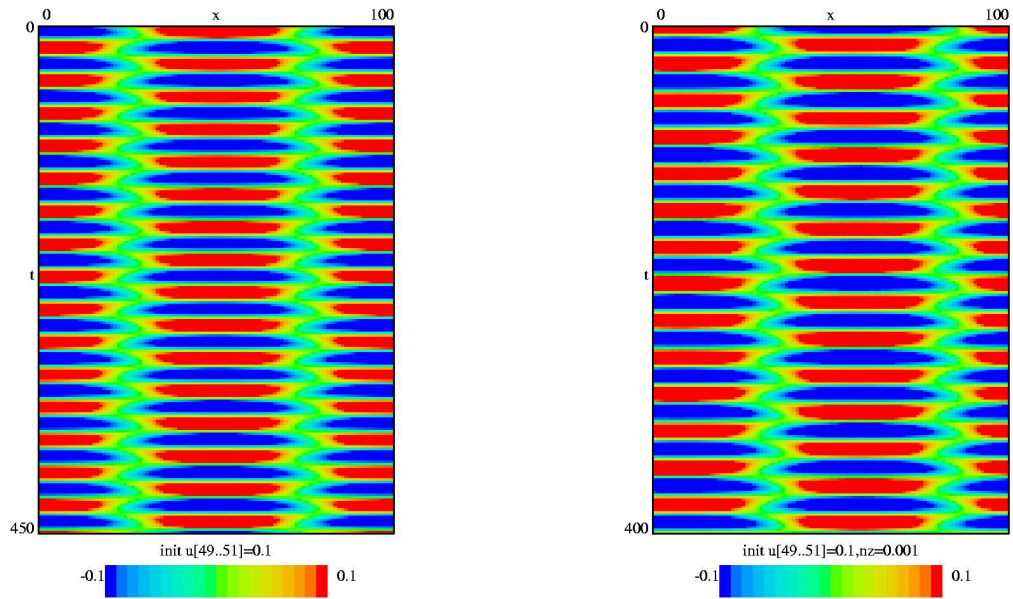
Figure 2.5. (a) SW is the pattern obtained at $g = 0.45$, $\theta = 0.3$, and set 2 of initial conditions and it is stable since (b) in the presence of noise SW is preserved.
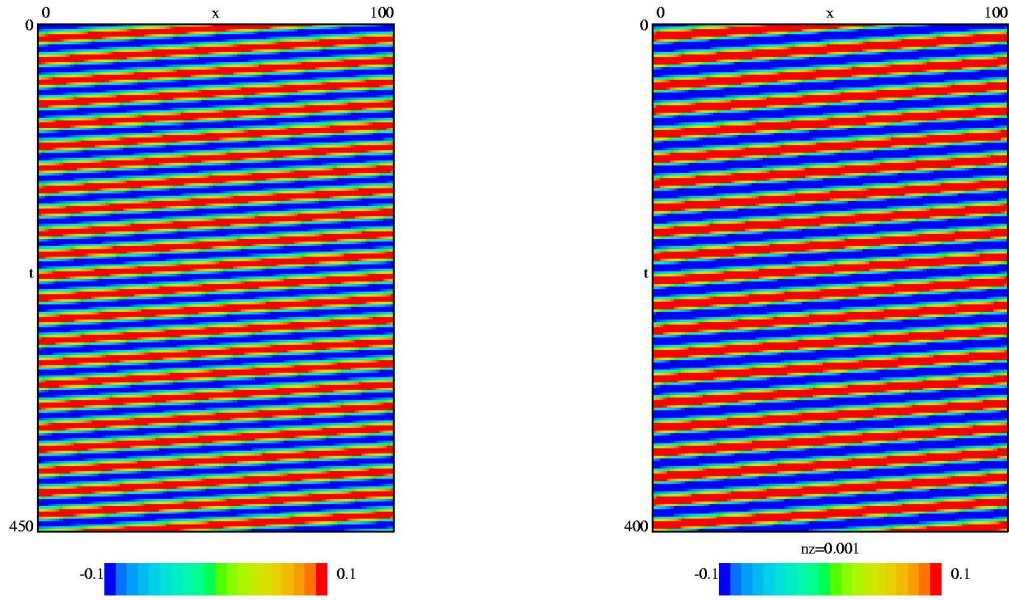
Figure 2.6. (a) TW is the pattern obtained at $g = 0.7$, $\theta = 0.3$, and set 1 of initial conditions; (b) in the presence of noise TW is preserved.
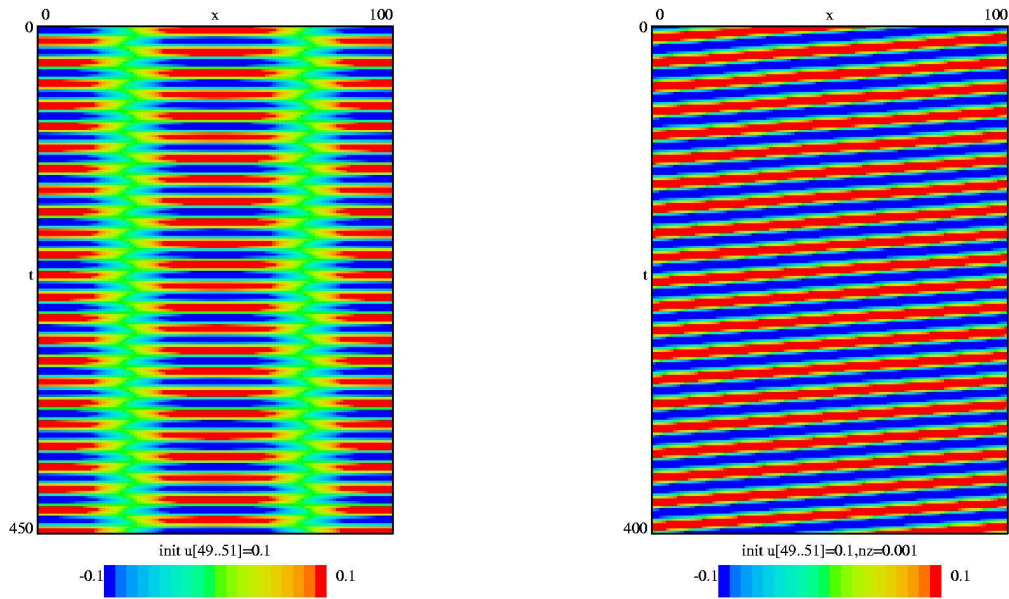
Figure 2.7. (a) SW is the pattern obtained at $g = 0.7$, $\theta = 0.3$, and set 2 of initial conditions but it is unstable since (b) in the presence of noise SW is replaced by TW.
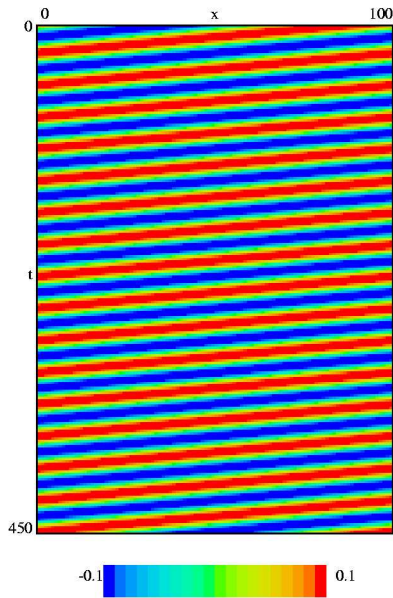
Figure 2.8. TW is the pattern obtained at $g = 0.45$, $\theta = 0$, and set 1 of initial conditions.
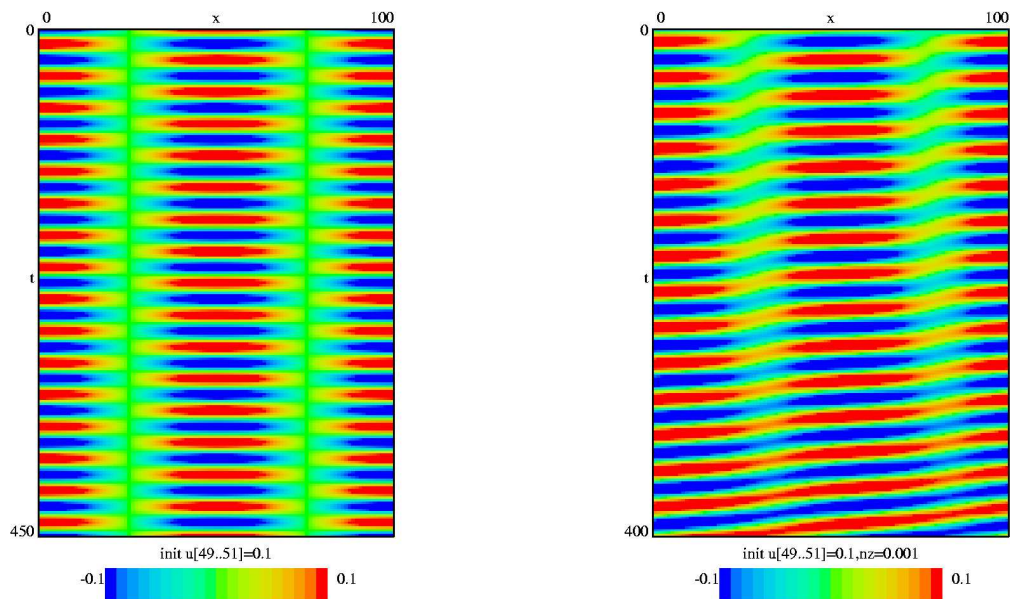
Figure 2.9. (a) SW is the pattern obtained at $g = 0.45$, $\theta = 0$, and set 2 of initial conditions and it is unstable since (b) in the presence of noise SW is replaced by TW.

43
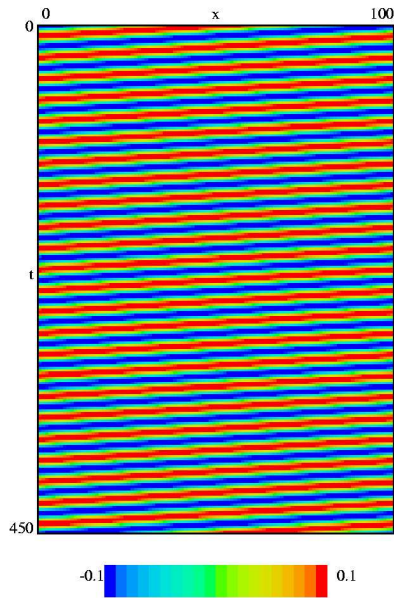
Figure 2.10. TW is the pattern obtained at $g = 0.7$, $\theta = 0$, and set 1 of initial conditions.
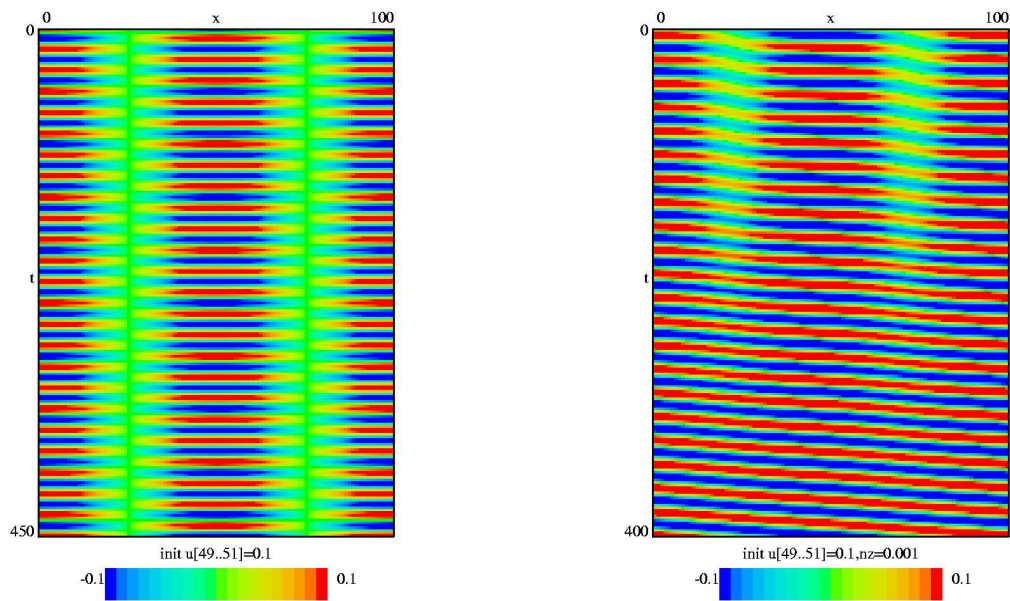
Figure 2.11. (a) SW is the pattern obtained at $g = 0.7$, $\theta = 0$, and set 2 of initial conditions and it is unstable since (b) in the presence of noise SW is replaced by TW.

2.3   Spatio-temporal patterns obtained by a loss of stability at a double-zero eigenvalue

We analyzed in the previous section, the case of traveling wave and standing wave spatio-temporal patterns that occur when the parameters in the system (2.3) are chosen such that at the most unstable mode the trace of the linearized part vanishes while the determinant is still positive. The resulting solutions change with both time and space position. Another possible situation is when the choice of parameters is such that the determinant vanishes first and the trace is still negative. In this case a zero eigenvalue occurs and the resulting pattern oscillates with respect to space position due to the unstable mode k_0, but it is independent of time. We call this pattern a *steady state* or *stationary pattern*.

An obvious question is how these possible patterns in the system (2.3) interact, that is how the system's behavior changes from traveling wave or standing wave to a stationary pattern or vice-versa. The issue of transition between spatio-temporal and only spatial patterns can be addressed by the analysis of the case when the trace and the determinant of the linearized system vanish simultaneously. Then at the most unstable mode we obtained a double-zero eigenvalue. The double-zero eigenvalue case is approached from two different directions: one when we already have a zero eigenvalue and now obtain another one (that is coming from the domain of spatial/stationary patterns), and the other when we have a pair of pure imaginary eigenvalues $\pm i\omega_0$ that collide (that is coming from the domain of spatio-temporal patterns).

As a result of the above remarks, the aim of the present section is to see how behaviors in the system (2.3) look like at the transition between stationary states and traveling/standing waves. Therefore we assume that at the most unstable mode k_0 we have $Tr(\hat{L}(k_0)) = det(\hat{L}(k_0)) = 0$. This is true when the parameters satisfy the conditions

$$g^* = 1/\tau \quad \text{and} \quad \alpha^* = \frac{1 + 1/\tau}{\hat{J}(k_0)} \, . \tag{2.30}$$

Remark 2.9. In the following we fix the value of τ, and take α and g as bifurcation parameters. The bifurcation values around which we will consider the singular perturbation analysis are α^* and g^*. Therefore on the entire Section 2.3, the operator L_0 defined by (2.10), and the matrix $\hat{L}(k)$

defined by (2.11) for all k where it makes sense, will be evaluated at $\alpha = \alpha^*$ and $g = g^*$.

At $\pm k_0$ the associated ODE $\frac{d\xi}{dt} = \hat{L}(k_0)\xi$ has a double-zero eigenvalue. For all other values $k \neq \pm k_0$ we have $Tr(\hat{L}(k)) < 0$ and $det(\hat{L}(k)) > 0$, and the corresponding eigenvalues have negative real part.

Let us construct the (generalized) eigenvectors of $\hat{L}(k_0)$ and $\hat{L}(k_0)^T$ as follows

$$\Phi_0 = \frac{1}{\sqrt{\tau}} \begin{pmatrix} 1 \\ 1 \end{pmatrix}, \ \Psi_1 = \frac{1}{\sqrt{\tau}} \begin{pmatrix} 1 \\ -1 \end{pmatrix}, \ \Phi_1 = \sqrt{\tau} \begin{pmatrix} 1 \\ 0 \end{pmatrix}, \ \Psi_0 = \sqrt{\tau} \begin{pmatrix} 0 \\ 1 \end{pmatrix}, \tag{2.31}$$

according to the conditions

$$\begin{cases} \hat{L}(k_0)\Phi_0 = \mathbf{0}, \ \hat{L}(k_0)\Phi_1 = \Phi_0, \ \hat{L}(k_0)^T\Psi_1 = \mathbf{0}, \ \hat{L}(k_0)^T\Psi_0 = \Psi_1, \\ \Phi_0 \cdot \Psi_0 = \Phi_1 \cdot \Psi_1 = 1, \ \Phi_0 \cdot \Psi_1 = \Phi_1 \cdot \Psi_0 = 0. \end{cases} \tag{2.32}$$

Around the double-zero bifurcation point, the first order approximation of the solution of the nonlinear system (2.3) is given by its projection on the generalized eigenspace. That means U can be approximated by

$$U(x,t) \approx 2\text{Re}\left[z(t)\,\Phi_0\,e^{ik_0x} + w(t)\,\Phi_1\,e^{ik_0x}\right] \tag{2.33}$$

where z, w are time-dependent functions that satisfy the ODE system with real coefficients

$$\begin{cases} z' = w, \\ w' = \zeta_1 z + \zeta_2 w + A|z|^2 z + Cz[\overline{z}\,w + z\,\overline{w}] + D|z|^2 w, \end{cases} \tag{2.34}$$

called *the normal form for the double-zero (Takens-Bogdanov) bifurcation with O(2)-symmetry* [27].

Indeed the linear part of the system (2.34) has two eigenvalues equal to zero at $\zeta_1 = \zeta_2 = 0$. That is why we call this type of bifurcation as 'double-zero', or 'Takens-Bogdanov'. The additional name of 'O(2)-symmetry' comes from the fact that the system (2.34) exhibits symmetry under both rotations and reflections. This means that the vector field $G(z,w)$ (the right hand side of the equation (2.34)) commutes with the rotation $z \mapsto e^{i\theta}z$ for any angle $\theta \in \mathbb{R}$, i.e. we have $G(e^{i\theta}z, e^{i\theta}w) = e^{i\theta}G(z,w)$, and it also commutes with reflection $z \mapsto \overline{z}$, i.e. $G(\overline{z},\overline{w}) = \overline{G(z,w)}$. Therefore the system shows no directional preference and we say that it is *isotropic*. The technical

46

terminology is that the vector field G, and therefore the system (2.34), is covariant (or equivariant) with respect to the group $O(2)$ of rotations and reflections.

Recall that for (2.3) we seek spatially periodic solutions of the form $\psi_k\, e^{ikx} + cc$, where cc stands for the complex conjugate of the previous term. Since $\left[\psi_k\, e^{ik(x+d)} + cc = e^{ikd}\psi_k\, e^{ikx} + cc\right]$, a translation in space $[x \mapsto x + d]$ will be associated with a rotation of the time-dependent vector ψ_k. Furthemore a reflection in space $[x \mapsto (-x)]$ is associated with a reflection of the vector ψ_k since $\left[\psi_k\, e^{ik(-x)} + cc = \overline{\psi}_k\, e^{ikx} + cc\right]$. Let us notice that the vector field of the original system (2.3) satisfies the properties $G(\,u(x+d,t), v(x+d,t)\,) = G(u,v)(x+d,t)$ and $G(\,u(-x,t), v(-x,t)\,) = G(u,v)(-x,t)$, so we say that the system (2.3) is isotropic.

The system (2.3) has at least one solution that preserves the symmetry with respect to both rotations, $u(x+d,t) = e^{ikd}u(x,t)$, $v(x+d,t) = e^{ikd}v(x,t)$, and reflection $u(-x,t) = \overline{u(x,t)}$, $v(-x,t) = \overline{v(x,t)}$, and this is the trivial solution $u(x,t) = v(x,t) \equiv 0$. For different values of parameters other solutions may exist which do not necessarily preserve the symmetry. We say that the symmetry in the system is broken and call the phenomenon that leads to this situation, *symmetry breaking bifurcation*. The above mentioned correspondence between (2.3) and (2.34), together with formula (2.33), allows us to work with the system (2.34) and detect the solutions that break its symmetry, rather than working with (2.3).

Dangelmayr and Knobloch present in [27] a detailed analysis of the existence and stability properties for five types of possible solutions of the system (2.34). These are the trivial solution/T, steady state/SS, traveling waves/TW, standing waves/SW, and modulated waves/MW. Depending on the sign of the coefficient A, and then the signs of D and $M = 2C + D$ together with some nondegeneracy conditions based on the value of the ratio D/M, different regions in the parameter plane (ζ_1, ζ_2) were identified, and the corresponding bifurcation diagrams were drawn. That is, as a dependence on the values of parameters, all possible qualitative different behaviors in the system are described.

As an example, TWs break the symmetry with respect to reflection and keep the symmetry to rotations. On the other hand SWs break the symmetry with respect to rotations but keep the symmetry to reflection (see below).

We summarize in the following the basic ideas followed by Dangelmayr and Knobloch [27] in their analysis. Moreover in a similar approach to Section 2.2 we give a geometric interpretation of

the solutions SS, TW, SW and MW.

First we write z and w in polar coordinates and tranform the system (2.34) accordingly. Since $w = z'$ we need only the polar representation of z, say $z(t) = r\, e^{i\phi}$. Then by the separation of the real and imaginary parts, the system (2.34) is equivalent to

$$
\begin{cases}
r'' - r(\phi')^2 - r(\zeta_1 + Ar^2) - r'\,(\zeta_2 + Mr^2) = 0\,, \\
r\,\phi'' + 2r'\phi' - r\,\phi'\,(\zeta_2 + Dr^2) = 0\,.
\end{cases}
\tag{2.35}
$$

The trivial solution T corresponds to the solution $r = 0$ and exists for all parameter values. Therefore $z(t) = w(t) = 0$ and from (2.33) we have $U(x,t) \equiv 0$. The solution is independent of time and position in space.

The linearization of (2.35) around $r = 0$, $\phi' = 0$, e.g. take $r = 0 + \xi$, $\phi' = 0 + \eta$ with ξ, η small, is the equation $\xi'' - \zeta_2\,\xi' - \zeta_1\,\xi = 0$. The eigenvalues have negative real part if and only if $\zeta_1 < 0$ and $\zeta_2 < 0$. The stability of the trivial solution T is lost at $\zeta_1 = 0$ through a zero eigenvalue when other constant solutions r_0 appear (with ϕ' still zero) (we denote the line $\zeta_1 = 0$ in the parameter space (ζ_1, ζ_2) by L_0 - see Figure 2.12), or at $\zeta_2 = 0$ and $\zeta_1 < 0$ (see the half-line H_0 in Figure 2.12) through a pair of pure imaginary eigenvalues $\pm i\omega_0$, when a small amplitude periodic solution $r = r(t)$ appears with ϕ' still zero. This case will correspond to a standing wave solution. We mention that the $O(2)$-symmetry of the system forces both types of TW and SW solutions to appear simultaneously from the trivial solution.

The steady state SS corresponds to solution of (2.35) *constant on the radial direction*, $r(t) = r_0$, and *with no orbital motion* $\phi' = 0$. This means that r_0 must satisfy the condition $\zeta_1 + Ar_0^2 = 0$ and obviously it does not exist for all parameter values. In order to get a SS we need $A\zeta_1 < 0$ so that $r_0 = \sqrt{-\zeta_1/A}$. Moreover $\phi' = 0$ implies $\phi(t) = \omega$, constant, and $z(t) = r_0\, e^{i\omega}$, $w(t) = z'(t) = 0$. The approximating formula (2.33) implies $U(x,t) = 2r_0\Phi_0 \cos(k_0 x + \omega) = 2\sqrt{-\frac{\zeta_1}{A}}\Phi_0 \cos(k_0 x + \omega)$, or up to a translation in space,

$$
U(x,t) \approx 2\sqrt{-\frac{\zeta_1}{A}}\,\cos(k_0 x)\,\Phi_0\,.
\tag{2.36}
$$

The steady state pattern SS consists in oscillations with respect to the position in space x, and it is independent of time; therefore it forms stationary stripes (see Figure 2.19 for an example).

The linearization of (2.35) around $r = r_0$, $\phi' = 0$, e.g. take $r = r_0 + \xi$, $\phi' = 0 + \eta$ with ξ, η small, is the system of equations $\xi'' - (\zeta_2 + Mr_0^2)\,\xi' - 2Ar_0^2\,\xi = 0$, $\eta' - (\zeta_2 + Dr_0^2)\eta = 0$, i.e. $\xi'' - (\zeta_2 - \frac{M}{A}\zeta_1)\xi' + 2\zeta_1\xi = 0$ and $\eta' - (\zeta_2 - \frac{D}{A}\zeta_1)\eta = 0$. The only possible bifurcations that result in appearance/disappearance of time independent solutions correspond to a zero eigenvalue. That can happen for $\zeta_1 = 0$ (we have already mentioned this case of new SS branch solution), or for $A\zeta_2 = D\zeta_1$, $A\zeta_1 < 0$ (see the half-line L_m in Figure 2.12) when a new ϕ' constant and nonzero solution is created, say $\phi' = \omega_0$ (see the TW case)

The traveling wave TW corresponds to a solution of (2.35) *constant on the radial direction*, $r(t) = r_0$, but *with orbital motion with constant angular frequency* $\phi' = \omega_0$. This means that r_0 and ω_0 must satisfy the conditions $\zeta_2 + Dr_0^2 = 0$ and $\omega_0^2 = -(\zeta_1 + Ar_0^2)$ and TW exists only in the parametric regime $D\zeta_2 < 0$, $\frac{A}{D}\zeta_2 - \zeta_1 > 0$. We have $r_0 = \sqrt{-\zeta_2/D}$ and $\omega_0 = \pm\sqrt{A\zeta_2/D - \zeta_1}$; then $z(t) = r_0\,e^{i(\omega_0 t + \omega)}$, $w(t) = z'(t) = ir_0\omega_0\,e^{i(\omega_0 t + \omega)}$ and from formula (2.33), the traveling wave equation, up to a translation in space is

$$U(x,t) \approx 2\sqrt{-\frac{\zeta_2}{D}}\,\operatorname{Re}\left[(\Phi_0 + i\omega_0\Phi_1)\,e^{i(\omega_0 t + k_0 x)}\right]\,, \tag{2.37}$$

with

$$\omega_0 = \pm\sqrt{\frac{A}{D}\zeta_2 - \zeta_1}\,. \tag{2.38}$$

The traveling wave solution TW changes with respect to time and position in space according to the traveling wave coordinate $\xi = ct - x$ where $c = \omega_0/k_0$ is the wave velocity; therefore the pattern is formed by non-stationary stripes, i.e. stripes with finite slope (see Figure 2.16 for an example). Equation (2.37) shows that TW solutions break the symmetry with respect to reflection, but respect the symmetry to rotations.

The modulated wave MW corresponds to a periodic solution $r(t)$ of (2.35) and a nonzero angular velocity ϕ'. This means that we have *oscillations in the radial direction* and *orbital motion* as well. The modulated waves bifurcate from a traveling wave through another Hopf bifurcation

that introduces a new frequency in the solution. Therefore the MW pattern is characterized by two different frequencies, one corresponding to the orbital motion and the other to radial oscillations (not shown in this thesis).

The standing wave SW corresponds to a periodic solution $r(t)$ of (2.35) and $\phi' = 0$. This means that we have *oscillations in the radial direction* and *no orbital motion*. SWs can occur as oscillations about the trivial solution or about a steady state. From (2.35), $r(t)$ satisfies the equation $r'' - r'(\zeta_2 + Mr^2) - r(\zeta_1 + Ar^2) = 0$ and $\phi = \omega$ is constant. Then $z(t) = r(t) e^{i\omega}$, $w(t) = z'(t) = r'(t) e^{i\omega}$, and (2.33) implies, up to a translation in space,

$$U(x,t) \approx 2\big[r(t)\,\Phi_0 + r'(t)\,\Phi_1\big]\,\cos(k_0 x)\,, \tag{2.39}$$

where $r(t)$ is the periodic solution of period, say, $2\pi/\omega_0$ of the ODE

$$r'' - r'\,(\zeta_2 + Mr^2) - r(\zeta_1 + Ar^2) = 0\,. \tag{2.40}$$

The standing wave solution SW oscillates with respect to time with frequency ω_0 for any fixed position in space, and oscillates with respect to space with frequency k_0 for any fixed t (see Figure 2.17 for an example of the SW pattern). Equation (2.39) shows that SW solutions break the symmetry with respect to rotations, but respect the symmetry to reflection.

Remark 2.10. We summarized above the properties of possible patterns in a system with $O(2)$-symmetry. Let us describe now the type of bifurcation diagram [27] that we need later in our study. It corresponds to $A < 0$ with $D < 0$, $M < 0$ and $0 < D/M < \frac{1}{2}$. The parameter plane (ζ_1, ζ_2) is divided into seven regions (Figure 2.12) by the following curves: $L_0 : \zeta_1 = 0$, $H_0 : [\zeta_2 = 0, \zeta_1 < 0]$, $L_M : [A\zeta_2 = M\zeta_1, \zeta_1 > 0]$, $SL_S : [5A\zeta_2 = 4M\zeta_1, \zeta_1 > 0]$, $SN_{S2} : [A\zeta_2 \approx 0.74M\zeta_1, \zeta_1 > 0]$, $L_m : [A\zeta_2 = D\zeta_1, \zeta_1 > 0]$. A bifurcation producing steady-state solutions occurs along L_0, and a Hopf bifurcation, from the trivial solution T, of a TW and SW_1 occurs along H_0. By crossing L_M, SL_S, SN_{S2} and L_m secondary bifurcations occur: along SN_{S2} we have a saddle-node for two standing waves, SW_1 and SW_2; along L_M a standing wave oscillation SW_3 about a non-trivial steady state bifurcates; then SW_3 and SW_2 undergo a global bifurcation and join smoothly to each
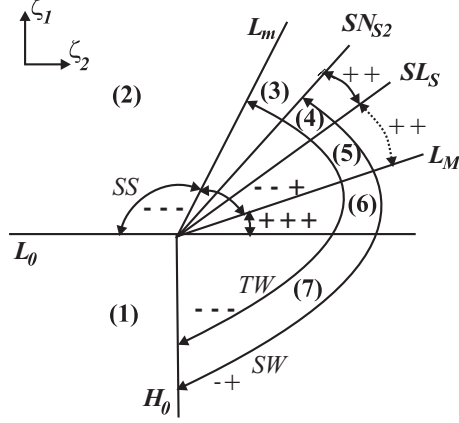
Figure 2.12. The bifurcation diagram corresponding to the system (2.34) with $A < 0$, $D < 0$, $M < 0$ and $0 < D/M < 1/2$.

other along SL_S; and TW bifurcates from a steady state along L_m.

Since our goal is to study how the SS, TWs and SWs solutions occur in the neural system (2.3) and how they interact, that is how the patterns change as the parameters α and g vary about α^* and g^*, the next necessary step in the analysis is to construct the normal form for the double-zero bifurcation, and determine its coefficients. That is the aim of the next section.

2.3.1 Double-zero bifurcation with $O(2)$-symmetry and pattern formation

In the case of a double-zero eigenvalue, we choose the singular perturbation expansion for α, g and the solution U as

$$\alpha - \alpha^* = \epsilon^2 \gamma, \;\; g - g^* = \epsilon^2 \eta, \;\; \gamma, \eta \in \mathbb{R},$$

$$U(x,t) = \epsilon\, U_0(x,t) + \epsilon^2\, U_1(x,t) + \epsilon^3\, U_2(x,t) + \epsilon^4\, U_3(x,t) + \cdots$$

and write the system (2.9) in its equivalent form,

$$L_0 U = (\alpha - \alpha^*)\, L_1 U + (g - g^*)\, L_2 U + B(U,U) + C(U,U,U) + Q(U,U,U,U) + \dots \qquad (2.41)$$

where $B(U,U)$, $C(U,U,U)$, $Q(U,U,U,U)$ represent the quadratic, cubic and fourth order terms, L_0 is defined according to Remark 2.9, and $L_1 = \begin{pmatrix} J * (\cdot) & 0 \\ 0 & 0 \end{pmatrix}$, $L_2 = \begin{pmatrix} 0 & -1 \\ 0 & 0 \end{pmatrix}$.

51

With the notation $\boldsymbol{E}$ for the unit vector $(1,0)^T$, equation (2.41) becomes

$$\epsilon L_0 U_0 + \epsilon^2 \left[L_0 U_1 - \frac{F''(0)}{2}[\alpha^* J * u_0 - g^* v_0]^2 \boldsymbol{E} \right] + \epsilon^3 [\, L_0 U_2 - \gamma L_1 U_0 - \eta L_2 U_0\,] + \epsilon^4 [\, L_0 U_3$$

$$- \gamma L_1 U_1 - \eta L_2 U_1\,]$$

$$= \epsilon^3 \left[F''(0)[\alpha^* J * u_0 - g^* v_0][\alpha^* J * u_1 - g^* v_1] + \frac{F'''(0)}{6}[\alpha^* J * u_0 - g v_0]^3 \right] \boldsymbol{E} +$$

$$\epsilon^4 \left[\frac{F''(0)}{2}[\alpha^* J * u_1 - g^* v_1]^2 + F''(0)[\alpha^* J * u_0 - g^* v_0][\alpha^* J * u_2 - g^* v_2 + \gamma J * u_0 - \eta v_0] \right.$$

$$\left. + \frac{F'''(0)}{2}[\alpha^* J * u_0 - g v_0]^2 [\alpha^* J * u_1 - g v_1] + \frac{F^{(4)}(0)}{24}[\alpha^* J * u_0 - g v_0]^4 \right] \boldsymbol{E} + \mathcal{O}(\epsilon^5). \qquad (2.42)$$

Remark 2.11. We give the details of the construction of the normal form in Appendix B.0.3. The main idea is to identify the functional equations that U_0, U_1, U_2 and U_3 satisfy and then solve for them.

The nullspace of L_0 corresponding to the center manifold is now only two-dimensional with the basis $\{\,\Phi_0\, e^{\pm i k_0 x}\}$ where Φ_0 is the real vector defined in (2.31). As a consequence, U_0 can be written as

$$U_0 = \left(z\, e^{i k_0 x} + \overline{z}\, e^{-i k_0 x} \right) \Phi_0$$

with z being ϵ-dependent. An appropriate time scale is $z = z(\epsilon t) = z(0) + z'(0)\epsilon t + \frac{z''(0)}{2}\epsilon^2 t^2 + \frac{z'''(0)}{6}\epsilon^3 t^3 + \mathcal{O}(\epsilon^4)$, therefore $U_0 = \left(z(0)\, e^{i k_0 x} + \overline{z}(0)\, e^{-i k_0 x} \right) \Phi_0 + \mathcal{O}(\epsilon)$.

The equation that defines U_1 reads as

$$L_0 U_1 = -\left[z'(0)\, e^{i k_0 x} + \overline{z'}(0)\, e^{-i k_0 x} \right] \Phi_0 + \frac{F''(0)}{2\tau} \boldsymbol{E} \left[z(0)^2\, e^{2 i k_0 x} + \overline{z}(0)^2\, e^{-2 i k_0 x} + 2 z(0)\, \overline{z}(0) \right]$$

and U_1 can be constructed as

$$U_1 = \left[w\, e^{i k_0 x} + \overline{w}\, e^{-i k_0 x} \right] \Phi_1 + z^2 \xi_1\, e^{2 i k_0 x} + \overline{z}^2 \xi_1\, e^{-2 i k_0 x} + 2 z\, \overline{z} \xi_2$$

with $w = w(\epsilon t) = w(0) + w'(0)\epsilon t + \frac{w''(0)}{2}\epsilon^2 t^2 + \mathcal{O}(\epsilon^3)$, and ξ_1, ξ_2 real vectors. The first equation of the normal form is obtained by solving for U_1 and it is $z'(0) = w(0)$. The next two steps consist in

finding U_2 as

$$U_2 = \left[zw e^{2ik_0x} + \overline{z}\,\overline{w} e^{-2ik_0x} \right] \beta_1 + [z\,\overline{w} + \overline{z}\,w]\beta_2 + \left[z^3 e^{3ik_0x} + \overline{z}^3 e^{-3ik_0x} \right] \beta_3$$

with β_1, β_2, β_3 real vectors to be computed, and then solving for U_3 (see Appendix B.0.3 for details). As a consequence we obtain the following result.

Theorem 2.2. *For any positive τ, in the neighborhood of the bifurcation values $\alpha^* = \frac{1+1/\tau}{\hat{J}(k_0)}$ and $g^* = 1/\tau$, the system (2.3) has the normal form (2.34) with $\zeta_1 = \frac{\alpha\,\hat{J}(k_0)-(g+1)}{\tau}$, $\zeta_2 = \alpha\,\hat{J}(k_0)-(1+\frac{1}{\tau})$, and the coefficients*

$$\begin{cases} A = \frac{1}{2\tau^2}[F'''(0) - 3F''(0)^2] + \frac{F''(0)^2}{\tau(\tau+1)} \cdot \left[\frac{\hat{J}(k_0)}{\hat{J}(k_0)-\hat{J}(0)} + \frac{\hat{J}(k_0)}{2\,[\,\hat{J}(k_0)-\hat{J}(2k_0)\,]} \right], \\[2mm] C = (\tau+1)A + \frac{F''(0)^2}{\tau(\tau+1)} \cdot \frac{\hat{J}(k_0)}{\hat{J}(k_0)-\hat{J}(0)}, \\[2mm] D = (\tau+1)A + \frac{F''(0)^2}{\tau(\tau+1)} \cdot \frac{\hat{J}(k_0)}{\hat{J}(k_0)-\hat{J}(2k_0)}. \end{cases}$$

Proof: The normal form obtained by the above constructive method is $z'(0) = w(0)$, $w'(0) = \left[\frac{\gamma\,\hat{J}(k_0)-\eta}{\tau} + A|z(0)|^2 \right] z(0) + \epsilon \left\{ \gamma\,\hat{J}(k_0)w(0) + Cz(0)[\,\overline{z}(0)\,w(0) + z(0)\,\overline{w}(0)\,] + D|z(0)|^2w(0) \right\} + \mathcal{O}(\epsilon^2)$, but this is equivalent to (2.34) for the scaling $\gamma = (\alpha - \alpha^*)/\epsilon^2$, $\eta = (g - g^*)/\epsilon^2$ and $\epsilon\,z(0) \leftrightarrow z$, $\epsilon^2\,w(0) \leftrightarrow w$, $\epsilon\,t \leftrightarrow t$.

Remark 2.12. If we consider the solution U of the nonlinear system approximated only by its projection on the generalized eigenspace, we have

$$U(x,t) \approx 2\epsilon\,\Phi_0\,\mathrm{Re}\left[z(0)\,e^{ik_0x} \right] + 2\epsilon^2\,\Phi_1\,\mathrm{Re}\left[w(0)\,e^{ik_0x} \right].$$

Since $\epsilon\,z(0) \leftrightarrow z$, $\epsilon^2\,w(0) \leftrightarrow w$ this becomes exactly the formula (2.33).

Theorem 2.3. *In the hypotheses of Theorem 2.2, the steady state SS, traveling wave TW and standing wave SW solutions that occur about the bifurcation point $\alpha^* = \frac{1+1/\tau}{\hat{J}(k_0)}$ and $g^* = 1/\tau$, are approximated by the following expressions*

$$SS\ :\ u(x,t) = v(x,t) \approx \frac{2}{\tau}\,\cos(k_0x)\,\sqrt{\frac{\alpha\,\hat{J}(k_0)-(g+1)}{(-A)}},$$

53

$$
TW \; : \;
\begin{cases}
u(x,t) \approx \left[\cos(\omega_0 t + k_0 x) - \tau\,\omega_0 \sin(\omega_0 t + k_0 x)\right]\sqrt{\tfrac{2[\alpha\,\hat{J}(k_0)-(1+1/\tau)]}{(-D)\,\tau}}\,, \\[3mm]
v(x,t) \approx \cos(\omega_0 t + k_0 x)\,\sqrt{\tfrac{2[\alpha\,\hat{J}(k_0)-(1+1/\tau)]}{(-D)\,\tau}}\,,
\end{cases}
$$

$$
SW \; : \;
\begin{cases}
u(x,t) \approx \tfrac{2}{\sqrt{\tau}}\left[r(t) + \tau\,r'(t)\right]\cos(k_0 x)\,, \\[3mm]
v(x,t) \approx \tfrac{2}{\sqrt{\tau}}\,r(t)\,\cos(k_0 x)\,,
\end{cases}
$$

where $r(t)$ is the periodic solution of

$$
r'' - r'\left[[\alpha\,\hat{J}(k_0)-(1+1/\tau)]+(2C+D)r^2\right] - r\left[\frac{\alpha\,\hat{J}(k_0)-(g+1)}{\tau}+Ar^2\right]=0
$$

and

$$
\omega_0 = \pm\sqrt{\frac{A}{D}[\alpha\,\hat{J}(k_0)-(1+1/\tau)]-\frac{1}{\tau}[\alpha\,\hat{J}(k_0)-(g+1)]}\,.
$$

Proof: The above formulas result directly from equations (2.36), (2.37) and (2.39) with Φ_0 and Φ_1 defined by (2.31) and ζ_1, ζ_2 as in Theorem 2.2.

Theorem 2.4. *Let us assume that the most unstable mode k_0 of the system (2.3) satisfies the conditions (2.13), (2.14), and at k_0 a double-zero eigenvalue occurs.*

If the firing rate function F is such that $F(0)=0$, $F'(0)>0$, $F''(0)=0$, and $F'''(0)<0$, then about $\alpha^* = \frac{1+1/\tau}{\hat{J}(k_0)}$, $g^* = 1/\tau$, the system (2.3) has the bifurcation diagram from Figure 2.13 (equivalent to Figure 2.12). The curves that divide the parametric plane (α, g) into seven regions have the following equations

$$
\begin{cases}
L_0 \; : \; \alpha\,\hat{J}(k_0)=g+1\,, \\[2mm]
H_0 \; : \; \alpha\,\hat{J}(k_0)=1+1/\tau\,,\; g>1/\tau\,, \\[2mm]
L_M \; : \; \alpha\,\hat{J}(k_0)=\frac{\tau+1}{2\tau+3}(3g+2)\,,\; g>1/\tau\,,
\end{cases}
\qquad
\begin{cases}
SL_S \; : \; \alpha\,\hat{J}(k_0)=\frac{\tau+1}{7\tau+12}(12g+7)\,,\; g>1/\tau\,, \\[2mm]
SN_{S2} \; : \; \alpha\,\hat{J}(k_0)\approx\frac{\tau+1}{61\tau+111}(111g+61)\,,\; g>1/\tau\,, \\[2mm]
L_m \; : \; \alpha\,\hat{J}(k_0)=(\tau+1)g\,,\; g>1/\tau\,.
\end{cases}
$$

$$(2.43)$$

Proof: Since $F''(0)=0$ and $F'''(0)<0$, we have $A<0$, $C=D=(\tau+1)A<0$ and then $M<0$, $D/M=\frac{1}{3}\neq\frac{1}{2},\frac{3}{5},0.7,0.74,\frac{3}{4},\frac{4}{5},1$ (the nondegeneracy conditions). This is exactly the case described by Figure 2.12. With the formulas provided by Theorem 2.2 we obtain immediately the equations (2.43).
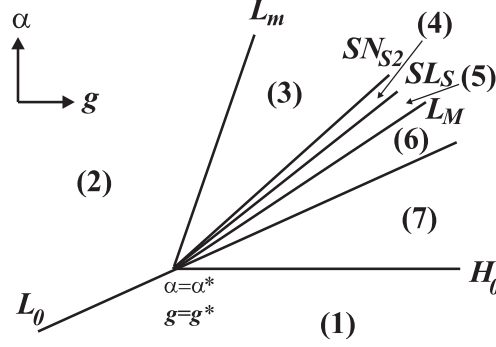
Figure 2.13. The bifurcation diagram corresponding to the system (2.3) about (α^*, g^*) when $\theta = 0$ in F.

2.3.2 Numerical results

We run the numerical simulations for the same hypotheses as in Section 2.2.3. The full system (2.3) is simulated with synaptic coupling (2.7) that has the coefficients $a = -0.2$, $b = 2.5$, $c = 2$; the gain function F is chosen with $r = 3$ and $\theta = 0$, and the parameter τ is fixed at $\tau = 4$. The horizontal axis represents the space x, the vertical axis corresponds to time t, and the variable $u(x,t)$ is plotted by the change in the level of color.

Therefore we have $F''(0) = 0$, $k_0 = 1$, $\hat{J}(0) = -0.2$, $\hat{J}(k_0) = 1.25$, $\hat{J}(2k_0) = 1$ and $\alpha^* = 1$, $g^* = 0.25$. The coefficients in the normal form are $A = -0.1406$, $C = D = -0.7031$, and then $M = -2.1094$, $D/M = \frac{1}{3}$. From Theorem 2.4 we obtain: $L_0 : \alpha = \frac{4}{5}(g+1)$, $H_0 : [\alpha = 1, g > 0.25]$, $L_M : [\alpha = \frac{12}{11}(g+\frac{2}{3}), g > 0.25]$, $SL_S : [\alpha = \frac{6}{5}(g+\frac{7}{12}), g > 0.25]$, $SN_{S2} : [\alpha = \frac{444}{355}(g+\frac{61}{111}), g > 0.25]$, $L_m : \alpha = 4g, g > 0.25]$.

We choose parameters in different regions.

Along the bifurcation line L_0 we take $\alpha = 0.95$, $g = 0.2$ in the region (1) and obtain the trivial solution T, and take $\alpha = 0.98$, $g = 0.2$ in region (2) and obtain the steady-state SS pattern (Figure 2.14). The same set of initial conditions, say Ic1, is considered in both cases. This set of initial conditions will be used later for other parameter values.

Along the bifurcation line H_0 let us take $\alpha = 0.98$, $g = 0.26$ in the region (1) (Figure 2.15), and $\alpha = 1.004$, $g = 0.26$ in region (7) . We consider two distinct sets of initial conditions, Ic1, the same as above, and Ic2. By crossing H_0 the patterns that bifurcate from T are different: TW for Ic1 (Figure 2.16), and SW for Ic2, but this is unstable (Figure 2.17, Figure 2.18).

Along the bifurcation line L_m we consider $\alpha = 1.08$, $g = 0.26$ in region (2) with different initial

55

conditions: Ic1 and Ic2. A steady-state pattern SS is selected (Figure 2.19). At $\alpha = 1.03$, $g = 0.26$ in region (3) we obtain a TW pattern for Ic1, and a SS pattern for Ic2 (Figure 2.20). The SS pattern is unstable as we see when we introduce in the system white noise scaled by a factor $nz = 0.001$ (Figure 2.21)

We consider $\alpha = 1.0122$, $g = 0.26$ in region (4), between SN_{S2} and SL_S, and $\alpha = 1.01122$, $g = 0.26$ in region (5), between SL_S and L_M. For different initial conditions, Ic1, Ic2 and Ic3, patterns as TW, SW and SS respectively can occur, but the last two are destabilized in time to a TW. We present, for example, the numerical results for the $\alpha = 1.0122$, $g = 0.26$. Starting with Ic1 initial condition we obtain a TW pattern (Figure 2.22); starting with Ic2, a SW pattern is formed but it destabilizes in time to a TW (Figure 2.23); starting with Ic3, a SS pattern is formed but it destabilizes in time to a TW (Figure 2.24).

Similar pictures are obtained for $\alpha = 1.01122$, $g = 0.26$ in region (5).

At $\alpha = 1.009$, $g = 0.26$ in region (6) the patterns that might occur are TW and SW, but always SW is destabilized in time to a TW (Figure 2.25).

Remark 2.13. There is a nice agreement between the theoretical and numerical results. Numerically it is impossible to detect a pattern that has all the corresponding eigenvalues positive, i.e. it is completely unstable (as one of the SWs in regions (4) and (5) in the bifurcation diagram, or the SS in region (6)). Nevertheless the other patterns that present stability at least on one direction can be visualized in the numerical simulation. Of course, finally they will approach the only stable solution, i.e. TW.

Remark 2.14. We did not complete in this thesis the analysis of the system (2.3). A direction for future research is to investigate other possible cases (bifurcation diagrams) that might occur for different values of the parameter θ in the function F. We are especially interested in the case when the standing wave pattern is stable, and furthermore in the case that can give rise to an additional pattern not studied here that is the modulated waves pattern. These situations correspond to different kinds of bifurcation diagrams listed in [27].

2.4   Conclusions

We have analyzed a rate model with nonlinear sigma-shaped gain function for two homogeneous populations of neurons, one excitatory that displays adaptation, and one inhibitory. The coupling is characterized by local excitation and long range (lateral) inhibition, and the adaptation is assumed to be linear. When the strength of adaptation is sufficiently large (or the adaptation is slow enough) temporal oscillations occur in the system. In general they form traveling waves, but we were able to show that it is possible, when the threshold is sufficiently high, to obtain also standing waves. These are spatial oscillations with frequency k_0 and temporal oscillations with frequency ω_0 that can be computed as functions of parameters τ, g, and the strength of the coupling α. Numerical simulations indicate that for a fixed adaptation time constant τ, the standing wave pattern occurs for intermediate value of the strength g of adaptation, in a relatively small regime. When g is increased the local activity is disrupted and starts to travel along the network, resulting in a traveling wave pattern.

We have also investigated the transition between stationary patterns and spatio-temporal patterns in the neural network therefore explaining the patterns found in the numerical simulations of the full model.

We did not complete the analysis of the system (2.3). The general theory predicts, under certain conditions, the existence of a different spatio-temporal pattern, that is the modulated waves characterized by two different temporal frequencies in addition to the spatial frequency k_0. The questions if the conditions necessary to the existence of modulated waves are met in this neural system, and if this pattern can be made to be stable, remain open.
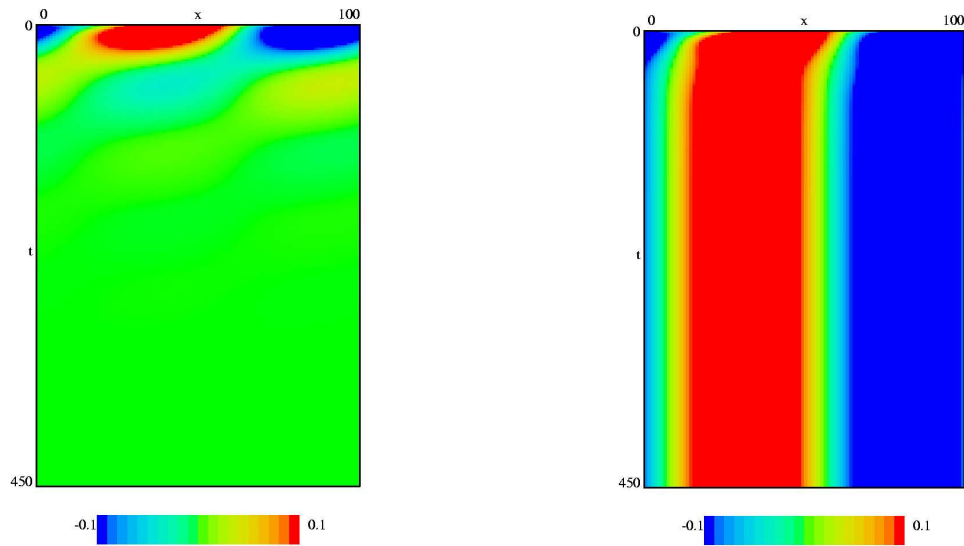
Figure 2.14. Along the bifurcation line L_0 we have (a) the trivial solution T in region (1), at $\alpha = 0.95, g = 0.2$, and (b) steady state SS in region (2), at $\alpha = 0.98, g = 0.2$. The same set of initial conditions Ic1 is used.
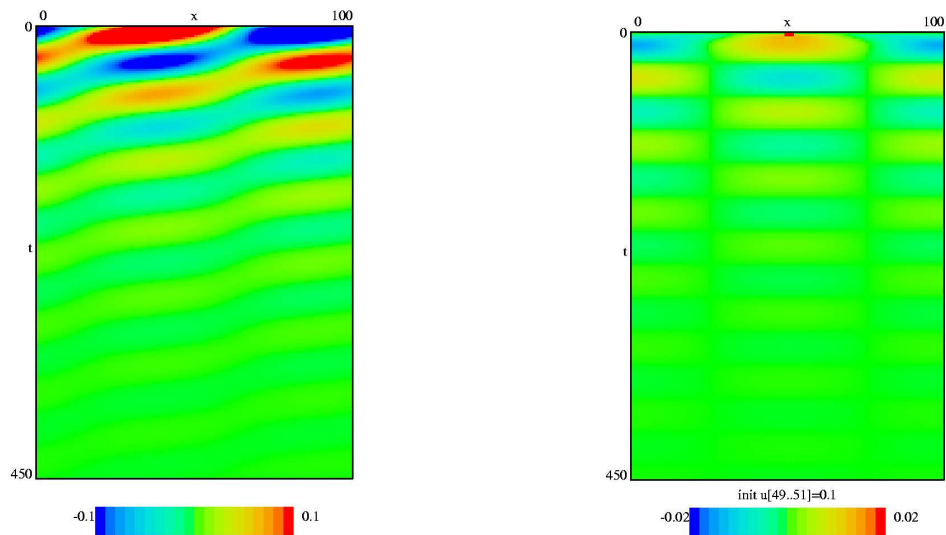
Figure 2.15. At $\alpha = 0.98, g = 0.26$ in region (1), close to the bifurcation line H_0, we obtain T for different sets of initial conditions (a) Ic1 will give rise in region (7) to a TW; (b) Ic2 will give rise in region (7) to an unstable SW.
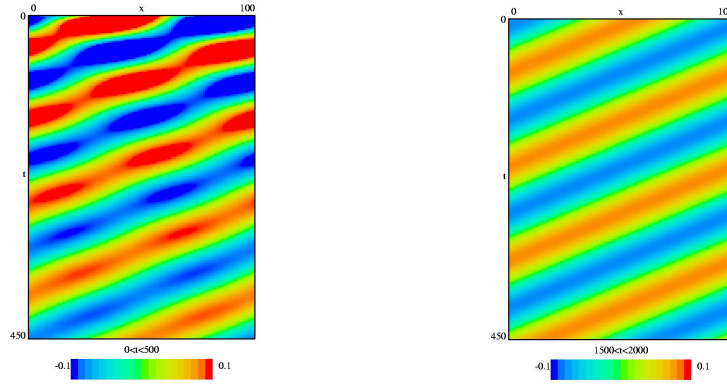
Figure 2.16. The TW pattern obtained for Ic1, at $\alpha = 1.004, g = 0.26$ in region (7).
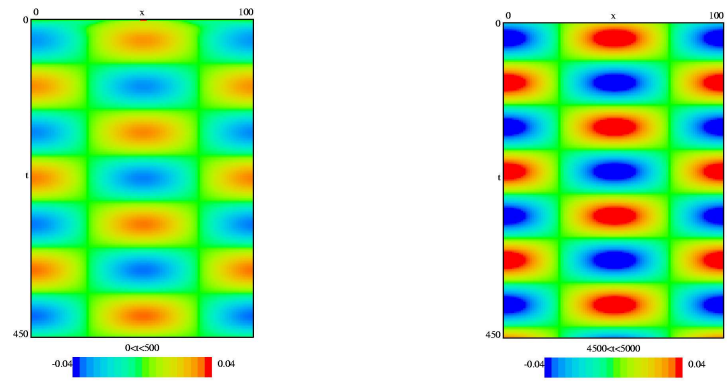
Figure 2.17. The SW pattern obtained for Ic2, at $\alpha = 1.004, g = 0.26$ in region (7). This pattern is unstable.
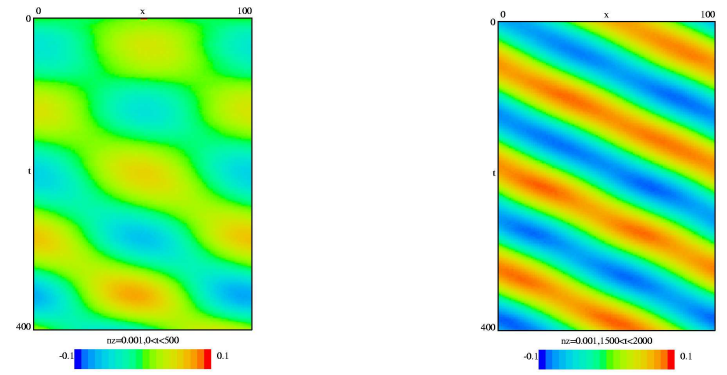
Figure 2.18. The SW pattern obtained at $\alpha = 1.004, g = 0.26$ for Ic2 is destabilized to TW in the presence of noise.
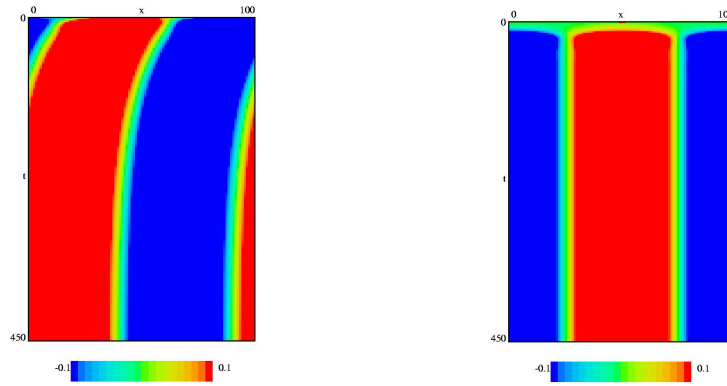
Figure 2.19. The SS pattern obtained at $\alpha = 1.08, g = 0.26$ in region (2), close to the bifurcation line L_m for initial conditions (a) Ic1; (b) Ic2.
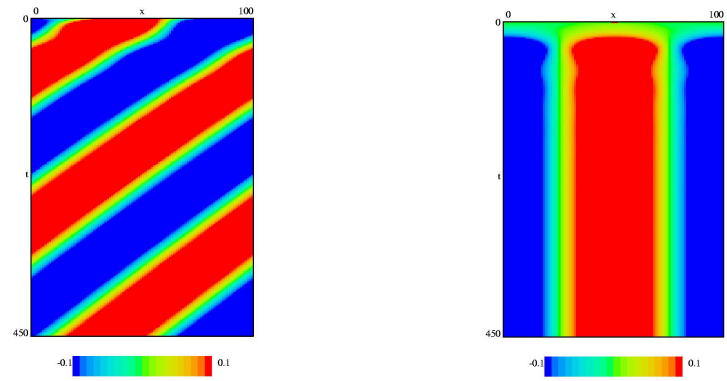
Figure 2.20. At $\alpha = 1.03, g = 0.26$ in region (3) we obtain (a) TW for Ic1; (b) SS for Ic2 (this pattern is unstable).
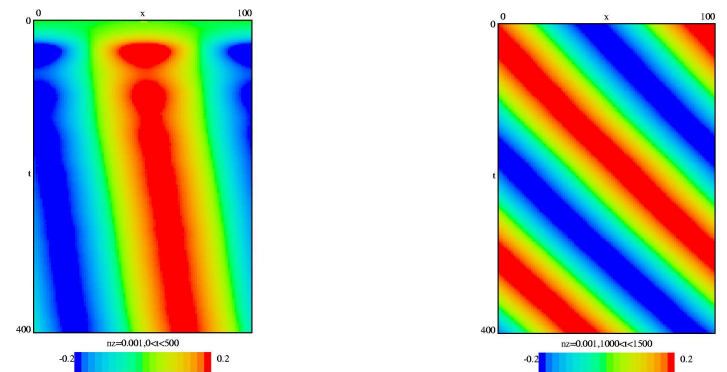
Figure 2.21. The SS pattern obtained at $\alpha = 1.03, g = 0.26$ for Ic2 is destabilized to TW in the presence of noise.

60
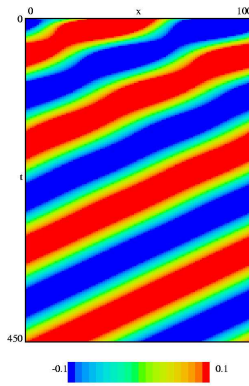
Figure 2.22. At $\alpha = 1.0122, g = 0.26$ in region (4), starting with Ic1 initial conditions a TW pattern is formed.
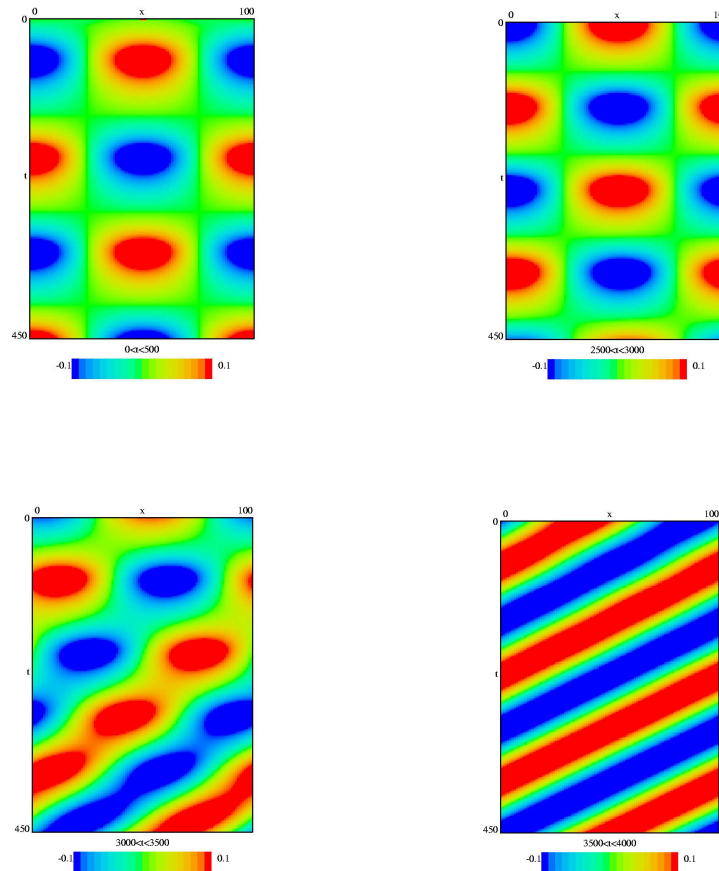
Figure 2.23. At $\alpha = 1.0122, g = 0.26$ in region (4), starting with Ic2 initial conditions, a SW pattern is formed. Nevertheless it is destabilized in time to a TW.
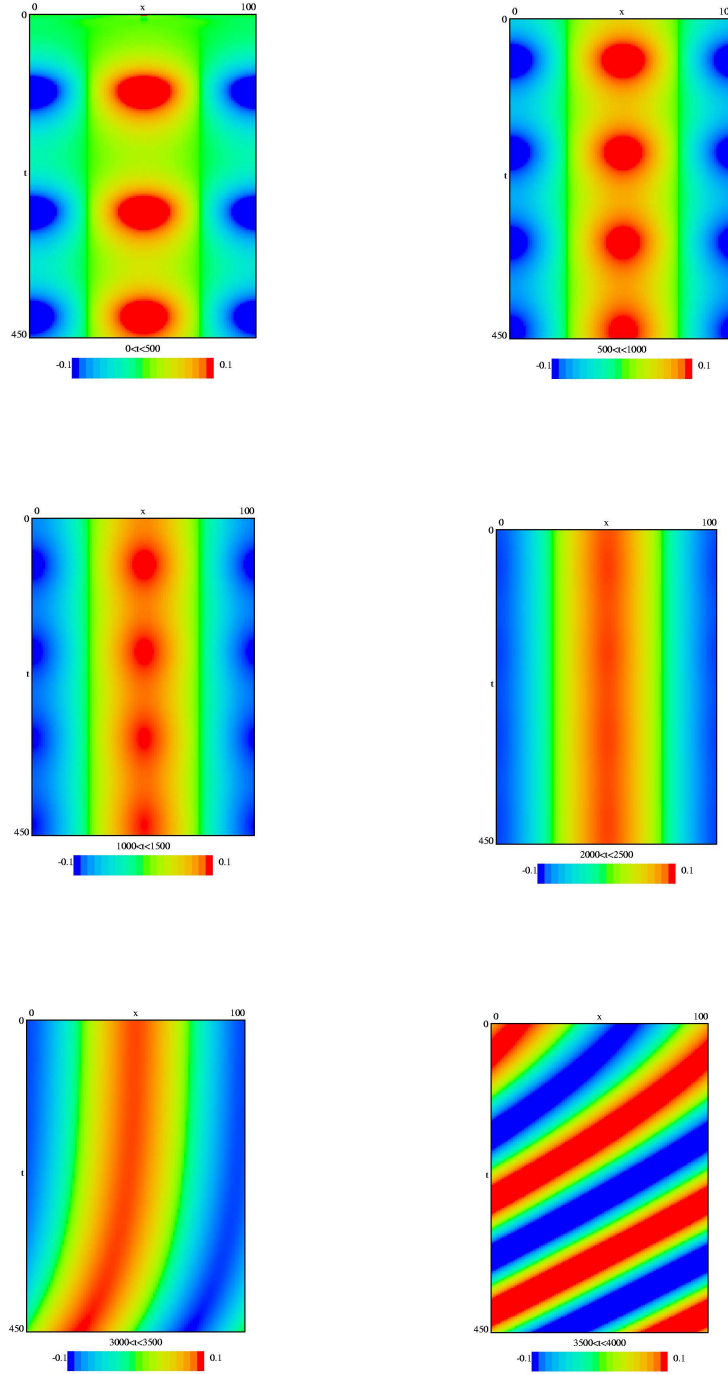
Figure 2.24. At $\alpha = 1.0122, g = 0.26$ in region (4), starting with Ic3 initial conditions, a SS pattern is formed. Nevertheless it is destabilized in time to a TW.
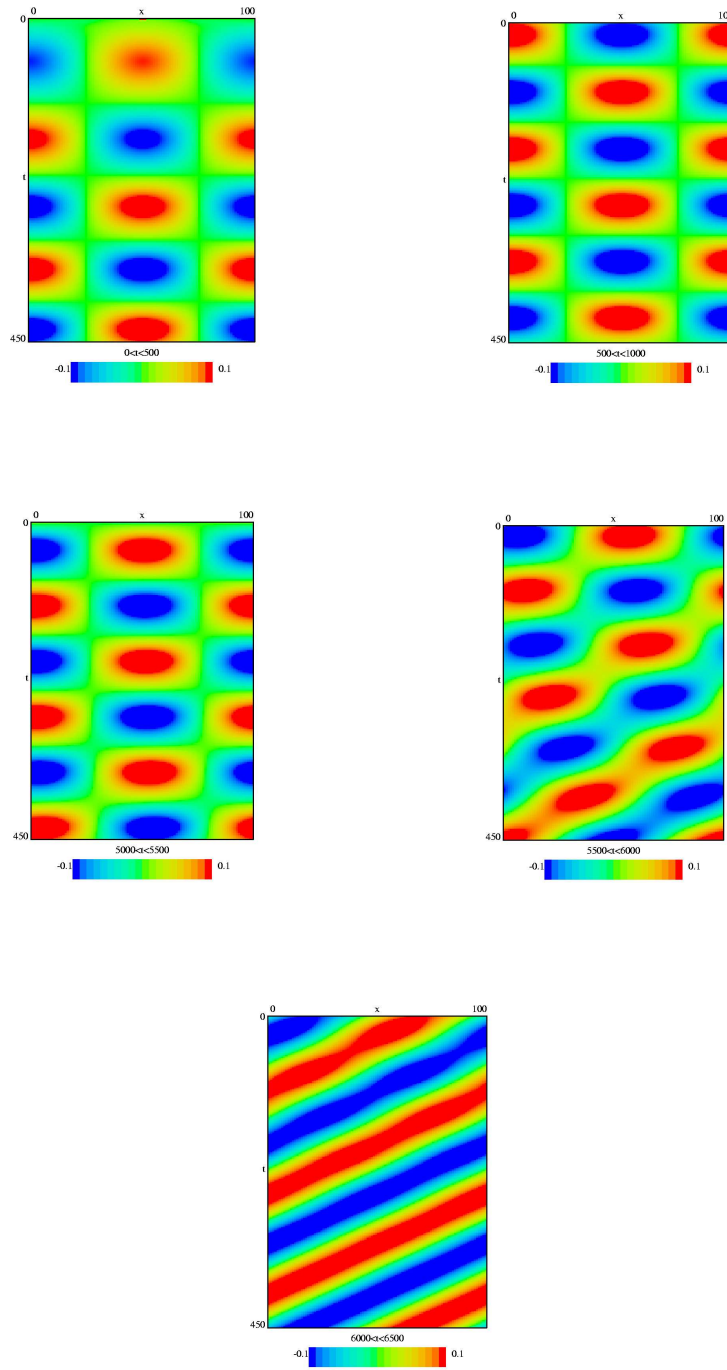
Figure 2.25. At $\alpha = 1.009, g = 0.26$ in region (6), a SW pattern may form, but it destabilizes in time to a TW.

Chapter 3

Multiple-spike waves in a one-dimensional integrate-and-fire neural network

3.1 Introduction

Traveling waves in networks of neurons with purely excitatory synaptic coupling have been the object of many recent theoretical studies [10, 11, 33, 40, 45, 44, 79, 81, 80, 82, 84]. These studies are motivated by experiments in which a slice of cortical tissue, with all inhibition blocked, is subjected to a local shock stimulus. This stimulus results in a wave of activity propagating across the network [17, 18, 43, 66, 98]. Theoretical models of this phenomenon range from continuum firing rate models [2], [84] to simplified spiking models [10, 33, 82] to detailed conductance-based models [43], [98].

Firing rate models do not include individual spikes; as a result, the temporal details of neuronal activity cannot be considered. In spiking models (and in experiments), it becomes apparent that after the first wave front passes through a network, a single neuron can fire many times [43]. However, theoretical analysis of spiking models has, with few exceptions, required that *each neuron fire exactly once* during wave propagation. This is either *a priori* imposed on the model or implemented by strong synaptic depression or after-hyperpolarization. In the single-spike case, the existence of traveling waves is reduced to solving a certain nonautonomous boundary value problem [33], [82]. This computation can be done explicitly when the individual neurons are modeled by the leaky integrate-and-fire (LIF) model. Ermentrout [33], Bressloff [10] and Golomb and Ermentrout [45], [44] developed methods for studying the existence of traveling waves of activity in networks of LIF cells, incorporating a variety of additional features such as synaptic delays, again under the assumption that each cell only fires once. Under this assumption it is also possible to obtain an expression for the wave velocity c [80].

The aim of this work is to address several questions related to networks of spiking neurons in which *each cell fires multiple spikes* during wave propagation. As with most previous analysis, we

will restrict our attention to an excitatorily coupled network of LIF neurons. Recall that the LIF model for an individual neuron has the form

$$\tau_1 \frac{dV}{dt} = -V + I(t),$$

where $I(t)$ represents inputs and τ_1 is the membrane time constant. If $V(t^-) = V_T$, the voltage threshold, then $V(t^+) = V_R$, the reset voltage, and the neuron emits a "spike." We can formally rewrite this equation to take into account the resetting as

$$\tau_1 \frac{dV}{dt} = -V + I(t) + \tilde{V}_R \sum_n \delta(t - t_n) \tag{3.1}$$

where $\tilde{V}_R = \tau_1(V_R - V_T)$ and t_n denotes the sequence of firing times of the neuron; that is, $V(t_n^-) = V_T$ for each $n \geq 1$. Henceforth, we omit the $-$ (minus) superscript when taking the limit of V as t approaches a firing time from the left.

We consider a continuous network of such neurons, coupled in a translationally invariant manner on an infinite one-dimensional domain and parameterized by the spatial variable, x. The model is identical to those studied in many of the papers mentioned above. Coupling between a neuron at position x and one at position y is mediated by a time-dependent current with maximal strength depending on the distance, $|x - y|$. Each time a neuron fires, it activates a potential defined by a fixed function, $\alpha(t)$, which vanishes for $t < 0$, is typically positive for $t > 0$, and decays to zero as $t > 0$ increases. With these considerations, the network of interest is:

$$\tau_1 \frac{\partial V}{\partial t} = -V(x,t) + g \sum_{n=-\infty}^{\infty} \int_{-\infty}^{\infty} dy\, J(x-y)\, \alpha(t - t_n^*(y)) + \sum_{n=-\infty}^{\infty} \delta(t - t_n^*(x))\, \tilde{V}_R \tag{3.2}$$

for $(x,t) \in \mathbb{R} \times \mathbb{R}$, where $\tilde{V}_R$ is given in (3.1); we assume that V_T is positive and $V_R < V_T$. In this continuous network, note that the firing times $t_n^*(x)$ have a spatial dependence. Integration of (3.2) yields $V(x, t_n^*(x)) = V_T$ and $V(x, t_n^{*+}(x)) = V_R$, which verifies that the constant $\tilde{V}_R$ is defined appropriately.

In (3.2), the parameter g denotes maximal synaptic coupling strength, while $J(x) : \mathbb{R} \to \mathbb{R}^+ \cup \{0\}$ is the synaptic coupling function, with integral 1. Any integrable, even, non-negative

function could be used here. We take

$$\alpha(t) = e^{-t/\tau_2} H(t) = \begin{cases} 0, & t < 0 \\ e^{-t/\tau_2}, & t \geq 0 \end{cases} \tag{3.3}$$

where $H(t)$ is the Heaviside step function, $\tau_1 < \tau_2$ and

$$J(x) = \frac{1}{2\sigma} e^{-|x|/\sigma} . \tag{3.4}$$

In this chapter, we provide a framework for the study of traveling waves with arbitrary (finite or countably infinite) collections of spike times. We first, in Section 3.2, provide a reformulation of (3.2) which is particularly suitable for the study of traveling waves. In Section 3.3, we use this to provide a necessary and sufficient condition for the existence of single-spike traveling waves, thereby completing the partial study of such waves begun in [10], [33], and to analyze two-spike traveling waves.

We analytically calculate the interspike interval for a two-spike wave, and then in Section 3.4 we consider traveling wave solutions for which each cell spikes at an infinite sequence $\{T_n(x)\}, n \geq 0$, of spike times. Our traveling wave formulation can be used naturally for the iterative computation of the interspike intervals $T_{n+1} - T_n$ that must arise for such a solution to be consistent with equations (3.2), (3.3), (3.4).

Further considerations regarding periodic solutions, the derivation of a three-branched dispersion relation between wave speed c and period T and the case when the absolute refractory period is included in the model are made in [78].

3.2   Traveling wave description

We begin by considering constant speed traveling wave solutions of (3.2) for which each cell has a finite first spike time.

For non-periodic solutions, the n-th spike time, $n \geq 0$, of the neuron at the position x can be written as $t_n^*(x) = \frac{x}{c} + T_n$. Here we assume $T_0 = 0$, and $\{T_n\}_{n\geq 0}$ is a sequence of nonnegative numbers $T_0 = 0 < T_1 \leq \ldots \leq T_N \leq \ldots$, with strict inequality as long as the T_n are finite. Traveling

wave solutions of (3.2) take the form $V(x, t) = V(\xi)$ for traveling wave coordinate $\xi = tc - x \in \mathbb{R}$, where c denotes the traveling wave velocity. In terms of this coordinate, and under the assumption that each cell's first spike occurs at a finite time, equation (3.2) becomes

$$\tau_1 c V'(\xi) = -V(\xi) + g \sum_{n=0}^{\infty} \int_{-\infty}^{\infty} du J(u - \xi) \alpha(u/c - T_n) + \sum_{n=0}^{\infty} \delta(\xi/c - T_n) \tilde{V}_R. \tag{3.5}$$

A traveling wave solution of (3.5) is obtained by direct integration. For such a solution to be valid, it must satisfy a self-consistency condition, which we state here. This consistency condition relates the asymptotic behavior of V as $\xi \to -\infty$ with the fact that V reaches threshold for the first time at $\xi = 0$. In the limit as $\xi \to -\infty$, the synaptic input to each cell becomes 0 (that is, all wave fronts become infinitely far away from each cell). Since solutions of the equation $\tau_1 c V'(\xi) = -V(\xi)$ decay to 0, the consistency condition states that the potential of each neuron must satisfy $\lim_{\xi \to -\infty} V(\xi) = 0$. Upon integration of (3.5) from $\xi = -\infty$ to $\xi = 0$, using $V(0) = V_T$, this condition formally yields

$$V_T = \frac{g \left(\sum_{n=0}^{\infty} e^{-\frac{c T_n}{\sigma}} \right)}{2 \left(\frac{\tau_1 c}{\sigma} + 1 \right) \left(1 + \frac{\sigma}{\tau_2 c} \right)}. \tag{3.6}$$

The derivation of the consistency condition (3.6) will become more clear in Section 3.2.2.

For expression (3.6) to be meaningful, a second condition must hold, namely that the series $\sum_{n=0}^{\infty} e^{-c T_n / \sigma}$ is convergent; we will only consider traveling wave solutions for which this is true. Clearly this holds if each neuron fires only a finite number M of times. In this case, we obtain $T_0 = 0 < T_1 < \ldots < T_{M-1} < \infty$ and set $T_n = \infty$ for all $n \geq M$; thus, the series becomes the finite sum $\sum_{n=0}^{\infty} e^{-c T_n / \sigma} = \sum_{n=0}^{M-1} e^{-c T_n / \sigma}$.

Using the consistency condition (3.6), integration of (3.5) up to arbitrary ξ yields

$$V(\xi) = V_T e^{-\xi/\tau_1 c} + I_{syn}(\xi) + R(\xi). \tag{3.7}$$

The function $R(\xi)$ is the "decaying reset," encoding the refractoriness of a cell after a spike. This is given by $R(\xi) = \sum_{n=0}^{\infty} \eta(\xi/c - T_n)$ where

$$\eta(t) = 0, \, t \leq 0; \quad \eta(t) = (V_R - V_T) e^{-t/\tau_1}, \, t > 0 \tag{3.8}$$

and $I_{syn}(\xi)$ is the "synaptic integral"

$$
\begin{aligned}
I_{syn}(\xi) &= \frac{g}{\tau_1 c} e^{-\xi/\tau_1 c} \int_0^\xi ds \left[\sum_{n=0}^\infty \int_0^\infty du\, J(u + cT_n - s)\alpha(u/c) \right] e^{s/\tau_1 c} \\
&\equiv (e^{-\xi/\tau_1 c}/\tau_1 c) \int_0^\xi ds \left(\sum_{n=0}^\infty I_n(s) \right) e^{s/\tau_1 c}.
\end{aligned}
\tag{3.9}
$$

On each interval between two consecutive spikes the decaying reset has the form

$$
R(\xi) = \begin{cases}
0 & , \xi \le 0 \\[2mm]
(V_R - V_T) \left(\sum_{n=0}^{N-1} e^{T_n/\tau_1} \right) e^{-\xi/\tau_1 c} & , cT_{N-1} < \xi \le cT_N \ (N \ge 1).
\end{cases}
$$

The balance between the input from the synaptic integral and the reset after spiking determines what types of constant speed wave fronts can propagate in the neural network.

3.2.1 Computation of synaptic currents

We now derive the synaptic current due to the n-th front of the traveling wave, $I_n(s) = g \int_0^\infty du\, J(u + cT_n - s)\alpha(u/c)$, at some point s on the traveling wave coordinate axis.

Suppose we freeze the time t and record what happens at each position in space along the neural network. Without loss of generality, we fix our point of reference at $x = 0$, where by assumption the first spike occurs at $t = 0$ (such that $\xi = ct - x = 0$).

For any fixed negative time t, none of the wave fronts has yet reached the point $x = 0$, and all synaptic current results from waves that will arrive in the future. The n-th front ($n \ge 0$) will reach $x = 0$ at time T_n. Hence, one can derive the position y_n of the n-th front at time $t < T_n$ from $0 - y_n = c(T_n - t)$, which gives $y_n = c(t - T_n) < 0$. Correspondingly, the current (measured at $x = 0$) that is induced by this front ("future wave")at time t is

$$
I_{n;f}(t) = g \int_{-\infty}^{c(t-T_n)} dy\, J(y)\, \alpha(t - y/c - T_n).
$$

Written in the wave coordinates ($s = ct - x = ct$, $u = ct - y - cT_n = s - y - cT_n$), and using the fact that J is an even function and that $u + cT_n - s = -y > 0$, this becomes

$$
I_n(s) \equiv I_{n;f}(s) = g \int_0^\infty du\, J(u + cT_n - s)\, \alpha(u/c) = \frac{g}{2\sigma} \int_0^\infty du\, e^{-(u + cT_n - s)/\sigma} e^{-u/\tau_2 c} = \frac{g\, e^{-cT_n/\sigma}}{2(1 + \frac{\sigma}{\tau_2 c})} e^{s/\sigma}
$$

68
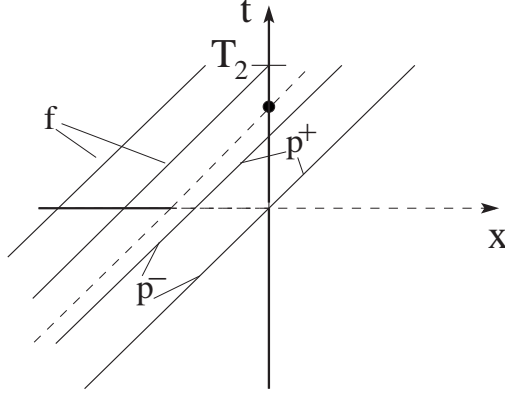
Figure 3.1. Illustration of incoming waves relative to the cell at $x = 0$.

In summary, for t (and thus s) negative, all the synaptic currents correspond to "future waves" $(I_{n;f})$ and the total current at s is

$$I_{total}(s) = \sum_{n=0}^{\infty} I_n(s) = \frac{g\left(\sum_{n=0}^{\infty} e^{-cT_n/\sigma}\right)}{2(1 + \frac{\sigma}{\tau_2 c})} e^{s/\sigma} . \tag{3.10}$$

At any fixed nonnegative time t (such that $s = ct \geq 0$), say between two consecutive spike-times $T_{N-1} < t \leq T_N$, there are "previous wave" fronts that have already passed through $x = 0$ and many others that have yet to arrive. The position reached by each front at the moment t can be found by the same formula, $y_n = c(t - T_n)$, as above; the only difference is that $y_n > 0$ for all previous waves $(n = 0, \ldots, N - 1)$ and $y_n \leq 0$ for all "future waves" $(n \geq N)$.

Remark 3.1. The above classification of waves is illustrated in Figure 3.1. At the time labelled with the solid black circle on the t-axis, the two waves labelled with 'f' are future waves for the cell at $x = 0$, as they have not yet reached $x = 0$; one of them will arrive at time T_2 and the other at time T_3 (not shown). The two waves to the right of the diagonal dashed line are previous waves, as they have already passed through $x = 0$. We subdivide the synaptic contribution from these waves into p^- and p^+, below and above the horizontal dashed line, respectively; these correspond to synaptic inputs from spikes that occurred for some $t < 0$ and from spikes that occurred for some time $t > 0$, respectively. The synaptic currents are characterized below.

Synaptic current due to a future wave $(n \geq N)$

$$I_n(s) = I_{n;\,f}(s) = g \int_{-\infty}^{c(t-T_n)} dy \, J(y) \, \alpha(t - y/c - T_n) = g \int_0^{\infty} du \, J(u + cT_n - s) \, \alpha(u/c)$$

$$= \frac{g \, e^{-cT_n/\sigma}}{2(1 + \frac{\sigma}{\tau_2 c})} \, e^{s/\sigma} \,.$$

Synaptic current due to a previous wave $(n = 0, \ldots, N - 1)$

$$I_n(s) = I_{n;\,p}(s) = g \int_{-\infty}^{c(t-T_n)} dy \, J(y) \, \alpha(t - y/c - T_n) = I_{n;\,p^-}(s) + I_{n;\,p^+}(s)$$

where

$$I_{n;\,p^-}(s) = g \int_{-\infty}^{0} dy \, J(y) \, \alpha(t - y/c - T_n) = g \int_{s-cT_n}^{\infty} du \, J(u + cT_n - s) \, \alpha(u/c)$$

$$= \frac{g}{2\sigma} \int_{s-cT_n}^{\infty} du \, e^{-(u+cT_n-s)/\sigma} e^{-u/\tau_2 c} = \frac{g \, e^{T_n/\tau_2}}{2(1 + \frac{\sigma}{\tau_2 c})} \, e^{-s/\tau_2 c} \,.$$

and

$$I_{n;\,p^+}(s) = g \int_0^{c(t-T_n)} dy \, J(y) \, \alpha(t - y/c - T_n) = g \int_0^{s-cT_n} du \, J(u + cT_n - s) \, \alpha(u/c)$$

$$= \frac{g}{2\sigma} \int_0^{s-cT_n} du \, e^{(u+cT_n-s)/\sigma} e^{-u/\tau_2 c} = \frac{g \, e^{T_n/\tau_2}}{2(1 - \frac{\sigma}{\tau_2 c})} \, e^{-s/\tau_2 c} - \frac{g \, e^{cT_n/\sigma}}{2(1 - \frac{\sigma}{\tau_2 c})} \, e^{-s/\sigma} \,.$$

Total current

$$I_{total}(s) = \sum_{n=0}^{\infty} I_n(s) = \sum_{n=0}^{N-1} I_{n;\,p}(s) + \sum_{n=N}^{\infty} I_{n;\,f}(s) = \tag{3.11}$$

$$= \frac{g \left(\sum_{n=0}^{N-1} e^{T_n/\tau_2} \right)}{1 - \frac{\sigma^2}{\tau_2^2 c^2}} \, e^{-s/\tau_2 c} - \frac{g \left(\sum_{n=0}^{N-1} e^{cT_n/\sigma} \right)}{2(1 - \frac{\sigma}{\tau_2 c})} \, e^{-s/\sigma} + \frac{g \left(\sum_{n=N}^{\infty} e^{-cT_n/\sigma} \right)}{2(1 + \frac{\sigma}{\tau_2 c})} \, e^{s/\sigma} \,.$$

3.2.2 The traveling wave solution

Once the synaptic integral $I_{syn}(\xi)$ in (3.9) is computed by integrating $I_{total}(s) = \sum_{n=0}^{\infty} I_n(s)$, the right hand side of expression (3.7) for the solution $V(\xi)$ is completely specified. The necessary

condition (3.6) that we imposed at the beginning of our analysis now appears in the form of $I_{syn}(s)$ for $\xi \leq 0$, i.e.

$$I_{syn}(\xi) = \frac{g\left(\sum_{n=0}^{\infty} e^{-cT_n/\sigma}\right)}{2(\frac{\tau_1 c}{\sigma} + 1)(1 + \frac{\sigma}{\tau_2 c})}\left(e^{\xi/\sigma} - e^{-\xi/\tau_1 c}\right).$$

That is, if (3.6) holds, then the terms $V_T e^{-\xi/\tau_1 c}$ and $I_{syn}(\xi)$ in (3.7) sum to $V_T e^{\xi/\sigma}$, such that $V(\xi) \to 0$ as $\xi \to -\infty$. Moreover, as we expected, the equations $V(0) = V_T$ and $V(cT_N^+) = \lim_{\xi \searrow cT_N} V(\xi) = (V_R - V_T) + V(cT_N) = V_R$ are valid. These results are summarized in Lemma 3.2.1 below. A more concise expression for $V(\xi)$ is provided in Theorem 3.1; however, we shall see that for practical purposes, Lemma 3.2.1 is very useful.

Lemma 3.2.1. *If condition (3.6) is true, then the following function $V(\xi)$, $\xi = tc - x$, is a traveling wave solution of the integro-differential equation (3.2), if all of the terms converge as $\xi, N \to \infty$.*

$$V(\xi) = V_T\, e^{\xi/\sigma}, \;\; \xi \leq 0,$$

$$V(\xi) = \left[V_T - \frac{g\left(\sum_{n=0}^{N-1} e^{-cT_n/\sigma}\right)}{2(\frac{\tau_1 c}{\sigma}+1)(1+\frac{\sigma}{\tau_2 c})}\right] e^{\xi/\sigma} + \frac{g\left(\sum_{n=0}^{N-1} e^{cT_n/\sigma}\right)}{2(\frac{\tau_1 c}{\sigma}-1)(1-\frac{\sigma}{\tau_2 c})} e^{-\xi/\sigma} + \frac{g\left(\sum_{n=0}^{N-1} e^{T_n/\tau_2}\right)}{(1-\frac{\sigma^2}{\tau_2^2 c^2})(1-\frac{\tau_1}{\tau_2})} e^{-\xi/\tau_2 c} -$$

$$-\frac{g\left(\sum_{n=0}^{N-1} e^{T_n/\tau_1}\right)}{(1-\frac{\sigma^2}{\tau_1^2 c^2})(1-\frac{\tau_1}{\tau_2})} e^{-\xi/\tau_1 c} + (V_R - V_T)\left(\sum_{n=0}^{N-1} e^{T_n/\tau_1}\right) e^{-\xi/\tau_1 c}, \; cT_{N-1} < \xi \leq cT_N(N \geq 1).$$

$$(3.12)$$

Theorem 3.1. [general traveling wave solution] *If condition (3.6) is true, then the following expression for $V(\xi)$, $\xi = tc - x$, denotes a traveling solution of the integrate-and-fire model (3.2), if it converges:*

$$V(\xi) = \sum_{n=0}^{\infty} \eta(\xi/c - T_n) + g\sum_{n=0}^{\infty} \int_0^{\infty} J(u - \xi + cT_n)\, A(u/c)\, du. \qquad (3.13)$$

In (3.13), η is defined by (3.8) and A is defined as the convolution function $A(t) = \alpha * \beta\,(t) = \int_0^t \alpha(s)\, \beta(t-s)\, ds$ with $\beta(t) = \frac{1}{\tau_1} e^{-t/\tau_1}$, i.e.

$$A(t) = 0, \; t \leq 0; \;\; A(t) = \frac{1}{1 - \tau_1/\tau_2}\left(e^{-t/\tau_2} - e^{-t/\tau_1}\right), \; t > 0.$$

Remark 3.2. For any traveling wave solution with a finite number of spikes, as discussed in the next section, convergence is not an issue.

71

3.3 Solutions with a finite number of spikes

3.3.1 One-spike traveling waves

We focus first on the case of a solitary wave with speed c and corresponding firing time $t^*(x) = x/c$. In the notation introduced in Section 3.2, $T_0 = 0$ and $T_N = \infty$ for all $N \geq 1$. Therefore equation (3.6) reads

$$V_T = \frac{g}{2\left(\frac{\tau_1 c}{\sigma} + 1\right)\left(1 + \frac{\sigma}{\tau_2 c}\right)} \qquad (3.14)$$

and can be solved exactly for c, if $g/V_T \geq 2\left(1 + \sqrt{\frac{\tau_1}{\tau_2}}\right)^2$. This necessary condition for the existence of a one-spike wave was used as an existence criterion in [11], [33], [80]. When this condition holds, there exist two candidate solutions, the *slow wave* and the *fast wave*, corresponding to

$$c_{\text{slow ; fast}} = \frac{\sigma}{2\tau_1}\left[\frac{g}{2V_T} - \frac{\tau_1}{\tau_2} - 1 \mp \sqrt{\left(\frac{g}{2V_T} - \frac{\tau_1}{\tau_2} - 1\right)^2 - 4\frac{\tau_1}{\tau_2}}\right].$$

As g/V_T increases from its minimal critical value to infinity, c_{slow} decreases from $\sigma/\sqrt{\tau_1 \tau_2}$ to zero and c_{fast} increases from $\sigma/\sqrt{\tau_1 \tau_2}$ to infinity. We will denote the curve $g/V_T = 2\left(1 + \sqrt{\frac{\tau_1}{\tau_2}}\right)^2$ as 1_F below.

Remark 3.3. In what follows, we analyze the fast one-spike traveling wave, since only this one is stable [10], [33]. We will simply write c for the velocity c_{fast}.

If a traveling wave solution to (3.2) exists, then it takes the form $V(\xi) = V_T\, e^{\xi/\sigma}$ when $\xi \leq 0$. When $\xi > 0$ it is given by, from Lemma 3.2.1,

$$V(\xi) = (V_R - V_T)\,e^{-\xi/\tau_1 c} + \frac{g\,e^{-\xi/\sigma}}{2(\frac{\tau_1 c}{\sigma} - 1)(1 - \frac{\sigma}{\tau_2 c})} + \frac{g\,e^{-\xi/\tau_2 c}}{(1 - \frac{\sigma^2}{\tau_2^2 c^2})(1 - \frac{\tau_1}{\tau_2})} - \frac{g\,e^{-\xi/\tau_1 c}}{(1 - \frac{\sigma^2}{\tau_1^2 c^2})(1 - \frac{\tau_1}{\tau_2})}.$$

Note that $\lim_{\xi \to \pm\infty} V(\xi) = 0$, $V(0) = V_T$, and $V(0^+) = V_R$.

The next step is to check that the candidate solution above indeed has no other spike after it passes $\xi = 0$; that is, the spiking threshold is never reached again. Therefore we must verify that $V(\xi) < V_T$ for all positive ξ. This is not true in general for reasons that are simple to understand. At fixed V_R, as $g/V_T \to \infty$, it becomes increasingly easier for the individual neurons to re-excite and spike again. We compute in the following the equation of a curve, call it 1_S, which separates

the $(g/V_T, -V_R/V_T)$ plane to the right of 1_F into two disjoint regions: a region where the one-spike fast wave solution exists and a region where it does not.

Theorem 3.2. [a necessary and sufficient condition for the existence of the fast one-spike traveling wave solution] *The integrate-and-fire model (3.2) has a one-spike fast wave solution if and only if*

$$g/V_T \geq 2 \left(1 + \sqrt{\frac{\tau_1}{\tau_2}} \right)^2 \tag{3.15}$$

and the reset voltage value satisfies

$$(-V_R/V_T) > (H(y^*) - 1), \tag{3.16}$$

where H is defined by

$$H(y) = \frac{1}{y^{\sigma/\tau_1 c}} \left[y - 1 + \frac{g/V_T}{1 - \frac{\tau_1}{\tau_2}} \left(\frac{y^{\sigma/\tau_2 c} - y}{1 - \frac{\sigma^2}{\tau_2^2 c^2}} - \frac{y^{\sigma/\tau_1 c} - y}{1 - \frac{\sigma^2}{\tau_1^2 c^2}} \right) \right] \tag{3.17}$$

and y^* is the unique solution in the interval $(0,1)$ of the equation $G(y) = 0$ with

$$G(y) = y - \frac{2\tau_2 c}{\tau_2 c + \sigma} y^{\sigma/\tau_2 c} + \frac{\sigma(\tau_2 c - \sigma)}{(\tau_1 c + \sigma)(\tau_2 c + \sigma)}. \tag{3.18}$$

When (3.15) holds, for values of V_R for which (3.16) fails, there exists a positive ξ where the threshold V_T is reached again, so the one-spike condition is violated.

Proof: We sketch the proof here and provide technical details in Appendix C.0.1.

Set $y = e^{-\xi/\sigma}$. The condition $V(\xi) < V_T$ for all positive ξ reads as $V(y) < V_T$ for all $y \in (0,1)$, which is equivalent to $H(y) < (-V_R/V_T + 1)$ with H defined by (3.17).

We analyze $H(y)$ and obtain that $H'(y) = \frac{\tau_2}{2\tau_1} \frac{\sigma}{\tau_2 c - \sigma} \frac{g}{V_T} y^{-(1+\sigma/\tau_1 c)} G(y)$. The sign of $H'(y)$ is the sign of $G(y)$ since for the fast wave we have $c \geq \sigma/\sqrt{\tau_1\tau_2} > \sigma/\tau_2$.

On the interval $[0,1]$, the function G satisfies

$$G(0) = \frac{\sigma(\tau_2 c - \sigma)}{(\tau_1 c + \sigma)(\tau_2 c + \sigma)} > 0, \ G(1) = -\frac{\tau_1 c(\tau_2 c - \sigma)}{(\tau_1 c + \sigma)(\tau_2 c + \sigma)} < 0;$$

Moreover it can be proved that G has exactly one zero in this interval, say y^*. Hence, $H(y)$ has a maximum at $y = y^*$, and further, $\lim_{y \searrow 0} H(y) = -\infty$ and $H(1) = 0$. Together, these imply $H(y^*) > 0$. In summary, $V(\xi) < V_T$ for all $\xi > 0$ if and only if $(-V_R/V_T) > (H(y^*) - 1)$.

Remark 3.4. A special case occurs at $g/V_T = 4(1 + \tau_1/\tau_2)$, where the fast wave has the velocity $c = \sigma/\tau_1$ and $V(\xi) = V_T \left(-\frac{2(\tau_2+\tau_1)}{\tau_2-\tau_1} \frac{\xi}{\sigma} e^{-\xi/\sigma} + \frac{4\tau_2^2}{(\tau_2-\tau_1)^2} e^{-\tau_1\xi/\tau_2\sigma} - \frac{3\tau_2^2+2\tau_1\tau_2-\tau_1^2}{(\tau_2-\tau_1)^2} e^{-\xi/\sigma} \right) + (V_R - V_T) e^{-\xi/\sigma}$. In this case, the definition of H changes in the following way: the ratio $\frac{y^{\sigma/\tau_1 c}-y}{1-\sigma^2/\tau_1^2 c^2} = -\left(\frac{y\tau_1 c}{\tau_1 c+\sigma}\right)\left(\frac{y^{\frac{\sigma}{\tau_1 c}-1}-1}{\frac{\sigma}{\tau_1 c}-1}\right)$ becomes $-\frac{\tau_1 c}{\tau_1 c+\sigma} y \ln(y)$, or equivalently $-\frac{1}{2} y \ln(y)$. In the computation of G, the logarithm cancels and we again end up with expression (3.18), i.e. y^* is again the unique solution of the equation $G(y) = 0$ on $(0, 1)$.

Remark 3.5. The curve 1_S which divides the plane $(g/V_T, -V_R/V_T)$ into the two regions mentioned above has the equation

$$-V_R/V_T = H(y^*) - 1 \,.$$

To see that this really forms a curve in the $(g/V_T, -V_R/V_T)$ plane, note that $y^* = y^*(\sigma, \tau_1, \tau_2, c)$, with c depending on g/V_T. If we fix all parameters except g/V_T, then we get $H(y^*) = H(y^*(g/V_T))$.

Remark 3.6. Recall that the equation $g/V_T = 2\left(1 + \sqrt{\frac{\tau_1}{\tau_2}}\right)^2$ defines the curve 1_F in the plane $(g/V_T, -V_R/V_T)$. Theorem 3.2 states that to obtain a one-spike traveling wave in the integrate-and-fire model, the parameters must lie to the right of the curve 1_F for firing to occur, and above the curve 1_S for firing to stop after one spike. That is, the first condition allows for self-sustained propagation of the traveling wave, while the second prevents multiple spikings by resetting the potential to low enough values. These curves are displayed in Figure 3.2 for a representative parameter set.

3.3.2   Two-spike traveling waves

In a two-spike traveling wave, each cell fires at times that we denote $T_0 = 0$ and $T_1 = T$. In our earlier notation, this also means $T_j = \infty$ for each $j \geq 2$. In this case, equation (3.6) and substitution of the condition $V(cT) = V_T$ into (3.12) in Lemma 3.2.1 read as

$$V_T = \frac{g\left(1 + e^{-cT/\sigma}\right)}{2(\frac{\tau_1 c}{\sigma} + 1)(1 + \frac{\sigma}{\tau_2 c})}, \tag{3.19}$$

$$V_T = (V_R - V_T)\,e^{-T/\tau_1} + \frac{g}{2(\frac{\tau_1 c}{\sigma} + 1)(1 + \frac{\sigma}{\tau_2 c})} + \frac{g\,e^{-cT/\sigma}}{2(\frac{\tau_1 c}{\sigma} - 1)(1 - \frac{\sigma}{\tau_2 c})} +$$

$$+ \frac{g\,e^{-T/\tau_2}}{(1 - \frac{\sigma^2}{\tau_2^2 c^2})(1 - \frac{\tau_1}{\tau_2})} - \frac{g\,e^{-T/\tau_1}}{(1 - \frac{\sigma^2}{\tau_1^2 c^2})(1 - \frac{\tau_1}{\tau_2})}\,. \tag{3.20}$$

74
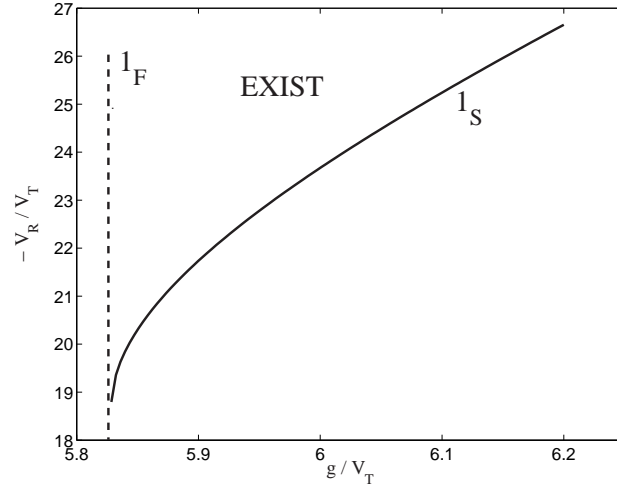
Figure 3.2. The curves 1_F and 1_S for $\tau_1 = 1, \tau_2 = 2, \sigma = 1, V_T = 1$. Parameter values must lie to the right of 1_F for cells to be able to fire upon receiving the one-spike synaptic input. Parameter values must lie above 1_S for cells to stop firing after just one spike. Between the two curves, one-spike waves exist in the region labelled EXIST. Note that 1_S terminates in an intersection with 1_F, at $g/V_T = 2(1 + \sqrt{\tau_1/\tau_2})^2$ with $-V_R/V_T$ finite and positive.
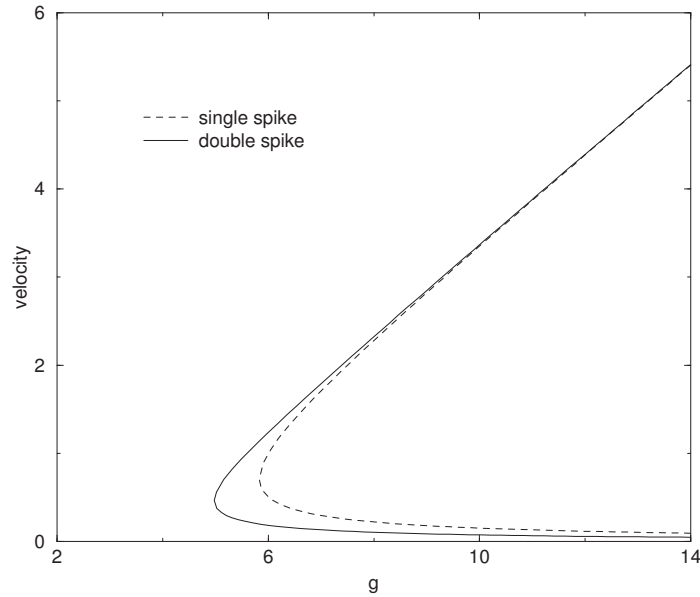
Figure 3.3. Numerically generated curves showing wave speed as a function of coupling strength for one- and two-spike waves.

With the definition

$$f(c) = \frac{2}{g/V_T} \left(\frac{\tau_1 c}{\sigma} + 1 \right) \left(1 + \frac{\sigma}{\tau_2 c} \right) - 1 \tag{3.21}$$

we obtain according to (3.19) an explicit equation for T,

$$T = -\frac{\sigma}{c} \ln f(c). \tag{3.22}$$

We are ready now to investigate under which conditions the system (3.19), (3.20) has a solution (c, T) with positive c and T, i.e. when $f(c)$ is between 0 and 1. Let us define

$$\begin{cases} \tilde{c}_{1;2} = \frac{\sigma}{2\tau_1} \left[\frac{g}{V_T} - \frac{\tau_1}{\tau_2} - 1 \mp \sqrt{\left(\frac{g}{V_T} - \frac{\tau_1}{\tau_2} - 1 \right)^2 - 4\frac{\tau_1}{\tau_2}} \right], \\ c_{1;2} = \frac{\sigma}{2\tau_1} \left[\frac{g}{2V_T} - \frac{\tau_1}{\tau_2} - 1 \mp \sqrt{\left(\frac{g}{2V_T} - \frac{\tau_1}{\tau_2} - 1 \right)^2 - 4\frac{\tau_1}{\tau_2}} \right] \end{cases} \tag{3.23}$$

and notice that $f(c) = 0$ at $c = c_{1;2}$ and $f(c) = 1$ at $c = \tilde{c}_{1;2}$.

The set $S_c = \{ c \in \mathbb{R}^+ \mid f(c) \in (0, 1) \}$ is easily computed: if $g/V_T < \left(1 + \sqrt{\frac{\tau_1}{\tau_2}} \right)^2$ then $S_c = \emptyset$; if $\left(1 + \sqrt{\frac{\tau_1}{\tau_2}} \right)^2 < g/V_T < 2 \left(1 + \sqrt{\frac{\tau_1}{\tau_2}} \right)^2$ then $c_{1;2}$ are complex with nonzero imaginary parts and $S_c = (\tilde{c}_1, \tilde{c}_2)$; if $2 \left(1 + \sqrt{\frac{\tau_1}{\tau_2}} \right)^2 \leq g/V_T$ then $0 < \tilde{c}_1 < c_1 \leq c_2 < \tilde{c}_2$ and $S_c = (\tilde{c}_1, c_1) \cup (c_2, \tilde{c}_2) \subset \mathbb{R}$.

Remark 3.7. $c_1 = c_{\text{slow}}^1$ and $c_2 = c_{\text{fast}}^1$; that is, c_1 and c_2 are the slow and fast velocities from the one-spike wave case. Moreover, $T(c) \to \infty$ as $c \to c_{1;2}$ since we have then $f(c) \searrow 0$.

Remark 3.8. As $g/V_T \to \infty$ we obtain $\tilde{c}_1, c_1 \to 0$, $c_2, \tilde{c}_2 \to \infty$ and $\tilde{c}_2/c_2 \to 2$, $\tilde{c}_1/c_1 \to 1/2$.

The equations (3.20) and (3.22) imply $F(c) = 0$, where

$$F(c) = \left(-\frac{V_R}{V_T} + 1 \right) f(c)^{\frac{\sigma}{\tau_1 c} - 1} + \frac{g/V_T}{1 - \frac{\tau_1}{\tau_2}} \left(\frac{\tau_2 c}{\tau_2 c + \sigma} f_{\tau_2}(c) - \frac{\tau_1 c}{\tau_1 c + \sigma} f_{\tau_1}(c) \right), \tag{3.24}$$

with

$$f_{\tau_i}(c) = \begin{cases} \frac{f(c)^{\frac{\sigma}{\tau_i c} - 1} - 1}{\frac{\sigma}{\tau_i c} - 1} & , \ c \neq \sigma/\tau_i \\ \ln f(\frac{\sigma}{\tau_i}) & , \ c = \sigma/\tau_i \end{cases} \quad (i = 1, 2).$$

The velocities of candidate two-spike traveling wave solutions are precisely the roots of F that belong to the set S_c. Such velocities correspond to true two-spike traveling wave solutions if $V(\xi) < V_T$

for all $\xi > cT$.

Lemma 3.3.1. *The function $F : S_c \to \mathbb{R}$ defined by (3.24) is continuous on S_c and satisfies $F(\tilde{c}_1^+) = F(\tilde{c}_2^-) = -\frac{V_R}{V_T} + 1 > 0$.*

Proof: The result comes directly from the definition of F and the fact that $\lim_{c \to \tilde{c}_{1;2}} f(c) = 1$. Here and below we use the notation $F(x_0^+) = \lim_{x \searrow x_0} F(x)$, $F(x_0^-) = \lim_{x \nearrow x_0} F(x)$.

Lemma 3.3.2. *Suppose that $g/V_T \geq 2\left(1 + \sqrt{\frac{\tau_1}{\tau_2}}\right)^2$, i.e. $S_c = (\tilde{c}_1, c_1) \cup (c_2, \tilde{c}_2)$. Then $F(c_2^+) = -\infty$ and $F(c_1^-) < 0$. Moreover*

i) if $2\left(1 + \sqrt{\frac{\tau_1}{\tau_2}}\right)^2 \leq g/V_T < 4\left(1 + \frac{\tau_1}{\tau_2}\right)$, then $\tilde{c}_1 < \frac{\sigma}{\tau_2} < c_1 \leq c_2 < \frac{\sigma}{\tau_1} < \tilde{c}_2$ and $F(c_1^-) = -\infty$,

ii) if $g/V_T = 4\left(1 + \frac{\tau_1}{\tau_2}\right)$, then $\tilde{c}_1 < c_1 = \frac{\sigma}{\tau_2} < \frac{\sigma}{\tau_1} = c_2 < \tilde{c}_2$ and $F(c_1^-) = -\infty$,

iii) if $g/V_T > 4\left(1 + \frac{\tau_1}{\tau_2}\right)$, then $\tilde{c}_1 < c_1 < \frac{\sigma}{\tau_2} < \frac{\sigma}{\tau_1} < c_2 < \tilde{c}_2$ and

$$F(c_1^-) = -\frac{g}{V_T}\left(1 + \frac{\tau_1}{\tau_2}\right)\frac{\sigma^2}{\tau_1^2 c_1^2 - \sigma^2}\frac{\tau_2^2 c_1^2}{\tau_2^2 c_1^2 - \sigma^2} < 0.$$

Proof: See Appendix C.0.2.

These two lemmas immediately imply the following result. The relation between velocities described in the theorem is shown in the numerical results in Figure 3.3.

Theorem 3.3. *If $g/V_T \geq 2\left(1 + \sqrt{\frac{\tau_1}{\tau_2}}\right)^2$, then for all $V_R \in \mathbb{R}^-$, there exist two distinct positive values $c_S \in (\tilde{c}_1, c_1)$, $c_F \in (c_2, \tilde{c}_2)$ such that $F(c_S) = F(c_F) = 0$. Therefore there exist two distinct solutions (c_S, T_S), (c_F, T_F) for the system (3.19), (3.20).*

When these correspond to two-spike traveling wave solutions, the velocity c_F (c_S) of the fast (slow) two-spike traveling wave solution is greater (less) than that of the fast (slow) one-spike traveling wave solution.

Remark 3.9. The above results apply for $g/V_T \geq 2(1 + \sqrt{\tau_1/\tau_2})^2$. We also expect two-spike traveling waves to exist for some $g/V_T < 2(1 + \sqrt{\tau_1/\tau_2})^2$, since $S_c \neq \emptyset$ for $(1 + \sqrt{\tau_1/\tau_2})^2 < g/V_T < 2(1 + \sqrt{\tau_1/\tau_2})^2$. In fact, in analogy to the one-spike case, we expect that there exist curves 2_F, given by $g/V_T = F_2(-V_R/V_T)$, and 2_S, given by $-V_R/V_T = S_2(g/V_T)$, in the $(g/V_T, -V_R/V_T)$ plane, such that for all g/V_T to the right of 2_F, cells can fire two spikes, while for all $-V_R/V_T$ above 2_S, cells fire at most two spikes.

It is perhaps non-intuitive that, for fixed V_R and V_T, a two-spike traveling wave should exist for smaller g than needed for a one-spike wave. This holds because in a two-spike wave, the two
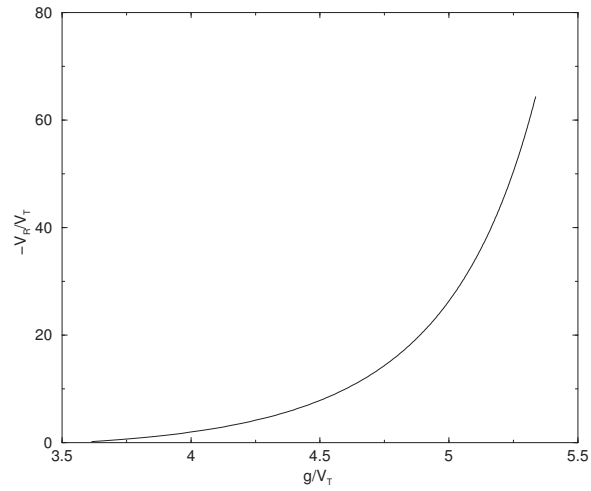
Figure 3.4. Numerically generated 2_F curve. To the right of this in parameter space, cells can propagate two-spike waves.
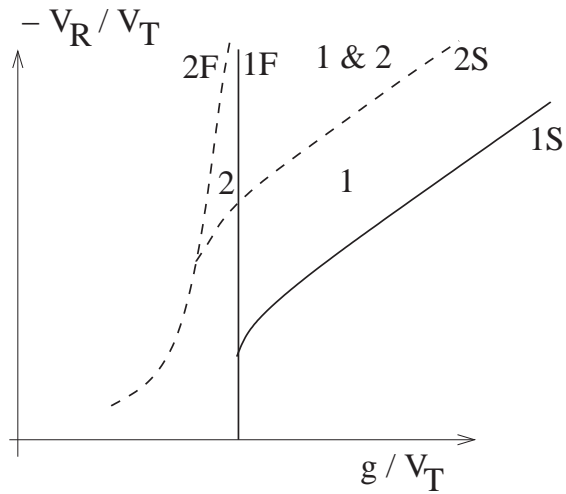
Figure 3.5. Schematic illustration of the expected relation of the $1_F, 1_S, 2_F$ and 2_S curves in parameter space. In the regions labelled 1 or 2, one-spike or two-spike waves exist; in the region labelled 1&2, these co-exist. Outside of the labelled regions, neither type of wave exists.

spikes fired by each cell produce a larger overall synaptic input to each cell in the medium, which promotes firing. We can carry these ideas further to make several reasoned conjectures. Recall that a cell's voltage is reset to V_R after a spike. For fixed V_T, as $|V_R|$ increases, a larger g is required to elicit a subsequent second spike. Hence, we expect the function F_2 to have a positive slope, with $F_2(-V_R/V_T) \to 2(1 + \sqrt{\tau_1/\tau_2})^2$ as $|V_R| \to \infty$. For fixed g and V_T, a sufficiently large value of $|V_R|$ (sufficiently strong reset) is required to prevent subsequent spikes after a second one, with a stronger reset needed for larger g. Hence, we also expect S_2 to have a positive slope. Finally, the same arguments should give corresponding curves for N-spike waves, for any positive integer N, such that N_F moves leftwards and N_S moves upwards in the $(g/V_T, -V_R/V_T)$ plane, as N increases. Figure 3.4 illustrates a numerically generated version of the curve 2_F, the shape of which agrees with our conjectures. The expected relation of the curves for one- and two-spike waves is drawn in Figure 3.5. The proofs of these conjectures remain open.

By solving the equation $F(c) = 0$ numerically for fixed parameters, one can analytically find the velocity c. Given this, equation (3.22) yields the time T between the two spikes in the corresponding traveling wave (if it really is a two-spike solution). These results match quite closely to those obtained from numerical simulation of fast two-spike traveling waves [78].

3.4   Arbitrary numbers of spikes and infinite spike trains

3.4.1   Computation of interspike intervals

Consider a traveling wave solution for which each cell spikes at an infinite sequence $\{x/c + T_n\}$, $n \geq 0$, of spike times. We will discuss here how the formulation given in Lemma 3.2.1 can be used to compute the interspike intervals $T_n - T_{n-1}$ between successive waves. In the traveling wave formulation, in which V is expressed as a function of $\xi = ct - x$, we have $V(cT_n) = V_T$ for each T_n. Correspondingly, Lemma 3.2.1 implies that for any $N \geq 1$,

$$
\begin{aligned}
V_T &= \left[V_T - \frac{g\left(\sum_{n=0}^{N-1} e^{-cT_n/\sigma}\right)}{2(\frac{\tau_1 c}{\sigma}+1)(1+\frac{\sigma}{\tau_2 c})} \right] e^{cT_N/\sigma} + \frac{g\left(\sum_{n=0}^{N-1} e^{cT_n/\sigma}\right)}{2(\frac{\tau_1 c}{\sigma}-1)(1-\frac{\sigma}{\tau_2 c})} e^{-cT_N/\sigma} + \frac{g\left(\sum_{n=0}^{N-1} e^{T_n/\tau_2}\right)}{(1-\frac{\sigma^2}{\tau_2^2 c^2})(1-\frac{\tau_1}{\tau_2})} e^{-T_N/\tau_2} \\
&\quad + \left((V_R - V_T) - \frac{g}{(1-\frac{\sigma^2}{\tau_1^2 c^2})(1-\frac{\tau_1}{\tau_2})} \right) \left(\sum_{n=0}^{N-1} e^{T_n/\tau_1} \right) e^{-T_N/\tau_1} .
\end{aligned}
$$

$$(3.25)$$

Suppose that there are a finite number of spikes in the traveling wave, say $N + 1$. For each spike, equation (3.25) applies. In fact, one obtains a system with $N + 1$ equations and $N + 1$ unknowns to be solved to obtain a valid $(N + 1)$-spike traveling wave solution. The unknowns are c, which denotes the velocity of the traveling wave, and the spike-times T_1 up to T_N (since $T_0 = 0$ by convention). The equations in the system are those corresponding to $V(cT_n) = V_T$, $1 \leq n \leq N$, and the equation (3.6). Based on the analysis in the previous section, it appears that this highly nonlinear system can only be solved numerically for most N.

The situation becomes even more complicated when an infinite number of spikes is considered. Thanks to the traveling wave description set out in Section 3.2, equation (3.25) is available, and one can iteratively solve for the spike time T_N from the previously known spike times $T_0 = 0, T_1, ..., T_{N-1}$ for every $N \geq 1$. To do so, however, an obstacle must first be overcome: since equation (3.6) involves all of the traveling fronts, it cannot be used independently from (3.25) in the case of infinitely many spikes. Thus, the velocity c that appears in each equation must be determined from some alternate source and then used here as a constant. Once c is specified from such a source, one can iteratively compute the spike times, and hence the interspike intervals $\Delta T_N = T_N - T_{N-1}$.

Remark 3.10. One source for the wave speed here is the fast two-spike wave speed calculated from the analytical formulas (3.19), (3.20). Numerics show [78] that the speeds of waves with large numbers of spikes are quite similar to those calculated for two-spike waves with corresponding parameter sets. Intuitively, this makes sense because in fast two-spike waves, the interspike interval cT is significantly greater than σ, the space constant or "footprint" of the synaptic coupling; see Figures 3.2, 3.4. Even for $cT = 2\sigma$, we have $J(cT) = (1/2\sigma)e^{-2}$, such that little interaction occurs between the synaptic inputs from different waves in the same solution. Thus, waves travel with roughly the same speed, no matter how many waves there are.

One might question the value of computing the interspike intervals from numerical solution of equation (3.25), given that one can perform a numerical simulation of traveling waves in the full network. However, such simulations are based on applying a localized shock somewhere in the network at a fixed time and allowing waves to propagate thereafter [81], [80]. This corresponds to a different, although closely related, form of traveling wave from that which we analyze analytically, for which all waves can be thought of as having existed somewhere in the infinite network for all

time. In fact, one interesting result that arises from using equation (3.25) to compute interspike intervals is that we can compare theory and analysis, to see just how closely related these forms of traveling wave solutions are.

Remark 3.11. By choosing the parameters $\tau_1 = 1$, $\tau_2 = 2$, $\sigma = 1$, $V_T = 1$, $V_R = -25$ and $g = 6$, the comparison leads to the following conclusion: For the first six interspike intervals, full numerical simulation of equation (3.2), labelled as 'Numerics,' and numerical solution of the analytical expression (3.25), labelled as 'Iterations,' produced excellent agreement, as shown in the following table. Note that for the analytical approach, we used $c = 1.256422$, the speed of the wave found in the numerical simulations.

	Numerics	*Iterations*	*Error*
$T1 - T0$	2.4258	2.4258	$2.83e - 006$
$T2 - T1$	2.0479	2.0479	$1.56e - 005$
$T3 - T2$	1.8844	1.8845	$9.72e - 005$
$T4 - T3$	1.7953	1.7964	$6.22e - 004$
$T5 - T4$	1.7417	1.7488	0.0040

We mention that R. Oşan [78] implemented the numerical scheme and the full numerical simulation. Errors in the table grow due to difficulty in solving equation (3.25) numerically, resulting from the fact that the first product in this equation consists of a factor that converges to 0 as $N \to \infty$ with a factor that diverges as $N \to \infty$. Thus the computation was stopped after the first six interspike intervals.

Remark 3.12. It can be shown, by induction on $N \geq 1$, that equation (3.25) is equivalent to

$$
\begin{aligned}
V_T &= \left[V_T - \frac{g \left(\sum_{n=0}^{N-1} e^{-c\,T_n/\sigma} \right)}{2(\frac{\tau_1 c}{\sigma}+1)(1+\frac{\sigma}{\tau_2 c})} \right] \cdot e^{c\,T_N/\sigma} \cdot \left[1 - e^{-(T_N - T_{N-1})(\frac{1}{\tau_1}+\frac{c}{\sigma})} \right] \\
&+ \frac{g \left(\sum_{n=0}^{N-1} e^{c\,T_n/\sigma} \right)}{2(\frac{\tau_1 c}{\sigma}-1)(1-\frac{\sigma}{\tau_2 c})} \cdot e^{-c\,T_N/\sigma} \cdot \left[1 - e^{-(T_N - T_{N-1})(\frac{1}{\tau_1}-\frac{c}{\sigma})} \right] \\
&+ \frac{g \left(\sum_{n=0}^{N-1} e^{T_n/\tau_2} \right)}{(1-\frac{\sigma^2}{\tau_2^2 c^2})(1-\frac{\tau_1}{\tau_2})} \cdot e^{-T_N/\tau_2} \cdot \left[1 - e^{-(T_N - T_{N-1})(\frac{1}{\tau_1}-\frac{1}{\tau_2})} \right] + V_R\, e^{-(T_N - T_{N-1})/\tau_1} \, .
\end{aligned}
\tag{3.26}
$$

This formulation proves its advantage when it is discussed the effect of adding an absolute refractory period to the integrate-and-fire model [78].

3.5 Conclusions

Traveling waves of activity are observed in slices of cortical tissue under various pharmacological manipulations. Previous works [33, 45, 44, 79, 82] studied how the velocity of traveling waves depends on various parameters by assuming that *each cell spiked once.* In particular, conditions on the parameters which prevent propagation are readily computed.

By studying propagation in the integrate-and-fire model, we have attempted to address here the following questions (i) is it possible to get multiple-spike waves; (ii) how does the existence of waves depend on having multiple spikes; (iii) how does the velocity depend on the number of spikes.

Lemma 3.2.1 and Theorem 3.1 provide two equivalent formulas for general traveling wave solutions to the continuum integrate-and-fire model (3.2), with the synaptic coupling functions $\alpha(t)$ and $J(x)$ given in (3.3) and (3.4), respectively. The functions defined by these formulas correspond to traveling wave solutions, for which the neuron at position x spikes at times $\{t_n^*(x) = x/c + T_n\}_{n=0}^{\infty}$, where $\xi = ct - x$, if and only if the consistency condition (3.6) holds and the sum $\sum_{n=0}^{\infty} e^{-cT_n/\sigma}$ converges. Convergence is not an issue, of course, when each cell fires only finitely many spikes (corresponding to $T_n = \infty$ for all but finitely many values of n). The same type of computations used to derive these formulas would be valid for other forms of $\alpha(t)$ and $J(x)$. With more complicated functions, however, difficulties in evaluating relevant integrals may arise.

We use these formulas to prove that there are curves that delineate the region on which single-spike traveling wave solutions exist, in a certain parameter space. These curves are shown in Figure 3.2. We also prove that in another region of parameter space, neurons can propagate a two-spike traveling wave. It remains open to determine where such solutions actually exist, by rigorously specifying the set of parameter values for which neurons stop spiking after exactly two spikes. Our reasoned conjecture on this result, illustrated in Figure 3.5, stems from the numerical results displayed in Figure 3.4. It also remains open to prove results about solutions with more than two spikes. We expect a similar pattern of regions in parameter space to extend to these cases.

The traveling wave formula in Lemma 3.2.1 is rewritten in (3.25), and equivalently (3.26) . This provides a relationship that can, in theory, be used in an iterative way to solve for as many spike times as desired in a traveling wave with any countable number of spikes, for fixed parameter values and a fixed wave speed. Numerics are needed here due to the highly nonlinear nature of (3.25).

Remark 3.13. An example that connects the present work with firing rate models (see the models in the previous chapters), in which spikes are completely ignored, is presented in [78]. We summarize here the main idea: We allow the neuron to spike continuously after shocking and suppose that the synapses saturate, i.e. once the neuron fires the synapse stays on for all time. Let $A(x, t)$ denote the firing rate of the neuron at spatial point x and time t, so $A(x, t) = F(I(x, t))$ where F is the firing rate of a neuron as a function of the applied current. For the integrate-and-fire model, this is almost a threshold linear curve ([28], p. 164). Since the current is given by $I(x, t) = g \sum_{n=-\infty}^{\infty} \int_{-\infty}^{\infty} dy\, J(x - y)\, \alpha(t - t_n^*(y))$, or, equivalent $I(x, t) = \int_{-\infty}^{t} \alpha(t - s) \int_{-\infty}^{\infty} J(x - y) \sum_n \delta(s - t_n^*(y))\, ds\, dy$, and the sum is essentially the firing rate of the neuron ([28],p. 233), the following closed system is obtained

$$A(x, t) = F\left(\int_{-\infty}^{t} \int_{-\infty}^{\infty} \alpha(t - s) J(x - y) A(y, s)\, ds\, dy \right).$$

Finally, if $\alpha(t) = \exp(-t/\tau)/\tau$, and $U(x, t) = \int_{-\infty}^{t} \alpha(t - s) A(x, s)\, ds$, we get at least formally,

$$A(x, t) = \tau \frac{\partial U(x, t)}{\partial t} + U(x, t) = F\left(\int_{-\infty}^{\infty} J(x - y) U(y, t)\, dy \right).$$

This is the familiar firing rate model that has been the subject of much analysis. Let us recall, for example, the rate model we investigated in Chapter 2 of this thesis. That assumed a smooth sigma-shaped F function and two different populations, one excitatory, and one inhibitory. When an additional adaptation equation was considered, we proved some sufficient conditions for the network to give rise to traveling waves solutions.

Chapter 4

Discussion

The first two chapters in this thesis discuss possible behaviors in two different rate models. The third chapter contains some analytical and computational results for a spiking model that is the leaky-integrate-and-fire (IF) model.

Chapter 1 studies the Wilson-Cowan model for a self-excited population of neurons with absolute refractory period. This is a rate model, the variable u of which, represents the proportion of excitatory cells firing per unit time at the instant time t. The spatial interactions are neglected and only the temporal dynamics of the network are considered ($u = u(t)$). R, the absolute refractory period of the neurons in the excitatory network is the parameter with respect to what the analysis is done.

Chapter 2 investigates a rate model that describes the feature selectivity in local cortical circuits (Hansel-Sompolinsky model). The spatial connectivity is now important and the "spatial" variable corresponds to a different "feature" presented to the system (e.g. $x \in [-\frac{\pi}{2}, \frac{\pi}{2}]$ the angle a bar is rotated in the subject receptive field). The rate variable u depends on the position x in the feature space and on the time value t, i.e. $u = u(x, t)$.

Similar mathematical methods are used in the first two chapters to analyze these models. The methods come from bifurcation theory and involve singular perturbation expansions. In both cases, normal form for typical bifurcations are constructed (Hopf bifurcation in Chapter 1, and Hopf and Takens-Bogdanov with $O(2)$-symmetry in Chapter 2). We were able to show that both rate models can lead to oscillations in some specific range of parameters.

In both cases, oscillations are driven by a 'delayed negative feedback' mechanism. In the Wilson-Cowan model the absolute refractory period is the biological mechanism that introduces negative feedback in the mathematical model. In the Hansel-Sompolinsky model the adaptation plays the role of negative feedback.

In chapter 2, due to the dependence of the rate variable $u(x, t)$ on spatial connectivity we were able to make a distinction between different types of oscillations. They occur as spatial-temporal

patterns in the form of traveling waves and standing waves.

As a result of our analysis, a new kind of pattern is found to be stable in the Hansel-Sompolinsky model and this is the standing wave pattern. In order to obtain it we need to consider a more general sigmoid gain function in the system. This pattern corresponds to oscillations in space for a given time t and oscillations in time for a given position (feature) x in space. The standing wave pattern can account for example, for the psychophysically investigated phenomenon of binocular rivalry [3], [9], [69], [70], [71]. Binocular rivalry phenomenon appears when two different stimuli (images) are presented in competition, that is when one image is shown to one eye simultaneously with showing another image to the other eye. In this case, subjects report that only one image is perceived at a moment in time with an alternation between perceived images. The time intervals between consecutive switches obey a Gamma distribution.

The standing wave solution we obtained in chapter 2 splits the neuronal network in two clusters the activity of which alternates in time. Therefore this result can be interpreted as corresponding to the effects on the neuronal network of the two images perceived alternatively in binocular rivalry. Nevertheless, the two problems cannot be directly connected because on one hand the standing wave pattern we obtained is a result of spatial connectivity in the system, so it arises as an intrinsic pattern; on the other hand in binocular rivalry, the pattern results as a consequence of the applied competing stimuli.

Chapter 3 studies the IF model. The mathematical methods used here are completely different from the previous chapters and they are more computational oriented. In chapter 3 we investigate again, this time in the context of spiking models, traveling wave patterns. Since temporal details are now taken into account, we can make the distinction between one-spike and multiple-spikes traveling wave solutions. The analysis focuses on this direction and results that characterize the existence of multiple-spike solutions are presented.

In conclusion, by studying three models in mathematical neuroscience we showed that oscillations and different kinds of wave patterns can be obtained in neuronal networks, and we analyze distinct possible mechanisms that can lead to these patterns.

Appendix A

Adjoint operator and coefficients in the normal form for the refractory neural network

A.0.1 Adjoint operator

We construct the adjoint operator of L, $Ly = \frac{dy}{dt} + A\tilde{r}_0 y + b\tilde{r}_0 \int_{t-1}^{t} y(s)\,ds$ in the space of solutions spanned by $\{1, e^{i\omega_0 t}, e^{-i\omega_0 t}, e^{2i\omega_0 t}, e^{-2i\omega_0 t}, \ldots\}$, which means we work with functions $x = x(t)$ that satisfy $x(0) = x(\frac{2\pi}{\omega_0})$. We define the primitive $X(t) := \int_0^t x(s)\,ds$ (so $X(0) = 0$), and the inner product as usual, $<\phi, \psi> = \int_0^{\frac{2\pi}{\omega_0}} \phi(t)\bar{\psi}(t)\,dt$. Now for any two functions x, y in this space $<x, Ly> = <L^* x, y>$, where L^* is the adjoint of the operator L. Compute $<x, Ly>$:

$$<x, Ly> = \int_0^{\frac{2\pi}{\omega_0}} x(t) \left[\overline{\frac{dy}{dt} + A\tilde{r}_0 y + b\tilde{r}_0 \int_{t-1}^{t} y(s)\,ds} \right]$$

$$= x(t)\,\bar{y}(t)\big|_0^{\frac{2\pi}{\omega_0}} - \int_0^{\frac{2\pi}{\omega_0}} \frac{dx}{dt}\,\bar{y}(t)\,dt + A\tilde{r}_0 \int_0^{\frac{2\pi}{\omega_0}} x(t)\,\bar{y}(t)\,dt + b\tilde{r}_0 \int_0^{\frac{2\pi}{\omega_0}} \left[x(t) \overline{\int_{t-1}^{t} y(s)\,ds} \right]$$

$$= -\int_0^{\frac{2\pi}{\omega_0}} \frac{dx}{dt}\,\bar{y}(t)\,dt + A\tilde{r}_0 \int_0^{\frac{2\pi}{\omega_0}} x(t)\,\bar{y}(t)\,dt + b\tilde{r}_0 \int_0^{\frac{2\pi}{\omega_0}} \left[x(t) \overline{\int_0^{t} y(s)\,ds} - x(t) \overline{\int_0^{t-1} y(s)\,ds} \right]$$

$$= \int_0^{\frac{2\pi}{\omega_0}} \left[A\tilde{r}_0\, x(t) - \frac{dx}{dt} \right] \bar{y}(t)\,dt + b\tilde{r}_0 \left[\int_0^{\frac{2\pi}{\omega_0}} x(t)\,\bar{Y}(t)\,dt - \int_0^{\frac{2\pi}{\omega_0}} x(t)\,\bar{Y}(t-1)\,dt \right].$$

Since $x = \frac{dX}{dt}$ and $y = \frac{dY}{dt}$ we use integration by parts and the properties of the functions X and Y to get $<x, Ly> = \int_0^{\frac{2\pi}{\omega_0}} \left[A\tilde{r}_0\, x(t) - \frac{dx}{dt} \right] \bar{y}(t)\,dt - b\tilde{r}_0 \int_0^{\frac{2\pi}{\omega_0}} \left(\int_0^{t} x(s)\,ds \right) \bar{y}(t)\,dt + b\tilde{r}_0 \int_{-1}^{\frac{2\pi}{\omega_0}-1} X(t+1)\,\bar{y}(t)\,dt + b\tilde{r}_0 X(t)\bar{Y}(t)\big|_0^{\frac{2\pi}{\omega_0}} - b\tilde{r}_0 X(t+1)\bar{Y}(t)\big|_{-1}^{\frac{2\pi}{\omega_0}-1}$ i.e.

$$<x, Ly> = \int_0^{\frac{2\pi}{\omega_0}} \left[A\tilde{r}_0\, x(t) - \frac{dx}{dt} + b\tilde{r}_0 \int_t^{t+1} x(s)\,ds \right] \bar{y}(t)\,dt$$
$$+ \int_{-1}^{0} \left[\int_0^{\frac{2\pi}{\omega_0}} x(s)\,ds - \int_{t+1}^{t+1+\frac{2\pi}{\omega_0}} x(s)\,ds \right] \bar{y}(t)\,dt.$$

Since the last integral is zero, the adjoint operator of L can be defined as

$$L^*x = -\frac{dx}{dt} + A\,\tilde{r}_0\,x + b\,\tilde{r}_0 \int_t^{t+1} x(s)\,ds\,.$$

By direct calculation we see that $L^*(e^{\pm i\omega_0 t}) = 0$. We use for this both $\lambda_0 = \pm i\omega_0$ and the characteristic equation (1.4).

A.0.2 Coefficients in the normal form

Directly from the definition of the operators L, Λ, B, C we can prove that $L(e^{\lambda t}) = \tilde{L}(\lambda)e^{\lambda t}$ where the function $\tilde{L}$ is defined as follows $\tilde{L}(\lambda) = \lambda + A\,\tilde{r}_0 + \frac{(1-e^{-\lambda})b\,\tilde{r}_0}{\lambda}$ if $\lambda \neq 0$, and $(A+b)\tilde{r}_0$ if $\lambda = 0$. Similarly, $\Lambda(e^{\lambda t}) = \tilde{\Lambda}(\lambda)e^{\lambda t}$ with $\tilde{\Lambda}(\lambda) = -A - \frac{1-e^{-\lambda}}{\lambda}b$ for $\lambda \neq 0$ and $-(A+b)$ for $\lambda = 0$, and $B(e^{\lambda_1 t}, e^{\lambda_2 t}) = \tilde{B}(\lambda_1, \lambda_2)e^{\lambda_1 t}e^{\lambda_2 t}$ with

$$\tilde{B}(\lambda_1, \lambda_2) = \begin{cases} \tilde{r}_0 \frac{1-\bar{u}}{2} f''(\bar{u}) - \frac{1}{2}\left[\frac{1-e^{-\lambda_1}}{\lambda_1} + \frac{1-e^{-\lambda_2}}{\lambda_2}\right] f'(\bar{u})\,\tilde{r}_0 & , \lambda_1 \neq 0, \lambda_2 \neq 0 \\[2mm] \tilde{r}_0 \frac{1-\bar{u}}{2} f''(\bar{u}) - \frac{1}{2}\left[1 + \frac{1-e^{-\lambda_1}}{\lambda_1}\right] f'(\bar{u})\,\tilde{r}_0 & , \lambda_1 \neq 0, \lambda_2 = 0 \\[2mm] \tilde{r}_0 \frac{1-\bar{u}}{2} f''(\bar{u}) - \frac{1}{2}\left[1 + \frac{1-e^{-\lambda_2}}{\lambda_2}\right] f'(\bar{u})\,\tilde{r}_0 & , \lambda_1 = 0, \lambda_2 \neq 0 \\[2mm] \tilde{r}_0 \frac{1-\bar{u}}{2} f''(\bar{u}) - f'(\bar{u})\,\tilde{r}_0 & , \lambda_1 = 0, \lambda_2 = 0 \end{cases}$$

and $C(e^{\lambda_1 t}, e^{\lambda_2 t}, e^{\lambda_3 t}) = \tilde{C}(\lambda_1, \lambda_2, \lambda_3)e^{\lambda_1 t}e^{\lambda_2 t}e^{\lambda_3 t}$. In our problem we are interested only in the case when all $\lambda_1, \lambda_2, \lambda_3$ are nonzero. Then $\tilde{C}(\lambda_1, \lambda_2, \lambda_3)$ is

$$\tilde{C}(\lambda_1, \lambda_2, \lambda_3) = \tilde{r}_0 \frac{1-\bar{u}}{6} f'''(\bar{u}) - \frac{1}{6}\left[\frac{1-e^{-\lambda_1}}{\lambda_1} + \frac{1-e^{-\lambda_2}}{\lambda_2} + \frac{1-e^{-\lambda_3}}{\lambda_3}\right] f''(\bar{u})\,\tilde{r}_0$$

We make the remark that $\tilde{L}(\bar{\lambda}) = \overline{\tilde{L}(\lambda)}$, $\tilde{\Lambda}(\bar{\lambda}) = \overline{\tilde{\Lambda}(\lambda)}$, $\tilde{B}(\lambda_1, \lambda_2) = \tilde{B}(\lambda_2, \lambda_1)$, $\tilde{B}(\bar{\lambda}_1, \bar{\lambda}_2) = \overline{\tilde{B}(\lambda_1, \lambda_2)}$ and $\tilde{C}(\bar{\lambda}_1, \bar{\lambda}_2, \bar{\lambda}_3) = \overline{\tilde{C}(\lambda_1, \lambda_2, \lambda_3)}$. In order to find the coefficient of $z^2(0)\bar{z}(0)$ in the normal form (1.12) we compute $L(te^{i\omega_0 t}) = e^{i\omega_0 t}\left[2 + A\,\tilde{r}_0 + i\left(\omega_0 - \frac{A\tilde{r}_0 + b\,\tilde{r}_0}{\omega_0}\right)\right]$ and $L(te^{-i\omega_0 t}) = e^{-i\omega_0 t}\left[2 + A\,\tilde{r}_0 + i\left(-\omega_0 + \frac{A\tilde{r}_0 + b\,\tilde{r}_0}{\omega_0}\right)\right]$.

Finally we have $\tilde{\Lambda}(i\omega_0) = \frac{i\omega_0}{\tilde{r}_0}$, $\tilde{L}(0) = (A+b)\,\tilde{r}_0$, $\tilde{L}(2i\omega_0) = \frac{A\omega_0^2}{b} + i\left[\omega_0 - \frac{\omega_0 \tilde{r}_0 A^2}{2b} + \frac{\omega_0^3}{2b\tilde{r}_0}\right]$,

$\tilde{B}(i\omega_0, -i\omega_0) = \tilde{r}_0 \frac{1-\bar{u}}{2} f''(\bar{u}) + \frac{A}{b} f'(\bar{u})\,\tilde{r}_0$, $\tilde{B}(i\omega_0, i\omega_0) = \left[\tilde{r}_0 \frac{1-\bar{u}}{2} f''(\bar{u}) + \frac{A}{b} f'(\bar{u})\,\tilde{r}_0\right] + i\frac{\omega_0}{b} f'(\bar{u})$,

$\tilde{B}(-i\omega_0, 2i\omega_0) = \left[\tilde{r}_0 \frac{1-\bar{u}}{2} f''(\bar{u}) + \left(\frac{A\tilde{r}_0}{b} - \frac{A\omega_0^2}{2b^2}\right) f'(\bar{u})\right] + i\frac{\tilde{r}_0 \omega_0}{4b^2}\left[A^2 - \frac{\omega_0^2}{\tilde{r}_0^2}\right] f'(\bar{u})$,

$\tilde{B}(i\omega_0, 0) = \left[\tilde{r}_0 \frac{1-\bar{u}}{2} f''(\bar{u}) + \frac{A}{2b} f'(\bar{u})\,\tilde{r}_0 - \frac{1}{2} f'(\bar{u})\,\tilde{r}_0\right] + i\frac{\omega_0}{2b} f'(\bar{u})$,

$\tilde{C}(i\omega_0, i\omega_0, -i\omega_0) = \left[\tilde{r}_0 \frac{1-\bar{u}}{6} f'''(\bar{u}) + \frac{A}{2b} f''(\bar{u})\,\tilde{r}_0\right] + i\frac{\omega_0}{6b} f''(\bar{u})$.

Appendix B

Normal forms in the case of the neural system with adaptation

B.0.1   Normal form for Hopf bifurcation in the neural system with adaptation

We present in the following the proofs for the results stated in Section 2.2.1. With the singular perturbation expansion (2.22), the first component of equation (2.23) reads as

$$[\epsilon L_0 U_0 + \epsilon^2 L_0 U_1 + \epsilon^3 L_0 U_2 + \mathcal{O}(\epsilon^4)]_{(1)} = \epsilon^2 \gamma J * u + \frac{F''(0)}{2}[\alpha^* J * u - gv + (\alpha - \alpha^*) J * u]^2$$

$$+ \frac{F'''(0)}{6}[\alpha^* J * u - gv + (\alpha - \alpha^*) J * u]^3 + \cdots = \epsilon^2 \frac{F''(0)}{2}[\alpha^* J * u_0 - gv_0]^2 + \epsilon^3 F''(0)[\alpha^* J * u_0$$

$$- gv_0][\alpha^* J * u_1 - gv_1] + \epsilon^3 \gamma (J * u_0) + \epsilon^3 \frac{F'''(0)}{6}[\alpha^* J * u_0 - gv_0]^3 + \mathcal{O}(\epsilon^4) , \text{ i.e.}$$

$$[L_0 U_0 + \epsilon L_0 U_1 + \epsilon^2 L_0 U_2 + \mathcal{O}(\epsilon^3)]_{(1)} = \epsilon \frac{F''(0)}{2}[\alpha^* J * u_0 - gv_0]^2 + \epsilon^2 \left[\gamma (J * u_0) \right.$$

$$\left. + F''(0)[\alpha^* J * u_0 - gv_0][\alpha^* J * u_1 - gv_1] + \frac{F'''(0)}{6}[\alpha^* J * u_0 - gv_0]^3 \right] + \mathcal{O}(\epsilon^3) ,$$

$$(\text{B.1})$$

and its second vector-component is zero,

$$[L_0 U_0 + \epsilon L_0 U_1 + \epsilon^2 L_0 U_2 + \mathcal{O}(\epsilon^3)]_{(2)} = 0 . \qquad (\text{B.2})$$

Solving for U_0

The first equation to be solved is $L_0 U_0 = \mathbf{0}$, and since the nullspace of L_0 corresponding to the center manifold has the basis $\left\{ \Phi_0 e^{i(\omega_0 t \pm k_0 x)}, \overline{\Phi}_0 e^{-i(\omega_0 t \pm k_0 x)} \right\}$ with Φ_0 and ω_0 defined by (2.18), (2.17), the solution U_0 can be written as

$$U_0 = z \, \Phi_0 \, e^{i(\omega_0 t + k_0 x)} + w \, \Phi_0 \, e^{i(\omega_0 t - k_0 x)} + \overline{z} \, \overline{\Phi}_0 \, e^{-i(\omega_0 t + k_0 x)} + \overline{w} \, \overline{\Phi}_0 \, e^{-i(\omega_0 t - k_0 x)} ,$$

with z and w being ϵ-dependent. Let us then consider $z = z(\epsilon^2 t)$ and $w = w(\epsilon^2 t)$ and expand them as $z = z(0) + z'(0)\epsilon^2 t + \mathcal{O}(\epsilon^4)$ and $w = w(0) + w'(0)\epsilon^2 t + \mathcal{O}(\epsilon^4)$ as $\epsilon \to 0$. We obtain

$$U_0 = \left[z(0)\,\Phi_0\,e^{i(\omega_0 t + k_0 x)} + w(0)\,\Phi_0\,e^{i(\omega_0 t - k_0 x)} + \overline{z}(0)\,\overline{\Phi}_0\,e^{-i(\omega_0 t + k_0 x)} + \overline{w}(0)\,\overline{\Phi}_0\,e^{-i(\omega_0 t - k_0 x)} \right]$$

$$+ t\epsilon^2 \left[z'(0)\Phi_0 e^{i(\omega_0 t + k_0 x)} + w'(0)\Phi_0 e^{i(\omega_0 t - k_0 x)} + \overline{z'}(0)\overline{\Phi}_0 e^{-i(\omega_0 t + k_0 x)} + \overline{w'}(0)\overline{\Phi}_0 e^{-i(\omega_0 t - k_0 x)} \right] + \mathcal{O}(\epsilon^4)$$

We have $L_0\left(\Phi_0\,e^{i(\omega_0 t \pm k_0 x)}\right) = i\omega_0 \Phi_0\,e^{i(\omega_0 t \pm k_0 x)} - \hat{L}(k_0)\Phi_0\,e^{i(\omega_0 t \pm k_0 x)} = 0$ and $L_0\left(\overline{\Phi}_0\,e^{-i(\omega_0 t \pm k_0 x)}\right) = -i\omega_0\overline{\Phi}_0\,e^{-i(\omega_0 t \pm k_0 x)} - \hat{L}(k_0)\overline{\Phi}_0\,e^{-i(\omega_0 t \pm k_0 x)} = 0$, and therefore $L_0 U_0 = \epsilon^2 \left[z'(0)\,L_0\left(\Phi_0\,t e^{i(\omega_0 t + k_0 x)}\right) + w'(0)\,L_0\left(\Phi_0\,t e^{i(\omega_0 t - k_0 x)}\right) + \overline{z'}(0)\,L_0\left(\overline{\Phi}_0\,t e^{-i(\omega_0 t + k_0 x)}\right) + \overline{w'}(0)\,L_0\left(\overline{\Phi}_0\,t e^{-i(\omega_0 t - k_0 x)}\right) \right] + \mathcal{O}(\epsilon^4)$.

By direct calculation, we obtain

$$L_0\left(\Phi_0 t e^{i(\omega_0 t \pm k_0 x)}\right) = \frac{d}{dt}\left(\Phi_0 t e^{i(\omega_0 t \pm k_0 x)}\right) - \begin{pmatrix} -1 + \alpha^* J * (\cdot) & -g \\ 1/\tau & -1/\tau \end{pmatrix} \Phi_0 t e^{i(\omega_0 t \pm k_0 x)} = \Phi_0 e^{i(\omega_0 t \pm k_0 x)} +$$

$$t\frac{d}{dt}\left(\Phi_0 e^{i(\omega_0 t \pm k_0 x)}\right) - t \begin{pmatrix} -1 + \alpha^* J * (\cdot) & -g \\ 1/\tau & -1/\tau \end{pmatrix} \Phi_0 e^{i(\omega_0 t \pm k_0 x)} = \Phi_0\,e^{i(\omega_0 t \pm k_0 x)} + t\,L_0\left(\Phi_0\,e^{i(\omega_0 t \pm k_0 x)}\right).$$

Then $L_0\left(\Phi_0\,t\,e^{i(\omega_0 t \pm k_0 x)}\right) = \Phi_0\,e^{i(\omega_0 t \pm k_0 x)}$. Similar $L_0\left(\overline{\Phi}_0\,t\,e^{-i(\omega_0 t \pm k_0 x)}\right) = \overline{\Phi}_0\,e^{-i(\omega_0 t \pm k_0 x)}$. The resulting expression for $L_0 U_0$ is

$$L_0 U_0 = \epsilon^2 \left[z'(0)\,\Phi_0\,e^{i(\omega_0 t + k_0 x)} + w'(0)\,\Phi_0\,e^{i(\omega_0 t - k_0 x)} + \overline{z'}(0)\,\overline{\Phi}_0\,e^{-i(\omega_0 t + k_0 x)} + \overline{w'}(0)\,\overline{\Phi}_0\,e^{-i(\omega_0 t - k_0 x)} \right]$$

$$+ \mathcal{O}(\epsilon^4) = \epsilon^2 \left[z'(0)\,\Phi_0\,e^{i(\omega_0 t + k_0 x)} + w'(0)\,\Phi_0\,e^{i(\omega_0 t - k_0 x)} + cc \right] + \mathcal{O}(\epsilon^4) \tag{B.3}$$

where here cc denotes the complex conjugation of the expression it follows.

L_0^* the adjoint operator of L_0

The solution $U = (u_1(x,t),\,u_2(x,t))^T$ from (2.22) belongs to the subspace of functions that satisfy

$$u_j(x,t) = u_j(x + \frac{2\pi}{k_0}, t), \quad u_j(x,t) = u_j(x, t + \frac{2\pi}{\omega_0}), \quad \forall x \in \mathbb{R}, \; \forall t \in \mathbb{R}, \; j = 1,2. \tag{B.4}$$

Let us consider now the following linear operator

$$L_0^* V = -\frac{d}{dt}V - \begin{pmatrix} -1 + \alpha^* J * (\cdot) & 1/\tau \\ -g & -1/\tau \end{pmatrix} V. \tag{B.5}$$

When looking for bounded solutions of $L_0^* V = \mathbf{0}$ of the form $\xi(t) e^{\pm ikx}$ with $k \in \mathbb{R}$, respectively $k \in \left(\pm \frac{\pi}{l} \mathbb{N} \right)$ when l is finite, we find that $\xi(t)$ must satisfy the ODE $\left[\frac{d\xi}{dt}(t) = -\hat{L}(k)^T \xi(t) \right]$. Since $det(-\hat{L}(k)^T) = det(\hat{L}(k))$, $tr(-\hat{L}(k)^T) = -tr(\hat{L}(k))$ and k_0 is the most unstable mode for (2.3), the eigenfunctions of L_0^* have the form $\xi_{1,2\,k}\, e^{\lambda_{1,2\,k} t \pm ikx}$, $\overline{\xi}_{1,2\,k}\, e^{\overline{\lambda}_{1,2\,k} t \mp ikx}$ where $\mathrm{Re}(\lambda_{1,2\,k}) > 0$ for $k \neq \pm k_0$ and $\lambda_{1,2 \pm k_0} = \pm i\omega_0$.

Remark B.1. The operator that corresponds to the restriction of L_0^* on the space of functions (B.4) has a four-dimensional nullspace with the basis $\{\ \Psi_0\, e^{i(\omega_0 t \pm k_0 x)}, \overline{\Psi}_0\, e^{-i(\omega_0 t \pm k_0 x)} \}$, where Ψ_0 is the two-dimensional complex vector defined by

$$\hat{L}(k_0)^T \Psi_0 = -i\omega_0 \Psi_0 \quad \text{and} \quad \Phi_0 \cdot \overline{\Psi}_0 = 1 \,. \tag{B.6}$$

We show that L_0^* is the adjoint operator of L_0 on the space of functions (B.4) with the inner product

$$< V, W > = \int_0^{\frac{2\pi}{\omega_0}} dt \int_0^{\frac{2\pi}{k_0}} dx\, V(x,t) \cdot \overline{W}(x,t) = \int_0^{\frac{2\pi}{\omega_0}} dt \int_0^{\frac{2\pi}{k_0}} dx\, [\, v_1(x,t)\overline{w}_1(x,t) + v_2(x,t)\overline{w}_2(x,t)\,] \,.$$

Let us consider $V = (v_1(x,t)\,, v_2(x,t))^T$, $W = (w_1(x,t)\,, w_2(x,t))^T$ with the property (B.4), and compute

$$< V, L_0 W > - < L_0^* V, W > = \int_0^{\frac{2\pi}{\omega_0}} dt \int_0^{\frac{2\pi}{k_0}} dx\, \Big[v_1 \frac{d\overline{w}_1}{dt} + \overline{w}_1 \frac{dv_1}{dt} + v_2 \frac{d\overline{w}_2}{dt}$$
$$+ \overline{w}_2 \frac{dv_2}{dt} - \alpha^* v_1 (J * \overline{w}_1) + \alpha^* \overline{w}_1 (J * v_1) \Big] \,.$$

Using integration by parts and the periodicity of v_j, w_j, $j = 1, 2$ with respect to t, we obtain

$$< V, L_0 W > - < L_0^* V, W > = \alpha^* \int_0^{\frac{2\pi}{\omega_0}} dt \int_0^{\frac{2\pi}{k_0}} dx\, [\overline{w}_1 (J * v_1) - v_1 (J * \overline{w}_1)]$$

which is zero, based of the fact that the inner integral is zero for any fixed t (see Appendix B.0.2 for a proof). Therefore $< V, L_0 W > = < L_0^* V, W >$ for all V, W functions in the space (B.4), that proves that L_0^* is the adjoint operator of L_0.

Solving for U_1

In order to compute U_1 we need to evaluate $J * u_0$ and $\alpha^* J * u_0 - g v_0$ where $(u_0\,, v_0)^T = U_0$ and

then introduce the result, together with (B.3), in equation (B.1). For $\Phi_0 = (\Phi_0^1,\, \Phi_0^2)^T$ as in (2.18), let us define $A \in \mathbb{C}$ as the inner product

$$A = \Phi_0^T \cdot (1 + 1/\tau,\, -g) = (1 + 1/\tau)\,\Phi_0^1 - g\,\Phi_0^2 = \phi + i\,\phi\frac{\sqrt{g\tau - 1}}{\tau} = \phi\,(1 + i\omega_0)\,. \tag{B.7}$$

Then we have

$$
\begin{aligned}
J * u_0 &= z\,\Phi_0^1\,\hat{J}(k_0)\,e^{i(\omega_0 t + k_0 x)} + w\,\Phi_0^1\,\hat{J}(k_0)\,e^{i(\omega_0 t - k_0 x)} + \overline{z}\,\overline{\Phi}_0^1\,\hat{J}(k_0)\,e^{-i(\omega_0 t + k_0 x)} \\
&\quad + \overline{w}\,\overline{\Phi}_0^1\,\hat{J}(k_0)\,e^{-i(\omega_0 t - k_0 x)} = \hat{J}(k_0)\left[\phi\,z(0)\,e^{i(\omega_0 t + k_0 x)} + \phi\,w(0)\,e^{i(\omega_0 t - k_0 x)}\right. \\
&\quad \left. + \overline{\phi}\,\overline{z}(0)\,e^{-i(\omega_0 t + k_0 x)} + \overline{\phi}\,\overline{w}(0)\,e^{-i(\omega_0 t - k_0 x)}\right] + \mathcal{O}(\epsilon^2)\,, \quad \text{i.e.}
\end{aligned}
$$

$$J * u_0 = \hat{J}(k_0)\left[\phi\,z(0)\,e^{i(\omega_0 t + k_0 x)} + \phi\,w(0)\,e^{i(\omega_0 t - k_0 x)} + cc\right] + \mathcal{O}(\epsilon^2)\,. \tag{B.8}$$

Similar, we obtain

$$
\begin{aligned}
\alpha^* J * u_0 - g v_0 &= (1 + 1/\tau)\left[z(0)\,\Phi_0^1\,e^{i(\omega_0 t + k_0 x)} + w(0)\,\Phi_0^1\,e^{i(\omega_0 t - k_0 x)} + \overline{z}(0)\,\overline{\Phi}_0^1\,e^{-i(\omega_0 t + k_0 x)} \right. \\
&\quad \left. + \overline{w}(0)\,\overline{\Phi}_0^1\,e^{-i(\omega_0 t - k_0 x)}\right] - g\left[z(0)\,\Phi_0^2\,e^{i(\omega_0 t + k_0 x)} + w(0)\,\Phi_0^2\,e^{i(\omega_0 t - k_0 x)} + \overline{z}(0)\,\overline{\Phi}_0^2\,e^{-i(\omega_0 t + k_0 x)} \right. \\
&\quad \left. + \overline{w}(0)\,\overline{\Phi}_0^2\,e^{-i(\omega_0 t - k_0 x)}\right] + \mathcal{O}(\epsilon^2) = A\left[z(0)\,e^{i(\omega_0 t + k_0 x)} + w(0)\,e^{i(\omega_0 t - k_0 x)}\right] + \overline{A}\left[\overline{z}(0)\,e^{-i(\omega_0 t + k_0 x)}\right. \\
&\quad \left. + \overline{w}(0)\,e^{-i(\omega_0 t - k_0 x)}\right] + \mathcal{O}(\epsilon^2)\,, \quad \text{i.e.}
\end{aligned}
$$

$$\alpha^* J * u_0 - g v_0 = \left[A\,z(0)\,e^{i(\omega_0 t + k_0 x)} + A\,w(0)\,e^{i(\omega_0 t - k_0 x)} + cc\right] + \mathcal{O}(\epsilon^2)\,. \tag{B.9}$$

Now, using the equations (B.1), (B.3), (B.8) and (B.9) we obtain

$$L_0 U_1 - \frac{F''(0)}{2}\,\boldsymbol{P} = \epsilon\left[-\left(z'(0)\,\Phi_0\,e^{i(\omega_0 t + k_0 x)} + w'(0)\,\Phi_0\,e^{i(\omega_0 t - k_0 x)} + cc\right) - L_0 U_2 + \boldsymbol{Q}\right] + \mathcal{O}(\epsilon^2) \tag{B.10}$$

where the second components of $\boldsymbol{P}$ and $\boldsymbol{Q}$ are zero, and their first components are

$$
\begin{aligned}
\boldsymbol{P}_{(1)} &= \left[A^2 z(0)^2\,e^{2i(\omega_0 t + k_0 x)} + A^2 w(0)^2\,e^{2i(\omega_0 t - k_0 x)} + 2A^2 z(0)w(0)\,e^{2i\,\omega_0 t} + cc\right] \\
&\quad + 2A\,\overline{A}\left[z(0)\overline{z}(0) + w(0)\overline{w}(0) + z(0)\overline{w}(0)\,e^{2ik_0 x} + \overline{z}(0)w(0)\,e^{-2ik_0 x}\right]
\end{aligned} \tag{B.11}
$$

$$\boldsymbol{Q}_{(1)} = \gamma \, \hat{J}(k_0) \left[\phi \, z(0) \, e^{i(\omega_0 t + k_0 x)} + \phi \, w(0) \, e^{i(\omega_0 t - k_0 x)} + cc \right] + \frac{F'''(0)}{6} \left[A^3 z(0)^3 \, e^{3i(\omega_0 t + k_0 x)} \right.$$

$$+ A^3 w(0)^3 \, e^{3i(\omega_0 t - k_0 x)} + 3A^3 z(0)^2 w(0) \, e^{i(3\omega_0 t + k_0 x)} + 3A^3 z(0) w(0)^2 \, e^{i(3\omega_0 t - k_0 x)}$$

$$+ 3A^2 \overline{A} \, z(0)^2 \overline{z}(0) \, e^{i(\omega_0 t + k_0 x)} + 3A^2 \overline{A} \, w(0)^2 \overline{w}(0) \, e^{i(\omega_0 t - k_0 x)} + 3A^2 \overline{A} \, z(0)^2 \overline{w}(0) \, e^{i(\omega_0 t + 3k_0 x)}$$

$$+ 3A^2 \overline{A} \overline{z}(0) w(0)^2 e^{i(\omega_0 t - 3ik_0 x)} + 6A^2 \overline{A} z(0) w(0) \overline{w}(0) e^{i(\omega_0 t + k_0 x)} + 6A^2 \overline{A} z(0) \overline{z}(0) w(0) e^{i(\omega_0 t - k_0 x)} + cc \Big]$$

$$+ F''(0) \left[A \, z(0) \, e^{i(\omega_0 t + k_0 x)} + A \, w(0) \, e^{i(\omega_0 t - k_0 x)} + cc \right] \left[\alpha^* \, J * u_1 - g v_1 \right]. \tag{B.12}$$

Based on equation (B.10), $U_1 = (u_1 \,, \, v_1)^T$ is the solution of $L_0 U_1 = \frac{F''(0)}{2} \boldsymbol{P}$ up to the order $\mathcal{O}(\epsilon)$. Using the form of $\boldsymbol{P}_{(1)}$ we may write U_1 in a similar manner as

$$U_1 = \left(\xi_1 \, z^2 \, e^{2i(\omega_0 t + k_0 x)} + \xi_2 \, w^2 \, e^{2i(\omega_0 t - k_0 x)} + \xi_3 \, z \, w \, e^{2i\omega_0 t} + \xi_4 \, z \, \overline{w} \, e^{2ik_0 x} + cc \right) + \xi_5 \, z \, \overline{z} + \xi_6 \, w \, \overline{w}$$

with ξ_i, $(i = \overline{1,6})$, vectors in $\mathbb{C}^2$. Therefore

$$U_1 = \left[\xi_1 \, z(0)^2 \, e^{2i(\omega_0 t + k_0 x)} + \xi_2 \, w(0)^2 \, e^{2i(\omega_0 t - k_0 x)} + \xi_3 \, z(0) \, w(0) \, e^{2i\omega_0 t} \right.$$

$$\left. + \xi_4 \, z(0) \, \overline{w}(0) \, e^{2ik_0 x} + cc \right] + \xi_5 \, z(0) \, \overline{z}(0) + \xi_6 \, w(0) \, \overline{w}(0) + \mathcal{O}(\epsilon^2)$$

This implies $L_0 U_1 = -z(0)\overline{z}(0)[\hat{L}(0)\xi_5] - w(0)\overline{w}(0)[\hat{L}(0)\xi_6] + \Big(z(0)^2 e^{2i(\omega_0 t + k_0 x)}[2i\omega_0\xi_1 - \hat{L}(2k_0)\xi_1] +$ $w(0)^2 e^{2i(\omega_0 t - k_0 x)}[2i\omega_0\xi_2 - \hat{L}(2k_0)\xi_2] + z(0) \, w(0) e^{2i\omega_0 t}[2i\omega_0\xi_3 - \hat{L}(0)\xi_3] - z(0) \, \overline{w}(0) \, e^{2ik_0 x}[\hat{L}(2k_0) \, \xi_4] +$ $cc \Big) + \mathcal{O}(\epsilon^2).$

In equation (B.10) we match the coefficients of the terms $z(0)^2 \, e^{2i(\omega_0 t + k_0 x)}$, $w(0)^2 \, e^{2i(\omega_0 t - k_0 x)}$, ... up to the order $\mathcal{O}(\epsilon)$. It results that

$$\xi_1 = \xi_2 = \frac{A^2 F''(0)}{2} [2i\omega_0 I - \hat{L}(2k_0)]^{-1} \begin{pmatrix} 1 \\ 0 \end{pmatrix}, \xi_4 = |A|^2 F''(0)[-\hat{L}(2k_0)]^{-1} \begin{pmatrix} 1 \\ 0 \end{pmatrix}$$

$$\xi_3 = A^2 F''(0)[2i\omega_0 I - \hat{L}(0)]^{-1} \begin{pmatrix} 1 \\ 0 \end{pmatrix}, \xi_5 = \xi_6 = |A|^2 F''(0)[-\hat{L}(0)]^{-1} \begin{pmatrix} 1 \\ 0 \end{pmatrix}$$

where, obviously, ξ_4, ξ_5, $\xi_6 \in \mathbb{R}^2$.

Remark B.2. The matrices involved in the equations above are invertible since $\hat{J}(k_0) > \hat{J}(nk_0)$,

$n = 0, 2$ and $g > 1/\tau$, $\alpha^* = \frac{1+1/\tau}{\hat{J}(k_0)}$. On one hand $det[\hat{L}(nk_0)] = \frac{1}{\tau}(g + 1 - \alpha^* \hat{J}(nk_0)) = \frac{1}{\tau}[g + 1 - \frac{(1+1/\tau)\hat{J}(nk_0)}{\hat{J}(k_0)}] > \frac{\tau+1}{\tau^2}[1 - \frac{\hat{J}(nk_0)}{\hat{J}(k_0)}] > 0$. On the other hand $det[2i\omega_0 I - \hat{L}(nk_0)]$ is nonzero since its imaginary part is equal to $2i\omega_0(1 + \frac{1}{\tau})[1 - \frac{\hat{J}(nk_0)}{\hat{J}(k_0)}] > 0$.

We find that

$$\xi_1 = \xi_2 = \frac{\frac{A^2 F''(0)}{2}}{\frac{3(1/\tau - g)}{\tau} + (\frac{1}{\tau} + 2i\omega_0)(1 + \frac{1}{\tau})[1 - \frac{\hat{J}(2k_0)}{\hat{J}(k_0)}]} \begin{pmatrix} \frac{1}{\tau} + 2i\omega_0 \\ \frac{1}{\tau} \end{pmatrix},$$

$$\xi_3 = \frac{A^2 F''(0)}{\frac{3(1/\tau - g)}{\tau} + (\frac{1}{\tau} + 2i\omega_0)(1 + \frac{1}{\tau})[1 - \frac{\hat{J}(0)}{\hat{J}(k_0)}]} \begin{pmatrix} \frac{1}{\tau} + 2i\omega_0 \\ \frac{1}{\tau} \end{pmatrix},$$

$$\xi_4 = \frac{|A|^2 F''(0)}{g + 1 - \frac{(1+1/\tau)\hat{J}(2k_0)}{\hat{J}(k_0)}} \begin{pmatrix} 1 \\ 1 \end{pmatrix}, \quad \xi_5 = \xi_6 = \frac{|A|^2 F''(0)}{g + 1 - \frac{(1+1/\tau)\hat{J}(0)}{\hat{J}(k_0)}} \begin{pmatrix} 1 \\ 1 \end{pmatrix}. \tag{B.13}$$

Solving for U_2

With the notation

$$\frac{A^2 F''(0)}{2} B := \alpha^* \hat{J}(2k_0)\xi_1^1 - g\xi_1^2 = \alpha^* \hat{J}(2k_0)\xi_2^1 - g\xi_2^2,$$

$$A^2 F''(0) C := \alpha^* \hat{J}(0)\xi_3^1 - g\xi_3^2, \quad |A|^2 F''(0) D := \alpha^* \hat{J}(2k_0)\xi_4^1 - g\xi_4^2,$$

$$|A|^2 F''(0) E := \alpha^* \hat{J}(0)\xi_5^1 - g\xi_5^2 = \alpha^* \hat{J}(0)\xi_6^1 - g\xi_6^2 \tag{B.14}$$

(notice that $D, E \in \mathbb{R}$) we have

$$\alpha^* J * u_1 - gv_1 = \Big[\frac{A^2 F''(0)}{2} Bz(0)^2 e^{2i(\omega_0 t + k_0 x)} + \frac{A^2 F''(0)}{2} Bw(0)^2 e^{2i(\omega_0 t - k_0 x)}$$

$$+ A^2 F''(0) Cz(0)w(0) e^{2i\omega_0 t} + |A|^2 F''(0) Dz(0)\overline{w}(0) e^{2ik_0 x} + cc\Big] + |A|^2 F''(0) Ez(0)\overline{z}(0)$$

$$+ |A|^2 F''(0) Ew(0)\overline{w}(0) + \mathcal{O}(\epsilon^2).$$

The terms in $\boldsymbol{Q}_{(1)}$ that will count in the computation of the normal form are those that include the exponential $e^{i(\omega_0 t + k_0 x)}$, $e^{i(\omega_0 t - k_0 x)}$ and their complex conjugates, therefore (B.12) reads as

$$\boldsymbol{Q}_{(1)} = \Big[\gamma \hat{J}(k_0)\phi z(0) + F'''(0) \cdot A|A|^2 \Big(\frac{1}{2} z(0)^2 \overline{z}(0) + z(0)w(0)\overline{w}(0) \Big) +$$

93

$$F''(0)^2 \cdot A|A|^2 \left((E + \frac{B}{2})z(0)^2 \overline{z}(0) + (E + D + C)z(0)w(0)\overline{w}(0) \right) \Bigg] e^{i(\omega_0 t + k_0 x)}$$

$$+ \left[\gamma \hat{J}(k_0)\phi \, w(0) + F'''(0) \cdot A|A|^2 \left(\frac{1}{2} w(0)^2 \overline{w}(0) + z(0)\overline{z}(0)w(0) \right) + \right.$$

$$\left. F''(0)^2 \cdot A|A|^2 \left((E + \frac{B}{2})w(0)^2 \overline{w}(0) + (E + \overline{D} + C)z(0)\overline{z}(0)w(0) \right) \right] e^{i(\omega_0 t - k_0 x)} + cc + \cdots$$

$$(\text{B.15})$$

The coefficient of ϵ in the expansion (B.10) gives us the functional equation that defines U_2. This is

$$L_0 U_2 = \boldsymbol{Q} - \left(z'(0) \, \Phi_0 \, e^{i(\omega_0 t + k_0 x)} + w'(0) \, \Phi_0 \, e^{i(\omega_0 t - k_0 x)} + cc \right).$$

In order to have a solution here we need the right term to be orthogonal on the basis of the nullspace of L_0^*, the adjoint operator of L_0. This is, as we noted in Remark B.1, the set $\left\{ \Psi_0 \, e^{i(\omega_0 t \pm k_0 x)}, \overline{\Psi}_0 \, e^{-i(\omega_0 t \pm k_0 x)} \right\}$.

Therefore we have $< \boldsymbol{Q} - \left(z'(0) \, \Phi_0 \, e^{i(\omega_0 t + k_0 x)} + w'(0) \, \Phi_0 \, e^{i(\omega_0 t - k_0 x)} + cc \right), \Psi_0 \, e^{i(\omega_0 t \pm k_0 x)} >=$ $\int_0^{\frac{2\pi}{\omega_0}} dt \int_0^{\frac{2\pi}{k_0}} dx \, \overline{\Psi}_0 \, e^{-i(\omega_0 t \pm k_0 x)} \cdot \left[\boldsymbol{Q} - \left(z'(0) \, \Phi_0 \, e^{i(\omega_0 t + k_0 x)} + w'(0) \, \Phi_0 \, e^{i(\omega_0 t - k_0 x)} + cc \right) \right] = 0.$

Based on the fact that $\overline{\Psi}_0 \cdot \Phi_0 = 1$ and using $\boldsymbol{Q}_{(1)}$ from (B.15) and $\boldsymbol{Q}_{(2)} = 0$, we obtain

$$\begin{cases} z'(0) = z(0) \left(\tilde{a} + bz(0)\overline{z}(0) + cw(0)\overline{w}(0) \right), \\ w'(0) = w(0) \left(\tilde{a} + bw(0)\overline{w}(0) + cz(0)\overline{z}(0) \right), \end{cases}$$

with $\tilde{a} = \gamma \hat{J}(k_0) \, \phi \, \overline{\Psi}_0^1$, $b = |A|^2 \cdot A \, \overline{\Psi}_0^1 \cdot \left[\frac{F'''(0)}{2} + (E + \frac{B}{2})F''(0)^2 \right]$ and $c = |A|^2 \cdot A \, \overline{\Psi}_0^1 \cdot \left[F'''(0) + (E + D + C)F''(0)^2 \right]$.

Coefficients of the normal form. Equations (2.18), (B.6) and (B.7) imply

$$\phi \, \overline{\Psi}_0^1 = \frac{1}{2} - i \frac{1}{2\sqrt{g\tau - 1}}, \tag{B.16}$$

$$A \, \overline{\Psi}_0^1 = \frac{1 + 1/\tau}{2} + i \frac{g - (1 + 1/\tau)}{2\sqrt{g\tau - 1}} \tag{B.17}$$

so we can write $\tilde{a}$, b and c as $\tilde{a} = \tilde{a}_1 + i\tilde{a}_2$, $b = b_1 + ib_2$, $c = c_1 + ic_2$ with

$$\tilde{a}_1 = \frac{\gamma \hat{J}(k_0)}{2} = \frac{\hat{J}(k_0)(\alpha - \alpha^*)}{2\epsilon^2}, \quad \tilde{a}_2 = -\frac{\gamma \hat{J}(k_0)}{2\sqrt{g\tau - 1}} = -\frac{\hat{J}(k_0)(\alpha - \alpha^*)}{2\epsilon^2 \sqrt{g\tau - 1}},$$

94

$$b_1 = \frac{\tau+1}{4\tau} \cdot |A|^2 \cdot F''(0)^2 \cdot \left[2E + \mathrm{Re}(B) + \frac{1 - g\tau/(\tau+1)}{\sqrt{g\tau - 1}} \, \mathrm{Im}(B) \right] + \frac{\tau+1}{4\tau} \cdot |A|^2 \cdot F'''(0),$$

$$c_1 = \frac{\tau+1}{4\tau} \cdot |A|^2 \cdot F''(0)^2 \cdot \left[2E + 2D + 2\mathrm{Re}(C) + 2\frac{1 - g\tau/(\tau+1)}{\sqrt{g\tau - 1}} \, \mathrm{Im}(C) \right] + \frac{\tau+1}{4\tau} \cdot |A|^2 \cdot 2F'''(0),$$

$$b_2 = \frac{g\tau - (\tau+1)}{4\tau\sqrt{g\tau - 1}} \cdot |A|^2 \cdot F''(0)^2 \cdot \left[2E + \mathrm{Re}(B) - \frac{\sqrt{g\tau - 1}}{1 - g\tau/(\tau+1)} \, \mathrm{Im}(B) \right]$$
$$+ \frac{g\tau - (\tau+1)}{4\tau\sqrt{g\tau - 1}} \cdot |A|^2 \cdot F'''(0),$$

$$c_2 = \frac{g\tau - (\tau+1)}{4\tau\sqrt{g\tau - 1}} \cdot |A|^2 \cdot F''(0)^2 \cdot \left[2E + 2D + 2\,\mathrm{Re}(C) \right.$$
$$\left. - 2\frac{\sqrt{g\tau - 1}}{1 - g\tau/(\tau+1)} \, \mathrm{Im}(C) \right] + \frac{g\tau - (\tau+1)}{4\tau\sqrt{g\tau - 1}} \cdot |A|^2 \cdot 2F'''(0).$$

Remark B.3. From (B.13) and (B.14) we have $D = -1 + \frac{1}{g+1-\frac{(1+1/\tau)\hat{J}(2k_0)}{\hat{J}(k_0)}} = -1 + \tilde{D}$, $E = -1 + \frac{1}{g+1-\frac{(1+1/\tau)\hat{J}(0)}{\hat{J}(k_0)}} = -1 + \tilde{E}$, $\mathrm{Re}(B) + \frac{1-g\tau/(\tau+1)}{\sqrt{g\tau - 1}} \, \mathrm{Im}(B) = -1 + \frac{M_B}{N_B}$, $\mathrm{Re}(C) + \frac{1-g\tau/(\tau+1)}{\sqrt{g\tau - 1}} \, \mathrm{Im}(C) = -1 + \frac{M_C}{N_C}$ with $\tilde{D}, \tilde{E}, N_B, N_C > 0$. We obtain

$$b_1 = \frac{\tau+1}{4\tau} |A|^2 \left[F'''(0) + F''(0)^2 \cdot \left(-3 + 2\tilde{E} + \frac{M_B}{N_B} \right) \right],$$
$$c_1 = \frac{\tau+1}{4\tau} |A|^2 \left[2F'''(0) + F''(0)^2 \cdot \left(-6 + 2\tilde{E} + 2\tilde{D} + 2\frac{M_C}{N_C} \right) \right], \text{ where}$$

$M_B = M\left(\frac{\hat{J}(2k_0)}{\hat{J}(k_0)} \right)$, $M_C = M\left(\frac{\hat{J}(0)}{\hat{J}(k_0)} \right)$, $N_B = N\left(\frac{\hat{J}(2k_0)}{\hat{J}(k_0)} \right)$, $N_C = N\left(\frac{\hat{J}(0)}{\hat{J}(k_0)} \right)$, and M, N are functions defined as

$$M(X) = (4g\tau - 3)[2g\tau - (\tau+1)(\tau+2)]X + 4(g\tau - 1)(\tau+1)^2 + (3g\tau - 4 - \tau)^2 + g\tau(g\tau + \tau - 2),$$

and

$$N(X) = (4g\tau - 3)(\tau+1)^2 X^2 + 2\tau(\tau+1)(3 - g - 4g\tau)X + [4(g\tau - 1)(\tau+1)^2 + (3g\tau - 4 - \tau)^2].$$

Therefore

$$c_1 + b_1 = \frac{\tau+1}{4\tau} |A|^2 \cdot \left[3\left[F'''(0) - 3F''(0)^2 \right] + F''(0)^2 \cdot \left(2\tilde{D} + 4\tilde{E} + 2\frac{M_C}{N_C} + \frac{M_B}{N_B} \right) \right],$$
$$c_1 - b_1 = \frac{\tau+1}{4\tau} |A|^2 \cdot \left[\left[F'''(0) - 3F''(0)^2 \right] + F''(0)^2 \cdot \left(2\tilde{D} + 2\frac{M_C}{N_C} - \frac{M_B}{N_B} \right) \right].$$

B.0.2 Some properties

In the sequel we prove that $\int_0^{\frac{2\pi}{k_0}} dx \, [\overline{w}_1(J * v_1) - v_1(J * \overline{w}_1)] = 0$ on the space of the complex functions at least $\mathbb{C}^2$ and such that $v(x) = v(x + \frac{2\pi}{k_0})$, $\forall x \in \mathbb{R}$, together with the inner product $<v, w> = \int_0^{\frac{2\pi}{k_0}} v(x)\overline{w}(x)dx$.

We define on this space the integral operator $J * v(x) = \int_{-l}^{l} J(x - y)v(y)\,dy$ where l and J are

either $l = \infty$ and J as in (2.6), or $l = \frac{\pi n_0}{k_0}$ for some $n_0 \in \mathbb{N} \setminus \{0\}$ and J a $2l$-periodic trigonometric polynomial. An additional condition is J real and $J(x) = J(-x)$ for all $x \in \mathbb{R}$.

Remark B.4. In our problem the choice of k_0 depends on l, not vice-versa. We recall that $k_0 \neq 0$ is the most unstable mode defined by (2.12) when $l = \infty$, or by (2.15) when l finite. Nevertheless the hypotheses we adopted here correspond to the conditions of the original problem.

The first step is to prove that $J * v$ also satisfy $(J * v)(x) = (J * v)(x + \frac{2\pi}{k_0})$, so that the inner products $< v, J * w >$ and $< J * v, w >$ make sense.

The case $l = \infty$: It is obvious , by the a change of variables and by the periodicity of v, that
$(J * v)(x + \frac{2\pi}{k_0}) = \int_{-\infty}^{\infty} J(x + \frac{2\pi}{k_0} - y)v(y)\, dy = \int_{-\infty}^{\infty} J(x - y)v(y + \frac{2\pi}{k_0})\, dy = \int_{-\infty}^{\infty} J(x - y)v(y)\, dy = (J * v)(x).$

The case l finite: We compute $(J*v)(x + \frac{2\pi}{k_0}) = \int_{-l}^{l} J(x + \frac{2\pi}{k_0} - y)v(y)\, dy = \int_{-l-\frac{2\pi}{k_0}}^{l - \frac{2\pi}{k_0}} J(x-y)v(y + \frac{2\pi}{k_0})\, dy = \int_{-l-\frac{2\pi}{k_0}}^{l-\frac{2\pi}{k_0}} J(x - y)v(y)\, dy = \int_{-l}^{l} J(x - y)v(y)\, dy = (J * v)(x).$ The equality $\int_{-l+a}^{l+a} J(x - y)v(y)\, dy = \int_{-l}^{l} J(x - y)v(y)\, dy$ is true for any real a since $J(x + 2l) = J(x)$ and $u(x + 2l) = u(x + \frac{2\pi}{k_0}n_0) = u(x)$, i.e. the function $f(y) = J(x - y)u(y)$ is $2l$-periodic.

We prove now that $< v, J * w >=< J * v, w >$, i.e that $\int_0^{\frac{2\pi}{k_0}} v(x) \cdot (J * \overline{w})(x)\, dx = \int_0^{\frac{2\pi}{k_0}} (J * v)(x) \cdot \overline{w}(x)\, dx.$

For this, let us consider the Fourier series corresponding to the functions v and w, $v(x) = \sum_{n=-\infty}^{\infty} c_n e^{ink_0 x}$, $w(x) = \sum_{n=-\infty}^{\infty} d_n e^{ink_0 x}$ with the coefficients $c_n = \frac{k_0}{2\pi} \int_{-\frac{\pi}{k_0}}^{\frac{\pi}{k_0}} v(y)\, e^{-ink_0 y}dy$, $d_n = \frac{k_0}{2\pi} \int_{-\frac{\pi}{k_0}}^{\frac{\pi}{k_0}} w(y)\, e^{-ink_0 y}dy$. Since $v, w \in C^2$, their attached Fourier series converge uniformly on each closed interval in $\mathbb{R}$ ([85]), and have the sum v and w respectively. Moreover the coefficients satisfy

$$c_n = \mathcal{O}(1/n^2)\,, \ d_n = \mathcal{O}(1/n^2)\,, \ \text{as} \ n \to \infty\,. \tag{B.18}$$

For any fixed $x \in \mathbb{R}$, we have

$$J * v(x) = \int_{-l}^{l} dy J(x - y) \sum_{n=-\infty}^{\infty} c_n e^{ink_0 y} = \int_{-l}^{l} dy J(x - y) \lim_{M \to \infty} \sum_{n=-M}^{M} c_n e^{ink_0 y}$$

96

$$= \int_{-l}^{l} \lim_{M \to \infty} \left(\sum_{n=-M}^{M} c_n J(x-y) \, e^{ink_0 y} \right) dy = \int_{-l}^{l} \lim_{M \to \infty} f_M(y) dy \, .$$

We have $\lim_{M \to \infty} f_M(y) = J(x-y)v(y)$ for any $y \in \mathbb{R}$, and based on conditions (B.18) there exists a function g such that $|f_M(y)| \leq g(y)$ for any integer M and $y \in \mathbb{R}$ with $\int_{-l}^{l} g(y)dy < \infty$, no matter l is finite or infinite (when $l = \infty$ the function J is a linear combination of Gaussians). Therefore we can apply Lebesgue's dominated convergence theorem ([88]) and obtain $J * v(x) = \int_{-l}^{l} \lim_{M \to \infty} f_M(y)dy = \lim_{M \to \infty} \int_{-l}^{l} f_M(y)dy$, i.e.

$$J * v(x) = \lim_{M \to \infty} \left(\sum_{n=-M}^{M} c_n e^{ink_0 x} \int_{-l}^{l} J(x-y)e^{ink_0(y-x)}dy \right) = \sum_{n=-\infty}^{\infty} \hat{J}(nk_0)c_n e^{ink_0 x}$$

where $\hat{J}(k)$ is defined by (2.5). Similar we obtain $J * \overline{w}(x) = \sum_{m=-\infty}^{\infty} \hat{J}(mk_0)\overline{d}_m e^{-imk_0 x}$. This implies $< v, J * w >= \int_0^{\frac{2\pi}{k_0}} v(x) \cdot (J * \overline{w})(x) \, dx = \sum_{n=-\infty}^{\infty} \sum_{m=-\infty}^{\infty} c_n \overline{d}_m \hat{J}(mk_0) \int_0^{\frac{2\pi}{k_0}} e^{ink_0 x} e^{-imk_0 x} dx = \frac{2\pi}{k_0} \sum_{n=-\infty}^{\infty} c_n \overline{d}_n \hat{J}(nk_0)$, and

$$< J * v, w >= \int_0^{\frac{2\pi}{k_0}} (J * v)(x) \cdot \overline{w}(x) \, dx = \sum_{m=-\infty}^{\infty} \sum_{n=-\infty}^{\infty} c_n \hat{J}(nk_0)\overline{d}_m \int_0^{\frac{2\pi}{k_0}} e^{ink_0 x} e^{-imk_0 x} dx =$$
$\frac{2\pi}{k_0} \sum_{m=-\infty}^{\infty} c_m \overline{d}_m \hat{J}(mk_0)$.

B.0.3 Normal form for double-zero bifurcation with $O(2)$-symmetry

We present in the following the proofs for the results stated in Section 2.3.

Solving for U_0

Since the nullspace of L_0 corresponding to the center manifold has the basis $\left\{ \Phi_0 \, e^{\pm ik_0 x} \right\}$, U_0 can be written as $U_0 = \left(z \, e^{ik_0 x} + \overline{z} \, e^{-ik_0 x} \right) \Phi_0$ where z is ϵ-dependent. We choose a new time scale, $z = z(\epsilon t) = z(0) + z'(0)\epsilon t + \frac{z''(0)}{2}\epsilon^2 t^2 + \frac{z'''(0)}{6}\epsilon^3 t^3 + \mathcal{O}(\epsilon^4)$, and therefore obtain

$$\epsilon \, L_0 U_0 = \epsilon^2 \left[z'(0) \, e^{ik_0 x} + \overline{z'}(0) \, e^{-ik_0 x} \right] \Phi_0 + \epsilon^3 t \left[z''(0) \, e^{ik_0 x} + \overline{z''}(0) \, e^{-ik_0 x} \right] \Phi_0 + \frac{\epsilon^4 t^2}{2} \left[z'''(0) \, e^{ik_0 x} \right.$$
$$\left. + \overline{z'''}(0) \, e^{-ik_0 x} \right] \Phi_0 + \mathcal{O}(\epsilon^5) \, ,$$

$$\alpha^* J * u_0 - g^* v_0 = \frac{1}{\sqrt{\tau}} \left[z(0) \, e^{ik_0 x} + \overline{z}(0) \, e^{-ik_0 x} \right] + \frac{\epsilon \, t}{\sqrt{\tau}} \left[z'(0) \, e^{ik_0 x} + \overline{z'}(0) \, e^{-ik_0 x} \right]$$
$$+ \frac{\epsilon^2 t^2}{2\sqrt{\tau}} \left[z''(0) \, e^{ik_0 x} + \overline{z''}(0) \, e^{-ik_0 x} \right] + \mathcal{O}(\epsilon^3) \, ,$$

$$\gamma J * u_0 - \eta v_0 = (\gamma \hat{J}(k_0) - \eta) \frac{1}{\sqrt{\tau}} \left[z(0) e^{ik_0 x} + \overline{z}(0) e^{-ik_0 x} \right] + \mathcal{O}(\epsilon) ,$$

$$\gamma L_1 U_0 + \eta L_2 U_0 = (\gamma \hat{J}(k_0) - \eta) \frac{1}{\sqrt{\tau}} \mathbf{E} \left[z(0) e^{ik_0 x} + \overline{z}(0) e^{-ik_0 x} \right] + \epsilon t (\gamma \hat{J}(k_0) - \eta) \frac{1}{\sqrt{\tau}} \mathbf{E} \left[z'(0) e^{ik_0 x} \right.$$

$$\left. + \overline{z'}(0) e^{-ik_0 x} \right] + \mathcal{O}(\epsilon^2) . \tag{B.19}$$

These will be distributed in equation (2.42) accordingly to ϵ power.

Solving for U_1

The equation that defines U_1 corresponds to the coefficient of ϵ^2 in expansion (2.42) and reads as

$$L_0 U_1 = - \left[z'(0) e^{ik_0 x} + \overline{z'}(0) e^{-ik_0 x} \right] \Phi_0 + \frac{F''(0)}{2\tau} \mathbf{E} \left[z(0)^2 e^{2ik_0 x} + \overline{z}(0)^2 e^{-2ik_0 x} + 2z(0) \overline{z}(0) \right] . \tag{B.20}$$

Remark B.5. The adjoint operator of L_0 is $L_0^* V = -\frac{d}{dt} V - \begin{pmatrix} -1 + \alpha^* J * (\cdot) & 1/\tau \\ -g^* & -1/\tau \end{pmatrix} V$ and it has a two-dimensional nullspace of basis $\{ \Psi_1 e^{\pm ik_0 x} \}$ where Ψ_1 is defined by equations (2.32) and (2.31).

Since $\Phi_0 \cdot \Psi_1 = 0$, the right hand side term of (B.20) is orthogonal on $\Psi_1 e^{\pm ik_0 x}$ with respect to the integration $\int_0^{\frac{2\pi}{k_0}} dx$ and so the solution U_1 can be constructed. We choose U_1 in the form $U_1 = \left[w e^{ik_0 x} + \overline{w} e^{-ik_0 x} \right] \Phi_1 + z^2 \xi_1 e^{2ik_0 x} + \overline{z}^2 \xi_1 e^{-2ik_0 x} + 2z \overline{z} \xi_2$ with $w = w(\epsilon t) = w(0) + w'(0)\epsilon t + \frac{w''(0)}{2} \epsilon^2 t^2 + \mathcal{O}(\epsilon^3)$, and find that

$$z'(0) = w(0) , \tag{B.21}$$

$$\hat{L}(2k_0)\xi_1 = -\frac{F''(0)}{2\tau} \mathbf{E} , \quad \hat{L}(0)\xi_2 = -\frac{F''(0)}{2\tau} \mathbf{E} , \tag{B.22}$$

i.e. $\xi_1 = (1,1)^T B_1 , \xi_2 = (1,1)^T B_2$ with

$$B_1 = \frac{F''(0)}{2(\tau+1)[1 - \frac{\hat{J}(2k_0)}{\hat{J}(k_0)}]} , \quad B_2 = \frac{F''(0)}{2(\tau+1)[1 - \frac{\hat{J}(0)}{\hat{J}(k_0)}]} . \tag{B.23}$$

Therefore

$$\gamma L_1 U_1 + \eta L_2 U_1 = \gamma \hat{J}(k_0) \sqrt{\tau} \mathbf{E} \left[w(0) e^{ik_0 x} + \overline{w}(0) e^{-ik_0 x} \right] + B_1 (\gamma \hat{J}(2k_0) - \eta) \mathbf{E} \left[z(0)^2 e^{2ik_0 x} + \right.$$

98

$$\overline{z}(0)^2\, e^{-2ik_0 x}\Bigg] + 2B_2(\gamma\,\hat{J}(0) - \eta)\boldsymbol{E}\,z(0)\,\overline{z}(0) + \mathcal{O}(\epsilon), \text{ and}$$

$$\alpha^* J * u_1 - g^* v_1 = (1 + \frac{1}{\tau})\sqrt{\tau}\Big[w(0)e^{ik_0 x} + \overline{w}(0)e^{-ik_0 x}\Big] + \Big[z(0)^2 e^{2ik_0 x} + \overline{z}(0)^2 e^{-2ik_0 x}\Big](B_1 - \frac{F''(0)}{2\tau})$$

$$+ (2B_2 - \frac{F''(0)}{\tau})\,z(0)\,\overline{z}(0) + \epsilon\,(1 + \frac{1}{\tau})\sqrt{\tau}\Big[tw'(0)\,e^{ik_0 x} + t\overline{w'}(0)\,e^{-ik_0 x}\Big] + \epsilon\Big[tz(0)z'(0)\,e^{2ik_0 x}$$

$$+ t\overline{z}(0)\,\overline{z'}(0)\,e^{-2ik_0 x}\Big](2B_1 - \frac{F''(0)}{\tau}) + \epsilon\,(2B_2 - \frac{F''(0)}{\tau})\,[tz(0)\,\overline{z'}(0) + t\,\overline{z}(0)z'(0)] + \mathcal{O}(\epsilon^2)\,.$$

Solving for U_2

By using the above calculations together with (B.19), (B.21), and the property (B.22), equation (2.42) becomes

$$L_0 U_2 = (\gamma\,\hat{J}(k_0) - \eta)\frac{1}{\sqrt{\tau}}\boldsymbol{E}\Big[z(0)\,e^{ik_0 x} + \overline{z}(0)\,e^{-ik_0 x}\Big] - \Phi_1\Big[w'(0)\,e^{ik_0 x} + \overline{w'}(0)\,e^{-ik_0 x}\Big] +$$

$$+ z(0)w(0)e^{2ik_0 x}\Big[-2\xi_1 + F''(0)(1 + 1/\tau)\boldsymbol{E}\Big] + \overline{z}(0)\overline{w}(0)e^{-2ik_0 x}\Big[-2\xi_1 + F''(0)(1 + 1/\tau)\boldsymbol{E}\Big]$$

$$+ [z(0)\overline{w}(0) + \overline{z}(0)w(0)]\Big[-2\xi_2 + F''(0)(1 + 1/\tau)\boldsymbol{E}\Big] + z(0)^2\,\overline{z}(0)e^{ik_0 x}\Big[\frac{F'''(0)}{2\tau\sqrt{\tau}} + \frac{F''(0)}{\sqrt{\tau}}(B_1$$

$$+ 2B_2 - \frac{3F''(0)}{2\tau})\Big]\boldsymbol{E} + z(0)\,\overline{z}(0)^2 e^{-ik_0 x}\Big[\frac{F'''(0)}{2\tau\sqrt{\tau}} + \frac{F''(0)}{\sqrt{\tau}}(B_1 + 2B_2 - \frac{3F''(0)}{2\tau})\Big]\boldsymbol{E}$$

$$+ z(0)^3 e^{3ik_0 x}\Big[\frac{F'''(0)}{6\tau\sqrt{\tau}} + \frac{F''(0)}{\sqrt{\tau}}(B_1 - \frac{F''(0)}{2\tau})\Big]\boldsymbol{E} + \overline{z}(0)^3 e^{-3ik_0 x}\Big[\frac{F'''(0)}{6\tau\sqrt{\tau}} + \frac{F''(0)}{\sqrt{\tau}}(B_1$$

$$- \frac{F''(0)}{2\tau})\Big]\boldsymbol{E} + \epsilon\boldsymbol{S} + \mathcal{O}(\epsilon^2) \tag{B.24}$$

where $\boldsymbol{S} = -L_0 U_3 + \gamma\,L_1 U_1 + \eta\,L_2 U_1 + ...$, the terms from (2.42) corresponding to ϵ^4.

The orthogonality condition on $\Psi_1 e^{\pm ik_0 x}$, necessary for the existence of U_2 becomes

$$w'(0) = \Big[\frac{F'''(0)}{2\tau^2} + \frac{F''(0)}{\tau}(B_1 + 2B_2 - \frac{3F''(0)}{2\tau})\Big]z(0)^2\overline{z}(0) + \frac{1}{\tau}(\gamma\,\hat{J}(k_0) - \eta)z(0)$$

$$+ \epsilon < \boldsymbol{S}, \Psi_1 e^{ik_0 x} > + \mathcal{O}(\epsilon^2)\,. \tag{B.25}$$

This, together with the fact that $\Big[\boldsymbol{E} - \frac{1}{\sqrt{\tau}}\Phi_1 = \boldsymbol{0}\Big]$, implies that U_2 can be chosen as

$$U_2 = \Big[zw e^{2ik_0 x} + \overline{z}\,\overline{w}e^{-2ik_0 x}\Big]\beta_1 + [z\,\overline{w} + \overline{z}\,w]\beta_2 + \Big[z^3 e^{3ik_0 x} + \overline{z}^3 e^{-3ik_0 x}\Big]\beta_3$$

with β_1, β_2, β_3 defined by $[-\hat{L}(2k_0)\beta_1] = -2\xi_1 + F''(0)(1+1/\tau)\boldsymbol{E}$, $[-\hat{L}(0)\beta_2] = -2\xi_2 + F''(0)(1+1/\tau)\boldsymbol{E}$, $[-\hat{L}(3k_0)\beta_3] = \left[\frac{F'''(0)}{6\tau\sqrt{\tau}} + \frac{F''(0)}{\sqrt{\tau}}(B_1 - \frac{F''(0)}{2\tau})\right]\boldsymbol{E}$.

Solving for U_3

The resulting equation for U_3 is then the following

$$
L_0 U_3 = -\boldsymbol{S} + \gamma\,\hat{J}(k_0)\sqrt{\tau}\,w(0)\,e^{ik_0x}\boldsymbol{E} + [z(0)^2\overline{w}(0) + z(0)\,\overline{z}(0)\,w(0)]\,e^{ik_0x}\boldsymbol{E}\left[\frac{F''(0)}{\sqrt{\tau}}(\alpha^*\hat{J}(0)\beta_2^1\right.
$$

$$
\left. - g^*\beta_2^2) + F''(0)(1+1/\tau)\sqrt{\tau}\left(B_1 - \frac{F''(0)}{2\tau}\right) + \frac{F'''(0)}{2\sqrt{\tau}}(1+1/\tau)\right]
$$

$$
+ z(0)\,\overline{z}(0)\,w(0)\,e^{ik_0x}\boldsymbol{E}\left[\frac{F''(0)}{\sqrt{\tau}}(\alpha^*\hat{J}(2k_0)\beta_1^1 - g^*\beta_1^2) + F''(0)(1+1/\tau)\sqrt{\tau}\left(2B_2 - B_1\right.\right.
$$

$$
\left.\left. - \frac{F''(0)}{2\tau}\right) + \frac{F'''(0)}{2\sqrt{\tau}}(1+1/\tau)\right] + cc + terms\left(1, e^{\pm2ik_0x}, e^{\pm3ik_0x}, e^{\pm4ik_0x}\right) + \mathcal{O}(\epsilon)
$$

and we need

$$
< \boldsymbol{S}, \Psi_1 e^{ik_0x} > = \gamma\,\hat{J}(k_0)\,w(0) + z(0)\,\overline{z}(0)\,w(0)\left[\frac{F''(0)}{\tau}(\alpha^*\hat{J}(2k_0)\beta_1^1 - g^*\beta_1^2) + F''(0)(1+1/\tau)\left(2B_2\right.\right.
$$

$$
\left. - B_1 - \frac{F''(0)}{2\tau}\right) + \frac{F'''(0)}{2\tau}(1+1/\tau)\right] + [z(0)^2\overline{w}(0) + z(0)\,\overline{z}(0)\,w(0)]\left[\frac{F''(0)}{\tau}(\alpha^*\hat{J}(0)\beta_2^1 - g^*\beta_2^2)\right.
$$

$$
\left. + F''(0)(1+1/\tau)\left(B_1 - \frac{F''(0)}{2\tau}\right) + \frac{F'''(0)}{2\tau}(1+1/\tau)\right] + \mathcal{O}(\epsilon)\,.
$$

Based on equations (B.21) and (B.25) we obtain the normal form for the double-zero bifurcation

$z''(0) - \epsilon\left\{\gamma\,\hat{J}(k_0)z'(0) + Cz(0)[\,\overline{z}(0)\,z'(0) + z(0)\,\overline{z'}(0)\,] + D|z(0)|^2z'(0)\right\} - \left[\frac{\gamma\,\hat{J}(k_0) - \eta}{\tau} + A|z(0)|^2\right]z(0) = \mathcal{O}(\epsilon^2)$, with coefficients $A = \frac{1}{2\tau^2}[F'''(0) - 3F''(0)^2] + \frac{F''(0)^2}{\tau(\tau+1)}\cdot\left[\frac{\hat{J}(k_0)}{\hat{J}(k_0) - \hat{J}(0)} + \frac{\hat{J}(k_0)}{2\,[\,\hat{J}(k_0) - \hat{J}(2k_0)\,]}\right]$, $C = (\tau+1)A + \frac{F''(0)^2}{\tau(\tau+1)}\cdot\frac{\hat{J}(k_0)}{\hat{J}(k_0) - \hat{J}(0)}$, $D = (\tau+1)A + \frac{F''(0)^2}{\tau(\tau+1)}\cdot\frac{\hat{J}(k_0)}{\hat{J}(k_0) - \hat{J}(2k_0)}$.

Appendix C

Details of proof for results presented in LIF model

C.0.1 Proof of Theorem 3.2 for one-spike traveling wave in the LIF model

The inequality $V(y) < V_T$ can be written as

$$\frac{g/V_T}{2(\frac{\tau_1 c}{\sigma}-1)(1-\frac{\sigma}{\tau_2 c})}\,y + \frac{g/V_T}{(1-\frac{\sigma^2}{\tau_2^2 c^2})(1-\frac{\tau_1}{\tau_2})}\,y^{\sigma/\tau_2 c} - \frac{g/V_T}{(1-\frac{\sigma^2}{\tau_1^2 c^2})(1-\frac{\tau_1}{\tau_2})}\,y^{\sigma/\tau_1 c} < 1 + (-V_R/V_T + 1)\,y^{\sigma/\tau_1 c},$$

or equivalently as

$$(y-1) + \frac{2(1+\tau_1/\tau_2)}{(\frac{\tau_1 c}{\sigma}-1)(1-\frac{\sigma}{\tau_2 c})}\,y + \frac{g/V_T}{1-\frac{\tau_1}{\tau_2}}\left(\frac{\tau_2^2 c^2}{\tau_2^2 c^2 - \sigma^2}\,y^{\sigma/\tau_2 c} - \frac{\tau_1^2 c^2}{\tau_1^2 c^2 - \sigma^2}\,y^{\sigma/\tau_1 c}\right) < (-V_R/V_T + 1)\,y^{\sigma/\tau_1 c}.$$

We used here $\frac{g/V_T}{2(\tau_1 c/\sigma-1)(1-\sigma/\tau_2 c)} - 1 = \frac{2(1+\tau_1/\tau_2)}{(\tau_1 c/\sigma-1)(1-\sigma/\tau_2 c)}$, which comes from (3.14). When we regroup

the terms, we obtain

$$y\left(\frac{2(1+\tau_1/\tau_2)}{(\frac{\tau_1 c}{\sigma}-1)(1-\frac{\sigma}{\tau_2 c})} - \frac{g/V_T\,(1+\tau_1/\tau_2)}{(\frac{\tau_1^2 c^2}{\sigma^2}-1)(1-\frac{\sigma^2}{\tau_2^2 c^2})}\right) + +(y-1) + \frac{g/V_T}{1-\frac{\tau_1}{\tau_2}}\left(\frac{y^{\sigma/\tau_2 c}-y}{1-\frac{\sigma^2}{\tau_2^2 c^2}} - \frac{y^{\sigma/\tau_1 c}-y}{1-\frac{\sigma^2}{\tau_1^2 c^2}}\right) < (-V_R/V_T +$$

$1)\,y^{\sigma/\tau_1 c}$. The difference inside the first set of parentheses is zero because of (3.14). Therefore, we

are left exactly with the inequality $H(y) < (-V_R/V_T + 1)$.

The next step is to compute the derivative of H. This is

$$H'(y) = \frac{y^{-(1+\sigma/\tau_1 c)}}{1-\frac{\tau_1}{\tau_2}}\left[\frac{\sigma(1-\frac{\tau_1}{\tau_2})}{\tau_1 c} - \left(\frac{\sigma(1-\frac{\tau_1}{\tau_2})\,g/V_T}{\tau_1 c}\right)\frac{\tau_2^2 c^2}{\tau_2^2 c^2 - \sigma^2}\,y^{\sigma/\tau_2 c}+\right.$$

$$\left.+y\left(\frac{(\tau_1 c-\sigma)(1-\frac{\tau_1}{\tau_2})}{\tau_1 c} + g/V_T\left(\frac{\sigma^2(\frac{\tau_2^2}{\tau_1^2}-1)}{\tau_2^2 c^2 - \sigma^2}\right)\left(\frac{\tau_1 c}{\tau_1 c+\sigma}\right)\right)\right].$$

By using again equation (3.14) we obtain

$$H'(y) = \frac{y^{-(1+\sigma/\tau_1 c)}}{1-\frac{\tau_1}{\tau_2}}\left[\frac{\sigma(1-\frac{\tau_1}{\tau_2})}{\tau_1 c} - \frac{2(\tau_1 c+\sigma)\cdot\frac{\tau_2}{\tau_1}\cdot(1-\frac{\tau_1}{\tau_2})}{\tau_2 c-\sigma}\,y^{\sigma/\tau_2 c} + y\,\frac{(\tau_1 c+\sigma)(\tau_2 c+\sigma)(1-\frac{\tau_1}{\tau_2})}{\tau_1 c(\tau_2 c-\sigma)}\right]$$

$$= \frac{(\tau_1 c+\sigma)(\tau_2 c+\sigma)}{\tau_1 c(\tau_2 c-\sigma)}\,y^{-(1+\sigma/\tau_1 c)}\left[\frac{\sigma(\tau_2 c-\sigma)}{(\tau_1 c+\sigma)(\tau_2 c+\sigma)} - \frac{2\tau_2 c}{\tau_2 c+\sigma}\,y^{\sigma/\tau_2 c} + y\right] = \frac{\tau_2}{2\tau_1}\,\frac{\sigma}{\tau_2 c-\sigma}\,\frac{g}{V_T}\,y^{-(1+\sigma/\tau_1 c)}\,G(y)$$

with G defined by (3.18).

The existence of the unique root $y^* \in (0,1)$ for G comes from the following observations.

Since $G'(y) = 1 - \frac{2\sigma}{\tau_2 c+\sigma}\,y^{\sigma/\tau_2 c-1}$, the derivative of G has exactly one zero in the interval $(0,1)$, at

$\tilde{y} = \left(\frac{2\sigma}{\tau_2 c + \sigma} \right)^{\tau_2 c / (\tau_2 c - \sigma)}$, G decreases on $(0, \tilde{y})$, and G increases on $(\tilde{y}, 1)$. Further, since we calculated that $c > \sigma / \sqrt{\tau_1 \tau_2}$, the assumption $\tau_2 > \tau_1$ implies that $G(0) > 0$ and $G(1) < 0$. Therefore, $G(\tilde{y})$ must be negative, and the unique root of G belongs to $(0, \tilde{y}) \subset (0, 1)$.

C.0.2 Proof of Lemma 3.3.2 for two-spike traveling waves in the LIF model

The inequalities from i), ii), iii) can be easily verified. To establish the limits of F, we use these inequalities, the assumption that $\tau_2 > \tau_1$, and the fact that $\lim_{c \to c_{1;2}} f(c) = 0$.

i) By direct calculation, we obtain $\lim_{c \searrow c_2} F(c) = \lim_{c \nearrow c_1} F(c) = -\infty$.

iii) By direct calculation, we have

$\lim_{c \nearrow c_1} F(c) = -\frac{g}{V_T} \left(1 + \frac{\tau_1}{\tau_2} \right) \frac{\sigma^2}{\tau_1^2 c_1^2 - \sigma^2} \frac{\tau_2^2 c_1^2}{\tau_2^2 c_1^2 - \sigma^2}$ and $\lim_{c \searrow c_2} F(c) = \lim_{c \searrow c_2} f(c)^{\frac{\sigma}{\tau_1 c} - 1} \left[-V_R/V_T \right.$

$\left. + 1 + \frac{g/V_T}{1 - \frac{\tau_1}{\tau_2}} \left(\frac{f(c)^{1 - \frac{\sigma}{\tau_1 c}} - f(c)^{-\frac{\sigma}{\tau_1 c} \left(1 - \frac{\tau_1}{\tau_2} \right)}}{1 - \frac{\sigma^2}{\tau_2^2 c^2}} - \frac{f(c)^{1 - \frac{\sigma}{\tau_1 c}} - 1}{1 - \frac{\sigma^2}{\tau_1^2 c^2}} \right) \right] = -\infty.$

ii) At $g/V_T = 4(1 + \tau_1/\tau_2)$, since $c_1 = \frac{\sigma}{\tau_2}$ and $c_2 = \frac{\sigma}{\tau_1}$, the calculation needs to be handled more carefully. We apply l'Hospital's rule repeatedly and obtain

$$\lim_{c \searrow \frac{\sigma}{\tau_1}} f(c)^{\frac{\sigma}{\tau_1 c} - 1} = 1 \,, \quad \lim_{c \searrow \frac{\sigma}{\tau_1}} \frac{f(c)^{\frac{\sigma}{\tau_1 c} - 1} - 1}{\frac{\sigma}{\tau_1 c} - 1} = -\infty \,, \quad \lim_{c \searrow \frac{\sigma}{\tau_1}} \frac{f(c)^{1 - \frac{\sigma}{\tau_2 c}} [f(c)^{\frac{\sigma}{\tau_1 c} - 1} - 1]}{\frac{\sigma}{\tau_1 c} - 1} = 0 \,,$$

and therefore $\lim_{c \searrow \frac{\sigma}{\tau_1}} F(c) =$

$\lim_{c \searrow \frac{\sigma}{\tau_1}} f(c)^{\frac{\sigma}{\tau_2 c} - 1} \left[(-V_R/V_T + 1) f(c)^{\frac{\sigma}{\tau_1 c} \left(1 - \frac{\tau_1}{\tau_2} \right)} + \frac{g/V_T}{1 - \frac{\tau_1}{\tau_2}} \left(\frac{f(c)^{1 - \frac{\sigma}{\tau_2 c}} - 1}{1 - \frac{\sigma^2}{\tau_2^2 c^2}} - \frac{f(c)^{1 - \frac{\sigma}{\tau_2 c}} (f(c)^{\frac{\sigma}{\tau_1 c} - 1} - 1)}{(1 + \frac{\sigma}{\tau_1 c})(\frac{\sigma}{\tau_1 c} - 1)} \right) \right] = -\infty.$

Similarly, $\lim_{c \nearrow \frac{\sigma}{\tau_2}} f(c)^{\frac{\sigma}{\tau_2 c} - 1} = 1$, $\lim_{c \nearrow \frac{\sigma}{\tau_2}} \frac{f(c)^{\frac{\sigma}{\tau_2 c} - 1} - 1}{\frac{\sigma}{\tau_2 c} - 1} = -\infty$, $\lim_{c \nearrow \frac{\sigma}{\tau_2}} f(c)^{\frac{\sigma}{\tau_1 c} - 1} = 0$, and thus $\lim_{c \nearrow \frac{\sigma}{\tau_2}} F(c) = -\infty.$

Bibliography

1. Ahrens K.F., Levine H., Suhl H., Kleinfeld D., *Spectral mixing of rhythmic neuronal signals in sensory cortex*, Proc.Natl.Acad.Sci. **99**(23), 15176-15181 (2002).

2. Amari S.I., *Dynamics of pattern formation in lateral-inhibition type neural fields*, Biol.Cyber. **27**, 77-87 (1977).

3. Andrews T.J., Purves D., *Similarities in normal and binocularly rivalrous viewing*, Proc. Natl. Acad. Sci. **94**, 9905-9908 (1997).

4. Arnold V., *Ordinary differential equations*, MIT Press, Cambridge MA, 1973.

5. Arrowsmith D.K., Place C.M., *An introduction to dynamical systems*, Cambridge University Press, 1990.

6. Bellman R., Cooke K.L., *Differential-difference equations*, Academic Press, New York, 1963.

7. Ben-Yishai R., Hansel D., Sompolinsky H., *Traveling waves and the processing of weakly tuned inputs in a cortical network module*, J.Comput.Neurosci. **4**, 57-77 (1997).

8. Ben-Yishai R., Lev Bar-Or R., Sompolinsky H., *Theory of orientation tuning in visual cortex*, Proc.Natl.Acad.Sci. **92**, 3844-3848 (1995).

9. Blake R., *A neural theory of binocular vision*, Phychol.Rev. **96**, 145-167 (1989).

10. Bressloff P.C., *Synaptically generated wave propagation in excitable neural media*, Phys. Rev. Lett. **82**, 2979-2982 (1999).

11. Bressloff P.C., *Traveling waves and pulses in a one-dimensional network of excitable integrate-and-fire neurons*, J.Math.Biol. **40**, 169-198 (2000).

12. Bressloff P.C., Cowan J.D., Golubitsky M., Thomas P.J., *Scalar and pseudoscalar bifurcations motivated by pattern formation on the visual cortex*, Nonlinearity **14**, 739-775 (2001).

13. Braun M., *Differential equations and their applications*, 3rd ed., Springer, New York, 1983.

14. Campbell S.A., Belair J., Ohira T., Milton J., *Complex dynamics and multistability in a damped harmonic oscillator with delayed negative feedback*, Chaos **5**, 640-645 (1995).

15. Carr J., *Applications of center manifold theory*, Springer, New York, 1981.

16. Castelfranco A.M., Stech H.W., *Periodic solutions in a model of recurrent neural feedback*, SIAM J.Appl.Math. **47**, 573-588 (1987).

17. Chagnac-Amitai Y., Connors B.W., *Horizontal spread of synchronized activity in neurocortex and its control by GABA-mediated inhibition*, J.Neurophysiol. **61**, 747-758 (1989).

18. Chervin R.D., Pierce P.A., Connors B.W., *Periodicity and directionality in the propagation of epileptiform discharges across neocortex*, J.Neurophysiol. **60**, 1695-1713 (1988).

19. Chow S-N, Li C., Wang D., *Normal forms and bifurcation of planar vector fields*, Cambridge University Press, New York, 1994.

20. Chu P.H., Milton J.G., Cowan J.D., *Connectivity and the dynamics of integrate-and-fire networks*, Int.J.Bif. and Chaos **4**, 237-243 (1994).

21. Coddington E., Levinson N., *Theory of ordinary differential equations*, McGraw-Hill, New York, 1955.

22. Connors B.W., Gutnick M.J., *Intrinsic firing patterns of diverse neocortical neurons*, Trends. Neurosci. **13**, 99-104 (1990).

23. Connors B.W., Gutnick M.J., Prince D.A., *Electrophysiological properties of neocortical neurons in vitro*, J.Neurophysiol. **48**, 1302-1320 (1982).

24. Contreras D., Destexhe A., Sejnowski T.J., Steriade M., *Spatiotemporal patterns of spindle oscillations in cortex and thalamus*, J.Neurosci. **17**, 1179-1196 (1997).

25. Curtu R., Ermentrout B., *Oscillations in a refractory neural net*, J. Math.Biol. **43**, 81-100 (2001).

26. Dangelmayr G., Armbruster D., *Steady-state mode interactions in the presence of $O(2)$-symmetry and in non-flux boundary value problems*, Contemporary Math. **56**, 53-68 (1986).

27. Dangelmayr G., Knobloch E., *The Takens-Bogdanov bifurcation with $O(2)$-symmetry*, Phil. Trans. R. Soc. Lond. A **322**, 243-279 (1987).

28. Dayan P., Abbott L.F., *Theoretical Neuroscience. Computational and mathematical modeling of neural systems*, MIT Press, 2001.

29. Destexhe A., Bal T., McCormick D.A., Sejnowski T., *Ionic mechanisms underlying synchronized oscillations and propagating waves in a model of ferret thalamic slices*, J.Neurophysiol. **76**(3), 2049-2070 (1996).

30. Diekmann O., van Gils S.A., Verduyn Lunel S.M, Walther H.O., *Delay Equations: Functional, Complex, and Nonlinear Analysis*, Springer, New York, Applied Mathematical Sciences, Vol.110, 1995.

31. Engel A.K., Konig P., Kreiter A.K., Singer W., *Interhemispheric synchronization of oscillatory neuronal responses in cat visual cortex*, Science **252**, 1177-1179 (1991).

32. Ermentrout B., *Simulating, analyzing, and animating dynamical systems: a guide to xppaut for researchers and students*, SIAM 2002.

33. Ermentrout G.B. *The analysis of synaptically generated traveling waves*, J.Comp.Neurosci. **5**, 191-208 (1998).

34. Ermentrout G.B. *Neural networks as spatio-temporal pattern-forming systems*, Rep.Prog.Phys. **61**, 353-430 (1998).

35. Ermentrout B., *Stripes or spots? Nonlinear effects in bifurcation of reaction-diffusion equations on the square*, Proc.R.Soc.Lond. A **434**, 413-417 (1991).

36. Ermentrout B., *XPPAUT, http://www.pitt.edu/∼phase*

37. Ermentrout G.B., *Symmetry breaking in homogeneous, isotropic, stationary neuronal nets*, Ph.D. Dissertation, The University of Chicago, 1979.

38. Ermentrout G.B., Campbell J., Oster G., *A model for shell patterns based on neural activity*, The Veliger **28**, 369-388 (1986).

39. Ermentrout G.B., Cowan J., *A mathematical theory of visual hallucination patterns*, Biol. Cybern. **34**, 137-150 (1979).

40. Ermentrout G.B., McLeod J.B., *Existence and uniqueness of traveling waves for a neural network*, Proc.Roy.Soc.Edinburgh A **123**, 461-478 (1993).

41. Faria T., Magalhães L., *Normal forms for retarded functional-differential equations with parameters and applications to Hopf bifurcation*, J.Differential Equations **122**, 182-200 (1995).

42. Flint A.C., Connors B.W., *Two types of network oscillations in neocortex mediated by distinct glutamate receptor subtypes and neuronal populations*, J. Neurophysiol. **75**, 951-957 (1996).

43. Golomb D., Amitai Y., *Propagating neuronal discharges in neocortical slices: Computational and experimental study*, J. Neurophysiol. **78**, 1199-1211 (1997).

44. Golomb D., Ermentrout G.B., *Effects of delay on the type and velocity of travelling pulses in neuronal networks with spatially decaying connectivity*, Network **11**, 221-246 (2000).

45. Golomb D., Ermentrout G.B., *Continuos and lurching traveling pulses in neuronal networks with delay and spatially decaying connectivity*, Proc.Natl.Acad.Sci. USA **96**, 13480-13485 (1999).

46. Golomb D., Wang X-J., Rinzel J., *Propagation of spindle waves in a thalamic slice model*, J.Neurophysiol. **75**, 750-769 (1996).

47. Golubitsky M., Schaeffer D., *Singularities and groups in bifurcation theory I*, Springer, New York, 1985.

48. Golubitsky M., Stewart I., Schaeffer D., *Singularities and groups in bifurcation theory II*, Springer, New York, 1988.

49. Gray C.M., König P., Engel A.K., Singer W., *Oscillatory responses in cat visual cortex exhibit inter-columnar synchronization which reflects global stimulus properties*, Nature **338**, 334-337 (1989).

50. Guckenheimer J., *A codimension two bifurcation with circular symmetry*, Contemporary Math. **56**, 175-184 (1986).

51. Guckenheimer J., Holmes P., *Nonlinear oscillations, dynamical systems and bifurcations of vector fields*, Springer, New York, 1983.

52. Gutnick M.J., Connors B.W., Prince D.A., *Mechanisms of neocortical epileptogenesis in vitro*, J.Neurophysiol. **48**, 1321-1335 (1982).

53. Hale J.K., *Local flows for functional differential equations*, Contemporary Math. **56**, 185-192 (1986).

54. Hale J.K., *Theory of functional differential equations*, Springer, New York, 1977.

55. Hale J.K., *Introduction to dynamical bifurcation*, LNM **1057**, Springer, Berlin, 1984.

56. Hale J., Huang W., *Periodic solutions to singularly perturbed delay equations*, Z. Angew. Math. Phys. **47**, 57-88 (1996).

57. Hale J., Huang W., *Square and pulse waves in matrix delay differential equations*, Dynamic Systems Appl. **1**, 51-70 (1992).

58. Hansel D., Sompolinsky H., *Modeling feature selectivity in local cortical circuits*, in Methods in Neuronal Modeling (Koch C., Segev I. editors), 2-nd ed., 1998.

59. Hansel D., Sompolinsky H., *Chaos and synchrony in a model of a hypercolumn in visual cortex*, J.Comput.Neurosci. **3**, 7-34 (1996).

60. Hartman P., *Ordinary differential equations*, Wiley & Sons, New York, 1964.

61. Hoppensteadt F., Izhikevich E., *Weakly connected neural nets*, Springer, Berlin, 1998.

62. Idiart M.A.P., Abbott L.F., *Propagation of excitation in neural network models*, Network **4**, 285-294 (1993).

63. James M.P., *Dynamics of synaptically interacting integrate-and-fire neurons*, Ph.D. Dissertation, Loughborough University, 2002.

64. Johnson D., Wu S.M-S., *Foundations of cellular neurophysiology*, MIT Press, Cambridge MA, 1995.

65. Kandel E.R., Schwartz J.H., Jessell T.M., *Principles of neural science*, 4-nd ed., McGraw-Hill, New York, 2000.

66. Kim U., Bal T., McCormick D.A., *Spindle waves are propagating synchronized oscillations in the ferret LGN in vitro*, J. Neurophysiol. **74**, 1301-1323 (1995).

67. Kleinfeld D., Delaney K.R., Fee M.S., Flores J.A, Tank D.W., Gelperin A., *Dynamics of propagating waves in the olfactory network of a terrestrial mollusk: an electrical and optical study*, J. Neurophysiol. **72**, 1402-1419 (1994).

68. Kuznetsov Yu.A., *Elements of applied bifurcation theory*, 2-nd ed., Springer, New York, 1998.

69. Laing C., Chow C., *A spiking neuron model for binocular rivalry*, J.of Comp.Neurosci. **12**, 39-53 (2002).

70. Leopold D.A., Logothetis N.K., *Multistable phenomena: changing views in perception*, Trends.Cogn.Sci. **3**(7), 254-264 (1999).

71. Logothetis N.K., Leopold D.A., Sheinberg D.L., *What is rivalling during binocular rivalry?*, Nature **380**, 621-624 (1996).

72. MacDonald N., *Biological delay systems: linear stability theory*, Cambridge University Press, 1989.

73. Mallet-Paret J., Nussbaum R.D., *Multiple transition layers in a singularly perturbed differential delay equation*, Proc.Roy. Soc.Edinburgh, Sect.A **123**, 1119-1134 (1993).

74. Marcus C.M., Westervelt R.M., *Stability of analog neural networks with delay*, Phys. Rev.A **39**, 347-359 (1989).

75. McLeod J.B., Sattinger D.H., *Loss of stability and bifurcation at a double eigenvalue*, J. of Func.Analysis **14**, 62-84 (1973).

76. Mehta M.R., Lee A.K., Wilson M.A., *Role of experience and oscillations in transforming a rate code into a temporal code*, Nature **417**, 741-746 (2002).

77. Murray J.D., *Mathematical biology*, 2-nd ed., Springer, New York, 1998.

78. Oşan R., Curtu R., Rubin J., Ermentrout G.B., *Multiple-spike waves in a one-dimensional integrate-and-fire neural network*, J.Math.Biol. accepted (2002).

79. Oşan R., Rubin J., Curtu R., and Ermentrout G.B., *Periodic traveling waves in a one-dimensional integrate-and-fire neural network*, Neurocomputing, In Press (2003).

80. Oşan R., Ermentrout G. B., *The evolution of synaptically generated waves in one- and two-dimensional domains*, Physica **D 163**, 217-235 (2002).

81. Oşan R., Ermentrout G. B., *Two dimensional synaptically generated traveling waves in a theta-neuron neural network*, Neurocomputing **38-40**, 789-795 (2001).

82. Oşan R., Rubin J., Ermentrout G. B., *Regular traveling waves in a one-dimensional network of theta neurons*, SIAM J.Appl.Math. **62**, 1197-1221 (2002).

83. Pinto D.J., *Computational, experimental, and analytic explorations of neuronal circuits in the cerebral cortex*, Ph.D. Dissertation, University of Pittsburgh, 1997.

84. Pinto D.J., Ermentrout G.B., *Spatially structured activity in synaptically coupled neuronal networks: I. Traveling fronts and pulses*, SIAM J.Appl.Math. **62**, 206-225 (2001).

85. Rees C.S., Shah S.M., Stanojević C.V., *Theory and applications of Fourier analysis*, Marcel Dekker Inc., New York, 1981.

86. Rinzel J., Keller J.B., *Traveling wave solutions of a nerve conduction equation*, Biophys. J. **13**, 1313-1337 (1973).

87. Rinzel J., Terman D., Wang X-J., Ermentrout B., *Propagating activity patterns in large-scale inhibitory neuronal networks*, Science **279**, 1351-1355 (1998).

88. Rudin W., *Principles of mathematical analysis*, 3-rd ed., McGraw-Hill, New York, 1976.

89. Sattinger D.H., *Group Theoretic Methods in Bifurcation Theory*, in Lectures Notes in Mathematics Series, Springer, Berlin, 1979.

90. Sattinger D.H., *Group representation theory, bifurcation theory and pattern formation*, J. of Func.Analysis **28**, 58-101 (1978).

91. Somers D., Nelson S., Sur M., *An emergent model of orientation selectivity in cat visual cortical cells*, J.Neurosci. **15**, 5448-5465 (1995).

92. Steriade M., McCormick D.A., Sejnowski T.J., *Thalamocortical oscillations in the sleeping and aroused brain*, Science **262**, 679-685 (1993).

93. Steriade M., Timofeev I., *Neuronal plasticity in thalamocortical networks during sleep and waking oscillations*, Neuron **37**, 563-576 (2003).

94. Stich M., *Target patterns and pacemakers in reaction-diffusion systems*, Ph.D. Dissertation, Technical University Berlin, 2002.

95. Strogatz S.H., *Nonlinear dynamics and chaos with applications to physics, biology, chemistry and engineering*, Addison-Wesley, New York, 1994.

96. Swindale N.V., *A model for the formation of ocular dominance stripes*, Proc.Roy.Soc.Lond. B **208**, 243-264 (1980).

97. Terman D.H., Ermentrout G.B., Yew A.C., *Propagating activity patterns in thalamic neuronal networks*, SIAM J.Appl.Math. **61**, 1578-1604 (2001).

98. Traub R.D., Jefferys J.G.R., Miles R., *Analysis of propagation of disinhibition-induced after-discharges along the guinea-pig hippocampal slice in vitro*, J. Physiol.Lond. **472**, 267-287 (1993).

99. van Vreeswijk C., Hansel D., *Patterns of synchrony in neural networks with spike adaptation*, Neural Computation **13**, 959-992 (2001).

100. Verhulst F., *Nonlinear differential equations and dynamical systems*, Springer, Berlin, 1990.

101. Whittington M.A., Traub R.D., Jefferys J.G.R., *Synchronized oscillations in interneuron networks driven by metabotropic glutamate receptor activation*, Nature **373**, 612-615 (1995).

102. Wiggins S., *Introduction to applied nonlinear dynamical systems and chaos*, Springer, New York, 1990.

103. Wiggins S., *Global bifurcations and chaos*, Appl.Math.Sci. **73**, Springer, New York, 1988.

104. Wilson H.R., Cowan J.D., *Excitatory and inhibitory interactions in localized populations of model neurons*, Biophys. J. **12**, 1-24 (1972).

105. Wu J-Y., Guan L., Tsau Y., *Propagating activation during oscillations and evoked response in neocortical slices*, J.Neurosci. **19**, 5005-5015 (1999).

106. Ye H., Michel A.N., Wang K., *Global stability and local stability of Hopfield neural networks with delays*, Phys.Rev.E **50**, 4206-4213 (1994).